DESIGN AND SIMULATION OF A DYNAMIC PCM INTEGRATED TROMBE WALL SYSTEM FOR ENSURING THERMAL COMFORT IN HIGHLY GLAZED BUILDINGS

A THESIS SUBMITTED TO
THE GRADUATE SCHOOL OF NATURAL AND APPLIED SCIENCES
OF
MIDDLE EAST TECHNICAL UNIVERSITY

BY

EGE SOYER

IN PARTIAL FULFILLMENT OF THE REQUIREMENTS
FOR
THE DEGREE OF MASTER OF SCIENCE
IN
BUILDING SCIENCE IN ARCHITECTURE

DECEMBER 2022

Approval of the thesis:

DESIGN AND SIMULATION OF A DYNAMIC PCM INTEGRATED TROMBE WALL SYSTEM FOR ENSURING THERMAL COMFORT IN HIGHLY GLAZED BUILDINGS

submitted by **EGE SOYER** in partial fulfillment of the requirements for the degree of **Master of Science in Building Science in Architecture, Middle East Technical University** by,

Prof. Dr. Halil Kalıpçılar
Dean, Graduate School of **Natural and Applied Sciences** _____

Prof. Dr. F. Cana Bilsel
Head of the Department, **Architecture** _____

Prof. Dr. Soofia Tahira Elias Ozkan
Supervisor, **Architecture, METU** _____

_____

Examining Committee Members:

Assoc. Prof. Dr. Ayşe Tavukçuoğlu
Architecture, METU _____

Prof. Dr. Soofia Tahira Elias Ozkan
Architecture, METU _____

Prof. Dr. İdil Ayçam
Architecture, Gazi University _____

Assoc. Prof. Dr. Ayşegül Tereci
Architecture, KTO Konya Karatay Uni. _____

Asst. Prof. Dr. Rukiye Çetin
Architecture, AYBÜ _____

Date: 02.12.2022

I hereby declare that all information in this document has been obtained and presented in accordance with academic rules and ethical conduct. I also declare that, as required by these rules and conduct, I have fully cited and referenced all material and results that are not original to this work.

Name Last name : Ege Soyer

Signature :

ABSTRACT

DESIGN AND SIMULATION OF A DYNAMIC PCM INTEGRATED TROMBE WALL SYSTEM FOR ENSURING THERMAL COMFORT IN HIGHLY GLAZED BUILDINGS

Soyer, Ege
Master of Science, Building Science in Architecture
Supervisor : Prof. Dr. Soofia Tahira Elias Ozkan

December 2022, 109 pages

In building design, there is an ongoing trend of research focused on various techniques for decreasing energy consumption in buildings, which can reduce the effect of global warming. This work is inspired by the passive heating system "Trombe Wall" which consists generally of a masonry unit located at the façades, covered with a glass layer, and collects heat energy from the sun due to a black coating at the exterior side of the wall. However, it has some drawbacks: e.g., Trombe Wall is static, heavy, hard to integrate into contemporary architectural facades.

To solve these problems, a dynamic Trombe Wall system called "Heat Pocket" has been designed. Heat Pocket consists of aluminum panels that are filled with phase change material (PCM), their exterior facing surface is painted with a selective black coating which converts solar energy to heat, and this thermal energy is stored in the PCM.

In this work, the proposed system was simulated to assess if the system would satisfy ASHRAE thermal comfort levels during the day for the virtual room having an interior space of 7.3 m x 5.4 m x 3.5 m; in cold climate conditions of Van, Turkey; in the month of December.

Findings show for the 100% PCM-filled panel, Heat Pocket is able to increase and retain the indoor by a minimum of 18.5 °C compared to outdoor temperatures. The system was able to satisfy ASHRAE thermal comfort levels completely throughout the analysis time, after the first 3.3 meters away from the glass façade.

Keywords: Sustainable Facade Design, Trombe Wall, Passive Heating, Heat Collection and Storage System, Phase Change Materials.

ÖZ

CAM CEPHELİ YAPILARDA TERMAL KONFORU SAĞLAMAYI HEDEFLEYEN FAZ DEĞİŞTİREN MALZEME ENTEGRE EDİLMİŞ DİNAMİK TROMBE DUVAR SİSTEMİ, TASARIMI VE SİMÜLASYONU

Soyer, Ege
Yüksek Lisans, Mimarlık
Tez Yöneticisi: Prof. Dr. Soofia Tahira Elias Ozkan

Aralık 2022, 109 sayfa

Küresel ısınmanın etkisini azaltmak için bina tasarımında binaların kullandığı enerjiyi düşürmeyi hedefleyen farklı teknikler, günümüzde birçok bina tekniği araştırmalarının ana konusudur. Bu çalışma Trombe Duvarı diye adlandırılan pasif ısıtma sisteminden esinlenmiştir. Trombe Duvarı tekniğinde, genellikle cepheye yerleştirilen tuğla duvarın dışarı bakan kısmı siyah ile boyanıp cam bir yüzey kaplanmıştır. Böylece, güneşten gelen enerji duvarda emilir ve duvar elemanı tarafından depolanır. Ne yazık ki, bu teknik bazı konularda eksik kalmaktadır, sabittir, ağırdır ve güncel binalara eklenmesi zor bir uygulamadır.

Bu problemleri çözmek için Isı Cebi projesi, Dinamik Trombe Duvarı Sistemi tasarlanmıştır. Sistem faz değiştiren malzeme ile dolu aluminyum panellerden oluşmaktadır. Bu panel, dışa bakan yüzeyinde bulunan seçici siyah boya ile güneşten gelen enerjiyi ısı enerjisine çevirir ve faz değiştiren malzeme içinde depolar.

Bu çalışmada sunulan sistem, 7.3 m x 5.4 m x 3.5 m ebatlarında bir oda modelinde Van, Türkiye Aralık iklim koşullarında simüle edilip, sistemin ASHRAE termal konfor seviyelerini karşılayıp karşılamadığı ölçülmüştür.

%100 faz değiştiren malzeme dolu Isı Cebi paneli, odanın içindeki sıcaklığı dışarıyla karşılaştırıldığında 18.5 °C arttırmış ve odanın sıcaklığını korumuştur. Sistem, ASHRAE termal konfor seviyelerini cam cepheden 3.3 m uzakta analiz zamanı boyunca sağlamıştır.

Anahtar Kelimeler: Sürdürülebilir Bina Tasarımı, Trombe Duvarı, Pasif Isıtma Sistemi, Isı Toplama Sistemi, Faz Değiştiren Malzeme

For my mother Nesrin and father Selahattin who always supported me dearly,

ACKNOWLEDGMENTS

The author wishes to express his deepest gratitude to his supervisor Prof. Soofia Tahira Elias-Ozkan for her faith from the start to end, guidance, critics, encouragements on repeated reworks and, understandings throughout the evolution of the project through many iterations.

The author wants to thank his teachers from Bilkent University, Dr. Alper Küçük, Architect M. Turhan Kayasü, Assoc. Prof. Dr. Yasemin Eren Afacan who guided me on a pathway to sustainable design, which eventually led to this research project.

The author wants to thank his mother Nesrin, father Selahattin and family who always supported him through his life. Also his friends, who were always by his side and supporting him.

For their critics in Erasmus Programme in TU Wien, the author wants to present his gratitude to Prof. Dr. Ardeshir Mahdavi and Dr. Ulrich Pont for their critiques.

Also, special thanks to the crafters of electronic music, its programs and electronic equipment of audio manipulation; dear workers in Ableton Live, NI, Soundtoys, Waves, Fabfilter, Dave Smith Instruments, Moog, Ibanez, Boss, Thermionic Culture, Overstayer Audio and many more who influenced others. You taught me that there are worlds out there to be found.

TABLE OF CONTENTS

LIST OF TABLES

TABLES

LIST OF FIGURES

FIGURES

LIST OF ABBREVIATIONS

PCM Phase Change Material

PV Photo Voltaic

SHS Sensible Heat Storage

TES Thermal Energy Storage

CHAPTER 1

INTRODUCTION

1.1 Problem Statement

Since the mid-20th century, scientists have been observing and explaining global warming and the "*greenhouse effect*". This phenomenon occurs because of the atmosphere trapping heat that is radiated from Earth to space, the main cause for this phenomenon to occur is certain gasses, called the "*greenhouse gasses*" such as water vapor, Carbon Dioxide, Methane, Nitrous oxide, Chlorofluorocarbons (CFCs), etc. The concentrations of greenhouse gases are increased due to energy production processes, and "the clearing of land for agriculture, industry, and other human activities" (*The Causes of Climate Change*, n.d.).

Global warming has impacts on the climate and therefore on natural systems, according to the Intergovernmental Panel on Climate Change (IPCC) 2014 Synthesis Report, it is seen that the influence of humankind on the world's climate system is clear where the greenhouse gas emissions are at their highest in history; and that human and natural systems are impacted by climate change (Pachauri et al., 2014). Increase of carbon dioxide and other man-made emissions into the atmosphere since the late 19th century caused average temperature of the planet's surface to rise about 1.14 °C (Global Climate Change: Evidence, 2008).

According to United Nations Environment Programme (UNEP) statistical data, buildings are responsible for 41% of the world's energy consumption causing 30% of the annual emission of greenhouse gas, and if nothing is done greenhouse gas emissions are expected to increase more than double in the next 20 years (UNEP, 2009). Between 30% and 50% of this energy is used for air-conditioning

systems to ensure buildings' thermal comfort (Noh-Pat, Gijón-Rivera, Xamán, Zavala-Guillén, Aguilar & Rodríguez-Pérez, 2019).

Also the energy demand is expected to increase by 50% in 2050 and cooling demand of the space to multiply by three between 2020 and 2050 (Souayfane, Fardoun & Biwole, 2016). In response to this crisis in the fields of construction and architecture, in order to prevent this increase in related CO2 emissions and energy demand due to buildings need for space heating and cooling, research is being focussed on reducing the energy consumed by buildings (Stritih, Tyagi, Stropnik, Paksoy, Haghighat & Joybari, 2018).

In the field of energy, one of the research topics that attracts attention is *thermal energy storage* (TES) since it has significant effects in energy utilization and provides energy efficiency by reducing the heating and cooling demands of buildings (Gencel, Hekimoglu, Sarı, Ustaoglu, Subasi, Marasli, Erdogmus & Memon, 2022). Applications of solar energy require an efficient thermal storage, for providing a successful solar energy application and, it is dependent on the practice of the energy storage used to a large extent (Khudhair & Farid, 2004). Energy storage reduces the mismatch between supply and demand while improving the energy systems reliability, which plays an important role in energy conservation (Gawande & Wasokar, 2016).

Thermal energy can be stored as sensible heat, latent heat and, thermochemical heat and, TES systems are mainly latent heat storage systems because this type of energy predominates over sensible heat storage (de Abreu, Neto, Aelenei & Silva, 2019). In *sensible heat storage* (SHS), the thermal energy is stored in the material by raising the temperature of a material using its heat capacity; and the amount that can be stored depends on the specific heat of the material, the change of temperature and amount of the storage material. With respect to SHS, water is considered as one of the best among other materials that has the ability to store thermal energy as sensible heat (Gawande & Wasokar, 2016). TES can be applied

to building elements such as walls, floor and roof or to HVAC systems and solar heating units (Kishore, Bianchi, Booten, Vidal & Jackson, 2021).

According to Wi, Yang, Lee, Yun, Park & Kim (2019), "One of the ways to reduce building energy is to actively release or store the thermal energy through phase change materials (PCMs) to use heat energy efficiently" (Wi et al, 2019).

Various articles in the literature about the subject state that the benefits of the PCM envelope include reducing the fluctuations of indoor temperature, reducing the maximum heat flux to indoor environment, increasing the thermal comfort of indoors and energy savings, peak load reduction, and a shift in peak load hours (Jin, Shi, Medina, Shi, Zhou & Zhang, 2017; Kishore et al, 2021). Kishore et al (2021) note that PCM in the building envelope undergoes phase change due to temperature variations that reduces the unwanted effects of outdoor temperature variations on indoor temperature; in this way, it stabilizes the indoor temperature fluctuations, reduces the peak heat flux and therefore provides energy savings by minimizing the use of HVAC.

Also, introduction of PCM can be used to shift the stored energy use to the peak hours which is the period when consumption of energy is at its highest during day (Kishore et al, 2021). Peak hours result in greater CO2 emissions and costs more for electricity because peaking power plants have marginal costs and lower efficiency to fulfill the additional demand than the base load plants (Kishore et al, 2021). According to the authors, prior studies have demonstrated that to minimize the variation in energy demand during peak hours and off-peak hours TES can be used as they store excess energy from available renewable sources during off-peak hours and releases it during peak hours. During off-peak hours storing energy in TES is less expensive as the required energy could be supplied by baseload or renewable energy generation plants and for this purpose, integrating the PCMs into the building envelopes is an easy to implement and cost effective technique which increases the energy storage capacity of the building (Kishore et al, 2021). As other

authors also point out, energy can be gathered and stored during off-peak hours and can be utilized during peak hours (Song, Niu, Mao, Hu & Deng, 2018).

To address the topics discussed above, the subject of this research is to present a new design called the “Heat Pocket” which can be considered as an improved or altered version of a PCM-Trombe Wall with more features included that allow a more flexible way for both product’s design and use scenarios. This study assesses the efficacy of the proposed Heat-Pocket on the indoor temperature changes by performing energy simulation for the system, on a virtual model in the ABAQUS software. The expected result is that the proposed system would work and harvest the solar heat from the sun efficiently and thus satisfy the ASHRAE indoor thermal comfort standards in winter conditions thereby, providing thermal comfort levels inside the building.

1.2 Research Objectives

The main objective of the research was to address the topics discussed in the problem statement and formulate an innovative solution that uses passive heating technology called “Heat Pocket”. The proposed solution for highly glazed facades was to be assessed for its effectiveness in the building interior in terms of establishing the ASHRAE thermal comfort levels, by simulating the model’s thermal behavior during the analysis period and calculating the equilibrium temperature at the end of the analysis.

1.3 Research Questions

In order to design a system that aims to provide heating in winter and cooling in summer by using lightweight materials the following questions were asked :

- What would be the best way to accomplish a passive heating and cooling design for a tall building with highly glazed walls?

- How can the proposed system be designed as a flexible solution rather than a fixed one like the classic Trombe Wall technique?

- How to create a more user-friendly product that is mountable on existing buildings?

- What is the best selection of materials and the best design approach for a dynamic Trombe Wall system?

- How will the proposed system perform under low solar gains and low-temperature conditions?

- What is the best fill rate for the panel to be performing safely and efficiently?

- Would the system satisfy the thermal comfort levels of ASHRAE in harsh winter conditions?

1.4 Methodology

In this research, a virtual model of a glazed envelope building type (for an offices or residences) with a room size of 7.3 m x 5.4 m x 3.5 m was generated. Then, as latent heat storage component, the proposed "Heat Pocket" was integrated into the model behind the glazing. The Heat Pocket is made out of aluminum panels, which are painted with solar selective coating on the exterior facing side for absorbing solar energy and are filled with a specific PCM product to store the solar heat energy.

Multiple heat transfer analyses were performed using ABAQUS software and the system's behaviour in different configurations were investigated. First, three energy analyses were simulated in order to select the best PCM fill rate for the panel by assessing different PCM fill rates of 50%, 75%, 100% using the same energy 3D model described in the Chapter 3. After this phase, the selected PCM fill rate scenario was calculated to observe the indoor air temperature values and the results were assessed if they satisfy the ASHRAE indoor thermal comfort levels.

The location for the analysis model was taken as Van, Turkey, and, the selected month for the analysis to take place was December when the lowest solar radiation input is present, because this design aims to provide thermal energy in the heating months. In the analysis model, $1/3^{rd}$ of the total solar collection area for the panels was used and multiple individual panels were combined into a single big panel to easily perform the heat transfer analysis. Material specifications were collected from various sources to perform the analyses. Natural convection analysis could not be performed due to software limitations however, in the air volumes forced convection node was applied.

1.5 Disposition

Chapter 1 : The introduction chapter of the thesis describes the topics of research problems, objectives, questions and methodology are discussed.

Chapter 2 : This chapter comprises of a literature review that covers the topics of PCM definition, PCM types, important factors for PCM selection given in prior studies, other PCM studies which used software simulations for assessing building energy performance, Trombe Wall definition, Trombe Wall types and ASHRAE thermal comfort levels. Various articles from the literature about the mentioned subjects were compiled and the required data gathered for the basis of the research.

Chapter 3 : This part includes detailed information about the design of the proposed product called the Heat Pocket; software used in the research, the energy analysis model and its boundary conditions, material properties used in the analysis, climate data of Van, Turkey, analysis phases, limitations for the study and the method of the research.

Chapter 4 : This chapter covers the temperature mapping results of the simulation that are taken from multiple points; such as air layers, aluminum box, PCM, etc. The best scenario for PCM fill rate is selected in this chapter and using the selected panel configuration same 3D model was tested to calculate indoor air temperatures

accordingly. Resulting temperature values of the air volumes are discussed and commented upon in relation to their satisfaction in terms of ASHRAE thermal comfort levels.

Chapter 5 : This last chapter covers the conclusion of the study and discusses the analysis limitations due to the used software and gives highlights for further research for the study.

CHAPTER 2

LITERATURE REVIEW

For providing the proposed system a basis to work on, the literature on the subjects of PCM, simulation works of PCM, Trombe wall and ASHRAE indoor thermal comfort standards are studied and summarized below.

2.1 Phase Change Material (PCM)

One of the techniques that can decrease energy consumption is implementing PCM which modulates heat in buildings with its latent heat storage capacity. Solid PCM can absorb large amounts of thermal energy from the environment by melting, then releases the stored energy in the form of latent heat by freezing therefore it becomes solid again (Hagenau & Jradi, 2020). In this way PCM can store energy in smaller volumes while compared with other materials which can generally store only sensible heat energy and therefore, enhancing the thermal storage capacity of the building (Khudhair & Farid, 2004). This could be demonstrated with comparison between sensible heat capacity of concrete which is 1.0 kJ/kg K with the latent heat of a PCM such as CaCl2·6H2O which is 193 kJ/kg (Khudhair & Farid, 2004). Also, PCM has additional advantage, its energy delivery happens in a fairly narrow temperature range (Khudhair & Farid, 2004).

With these characteristics, PCM applications in buildings allow to store more energy in the buildings winter times therefore increasing the heat storage of the building, and in the summer times it allows to absorb heat from the environment thus the excessive temperatures can be decreased by PCM and in the

night time the excess collected heat can be released which makes it possible to reduce the energy demand in buildings in the summer.

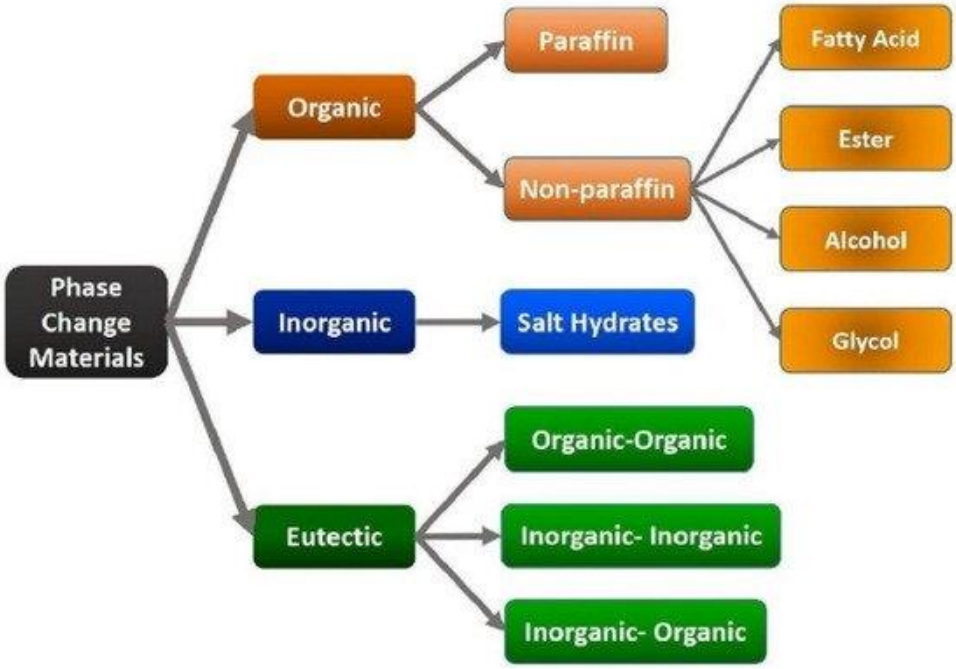

Figure 2.1 PCM Categorization (Barbi, Barbieri, Marinelli, Rimini, Merchiori, Bottarelli & Montorsi, 2022)

2.1.1 PCM Types

Tyagi & Buddhi (2007) categorized and gathered the PCMs from various sources which are shown in Table 2.1, Table 2.2 . There are various types (Figure 2.1) which are categorized as Organic PCMs, Inorganic PCMs, Eutectics (Barbi et al, 2022). These categories are explained in the following sections:

i. Organic PCMs

Organic materials are categorized as paraffin and non-paraffin. This type has the properties of self-nucleation (crystallization), congruent melting, and non-

corrosiveness to the container material (Table 2.1) (Tyagi & Buddhi, 2007). Paraffins have high latent heat per unit weight, negligible supercooling, a wide range of melting temperatures and are non-corrosive; however, as negative properties they have low density, high cost, low thermal conductivity and flammability (Ghoneim, Klein & Duffle, 1991). Additionally, they are not compatible with the plastic container, have low vapor pressure in the melted form and are stable below 500°C (Gawande & Wasokar, 2016). Paraffins are non-polar materials and are not subject to hydrogen bonding with other polar components of the building materials (Farid & Sheriff, 2016). They consist of a mixture of straight chain alkanes CH3 – (CH2) – CH3 and "the crystallization of the (CH3)-chain release a large amount of latent heat increase with chain length" (Gawande & Wasokar, 2016).

ii. Inorganic PCMs

Inorganic PCMs are classified as salt hydrate and metallic (Tyagi & Buddhi, 2007). This type has a high latent heat per unit mass and it is non-flammable, as well as being cheaper than the organic PCM type; but it has a disadvantage which is its tendency to decomposition and supercooling that can affect its phase change property (Table 2.1) (Tyagi & Buddhi, 2007). Hydrated salts have high thermal conductivity(~0.5 W/m °C), high volumetric storage density (~350 MJ/m3) and, moderate costs compared to paraffin waxes with few exceptions which makes them attractive materials however, high storage density of hydrated salts is difficult to maintain and decreases with cycling (Farid & Sheriff, 2016). To use hydrated salts safely microencapsulation is used as particles with a polymer shell as a coating which eliminates the leakage, the diffusion of the liquid or volatile components' evaporation over time and also reduces flammability (Farid & Sheriff, 2016). According to Madessa (2014), prior studies represent the use of inorganic salt hydrates has a lower environment impact than paraffin.

Table 2.1 Organic & Inorganic substances with potential use as PCM (Tyagi & Buddhi, 2007)

Table 1
Organic substances with potential use as PCM

Compound	Melting point (°C)	Heat of fusion (kJ/kg)
Butyl stearate	19	140
Paraffin C_{16}–C_{18}	20–22	152
Capric–Lauric acid	21	143
Dimethyl sabacate	21	120
Polyglycol E 600	22	127.2
Paraffin C_{13}–C_{24}	22–24	189
(34% Mistiric acid + 66% Capric acid)	24	147.7
1-Dodecanol	26	200
Paraffin C_{18} (45–55%)	28	244
Vinyl stearate	27–29	122
Capric acid	32	152.7

Table 2
Inorganic substances with potential use as PCM

Compound	Melting point (°C)	Heat of fusion (kJ/kg)
$KF \cdot 4H_2O$	18.5	231
$Mn(No_3)_2 \cdot 6H_2O$	25.8	125.9
$CaCl_2 \cdot 6H_2O$	29	190.8
$LiNO_3 \cdot 3H_2O$	30	296
$Na_2SO_4 \cdot 10H_2O$	32	251

iii. Eutectics

Eutectics have a minimum-melting composition consisting of two or more components, they melt and freeze congruently which during crystallization forms a mixture of crystals (Tyagi & Buddhi, 2007). Eutectic material has the advantage of a high volumetric thermal storage density, sharp melting temperature and, its properties can be adjusted to match specific, however it has a high cost and low heat of fusion per unit weight (Table 2.2) (Li, Wu, Wang, Liu & Arıcı, 2020).

Table 2.2 Inorganic eutectics with potential use as PCM and Commercial PCMs available in the International market (Tyagi & Buddhi, 2007)

Table 3
Inorganic eutectics with potential use as PCM

Compound	Melting temperature (°C)	Heat of fusion (kJ/kg)
66.6% $CaCl_2 \cdot 6H_2O + 33.3\%$ $Mgcl_2 \cdot 6H_2O$	25	127
48% $CaCl_2 + 4.3\%$ NaCl + 0.4% KCl + 47.3% H_2O	26.8	188
47% $Ca(NO_3)_2 \cdot 4H_2O + 53\%$ $Mg(NO_3)_2 \cdot 6H_2O$	30	136
60% $Na(CH_3COO) \cdot 3H_2O + 40\%$ $CO(NH_2)_2$	30	200.5

Table 4
Commercial PCMs available in the International market

PCM name	Type of product	Melting point (°C)	Heat of fusion (kJ/kg)	Source
RT 20	Paraffin	22	172	Rubitherm GmBH
Climsel C23	Salt hydrate	23	148	Climator
ClimselC24	Salt hydrate	24	216	Climator
RT 26	Paraffin	25	131	Rubitherm GmBH
RT 25	Paraffin	26	232	Rubitherm GmBH
STL 27	Salt hydrate	27	213	Mitsubishi chemical
S27	Salt hydrate	27	207	Cristopia
RT 30	Paraffin	28	206	Rubitherm GmBH
RT 27	Paraffin	28	179	Rubitherm GmBH
TH 29	Salt hydrate	29	188	TEAP
Climsel C32	Salt hydrate	32	212	Climator
RT32	Paraffin	31	130	Rubitherm GmBH

2.1.2 PCM Applications

There are two PCM application types in buildings, first one is active PCM application where the PCM modules can be applied to the building HVAC system which is used as an active energy storage component and, second one is the passive PCM application where the PCM is implemented into building envelope as an interdependent layer or in a mix with another material (Hagenau & Jradi , 2020). The use of PCMs in passive systems can be regarded as more promising because of its simplicity while comparing it with the PCMs in active system which have heat transfer problems (Peippo, Kauranen & Lund, 1991). Since to the proposed system, presented in this thesis is a passive solution type, an overview of widely used passive PCM applications in building design are gathered in this section.

i. PCM Wallboard

This technique is low-cost, applicable in new construction as well as for retrofitting, and it provides a structure for PCM and micro-encapsulation is the most suitable when using gypsum boards which prevents leakage of PCM (Vautherot, Maréchal & Farid, 2015). In the work of Kedl & Stovall (1989), paraffin wax is applied into a plasterboard's pores with immersion process to increase the heat storage capacity which shows that it has the potential to achieve higher storage capacity than adding pellets that are wax filled during its manufacturing process.

ii. PCM Shutter

In this concept, PCM is injected into the curtain plates, and this shading unit is placed inside the building that faces the exterior side (Figure 2.2). In the daytime, the plates absorb solar energy and collect heat. Silva, Vicente, Rodrigues, Samagaio & Cardoso (2015) researched in winter conditions comparing indoor temperatures between two separate rooms, one had PCM Filled blades in the shutters and the other one was with normal hollow blades, both facing outside. The results showed that the maximum indoor air temperature of the room with PCM (37.2 °C) was 16.6 °C lower than without PCM shutter (53.8 °C) which indicates the introduction of PCM shutter units indoors can provide energy efficiency in buildings in hot regions (Silva et al, 2015).

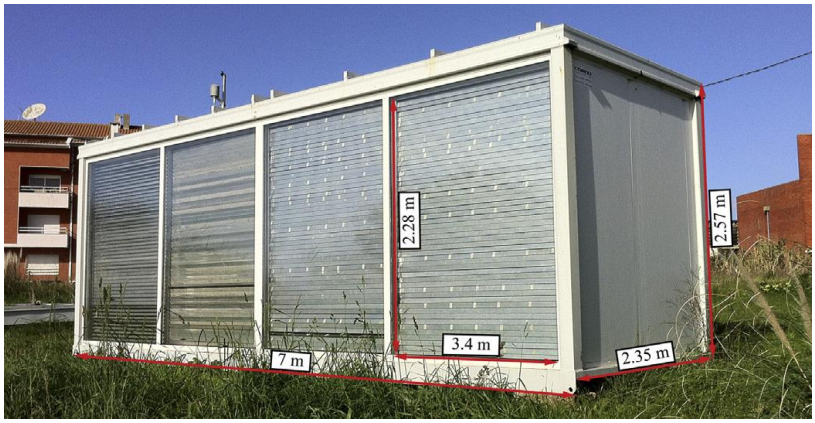

Figure 2.2 PCM Shutter located in Aveiro, Portugal (Silva et al, 2015)

iii. PCM Applied Glazing Units

Glazing Units have very low thermal resistance in comparison with other building elements therefore they are in a position of critical role in terms of energy consumption and thermal comfort (Li et al., 2020). In terms of heat loss, glazing units are responsible for 10-25% heat loss of buildings in cold climates (Ismail et al., 2020). In order to compensate for this, various methods have been proposed to increase the thermal resistance of glazing units "such as optimizing the spacing between panes of the glazing unit, filling the enclosure between glass panes with a participating gas or aerogel, applying multilayer glazing, and coating glass surfaces with low emissivity materials" (Li et al., 2020).

Another approach to improve the thermal performance of a glazing unit is to increase its thermal energy storage capacity by stacking it with water or PCM which reduces the energy demand, provides thermal comfort for the user, while extending the equipment lifetime (Figure 2.3) and, in this way, visible radiation is allowed to enter the building addition to that a part of solar energy is absorbed (Li et al., 2020). Due to available PCMs' low solar transmittance during the melting phase, used PCM products in the double-glazed windows can reduce the daylight factor, therefore, use of nano-treated PCMs should be considered to improve PCM transparency (Madessa, 2014).

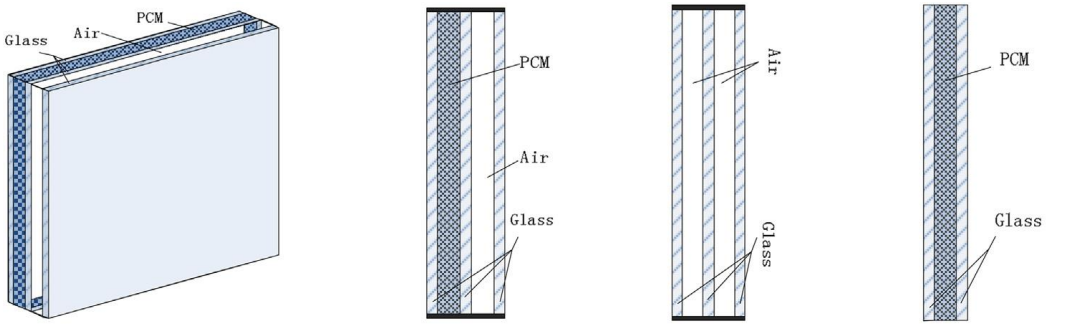

(a) Structure of the TW+PCM (b) Structure of the TW (c) Structure of the DW+PCM

Figure 2.3 Structure comparison of three different kinds of windows, TW(Triple Pane Window), DW (Double Pane Window) (Li et al., 2016)

iv. PCM Building Blocks

Building blocks or other building materials that encapsulate PCM are used in buildings for increasing the thermal inertia without the associated mass (Tyagi & Buddhi, 2007). It has been stated that cement masonry blocks with macro-encapsulating PCM increases the system performance over an equivalent volume of concrete (Collier & Grimmer, 1979).

v. Floor Heating

This technique is for reducing and shifting peak loads to night time when the electricity costs are lower (Tyagi & Buddhi, 2007). In their research, Farid and Chen used paraffin wax as PCM (30mm) which is placed between the flooring and the electrical underfloor heating system that is located below (Figure 2.4) with the application of the PCM, proposed computer simulation results show that the heat output could be increased from 30W/m2 to 75W/m2 (Farid & Chen, 1999).

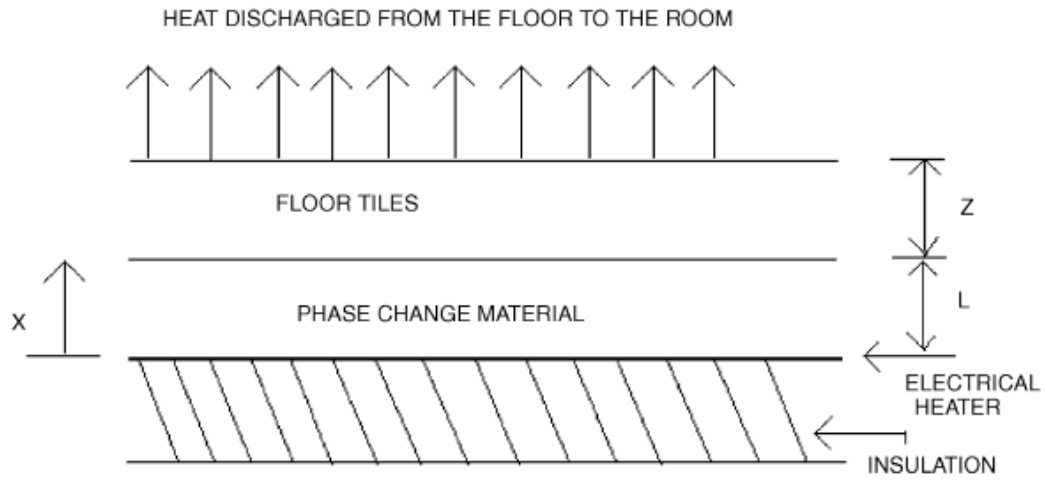

Figure 2.4 Section of the PCM applied electrical floor heating system used for computer simulation (Farid & Chen, 1999)

2.1.3 Optimal PCM Properties for PCM Application in Buildings

It is stated by Khudhair & Farid (2004) that not all PCMs can be used for thermal storage; a PCM that is ideal for use should satisfy the following features: high thermal conductivity to minimize thermal gradients, high heat of fusion, high specific heat, high density, long-term reliability during repeated cycling, non-toxic, non-corrosive, low vapor pressure and, should be exhibiting little or no supercooling. In building applications, PCMs should have a phase transition temperature range that is closer to the human comfort temperature (Khudhair & Farid, 2004). It is also mentioned, in the areas with high temperature fluctuations, PCMs do not have high efficiency (Sharifi, Shaikh & Sakulich, 2017).

2.1.4 Important Factors for PCM Applications in Buildings

When implementing PCM to a building envelope as a passive heat storage technique, there are various factors should be considered for a successful operation, it should be mentioned that in some cases, wrong use of PCM ends up with more energy consumption (Hagenau & Jradi, 2020). Following factors are investigated by gathering various studies in the literature.

i. Location

There are various studies that are trying to find the optimum location for the PCM in the wall however, it can be understood that the optimum location for the PCM alters as the system's different parameters alter. Therefore, some researches investigating this parameter are gathered to give an insight in the following section.

Childs and Stovall (2012) found that the performance of the PCM which is placed closer to the interior was very sensitive to the indoor temperature set point changes and concentrating PCM near the outer surface of the wall was not a good strategy for reducing cooling electricity demand.

Jin, Medina & Zhang (2016) found that the optimal PCM layer location in the wall was influenced by the exterior conditions and thermal properties of the PCM. They found when the PCM thickness, PCM heat of fusion or PCM melting temperature increase, optimal PCM location is shifted toward the exterior surface and, when the interior surface temperature was increased the optimal PCM location moved closer to the interior surface (Jin, Medina & Zhang, 2016).

Investigating prior research, Kishore et al state that the location of PCM in the wall depends on the thermophysical properties of the PCM, and the interior and exterior conditions for the optimum performance (Kishore, Bianchi, Booten,Vidal & Jackson, 2020).

In the work of Jin et al. which used the climate data of Nanjing, China , with the phase change temperature range of 26°C-28°C, the optimum PCM location for spring, summer, autumn, winter and whole year were 8/16L, 2/16L, 5/16L, 8/16L, 4/16L respectively (the wall section is divided to 16 parts and, L is the distance ratio from the internal gypsum layer to the exterior layer) . However, both the optimal phase change temperature ranges and their corresponding optimal PCM location change depended on the season, i.e. spring, summer, autumn, winter; which were 24°C-26°C with 0/16L, 26°C-28°C with 2/16, 24°C-26°C with 1/16L, 20°C-22°C with 3/16L, 24°C-26°C with 0/16L (Jin, Shi, Medina, Shi, Zhou & Zhang, 2017).

When the PCM is located near the exterior side, a larger amount of it gets melted which allows it to perform better in reducing the heat transfer (Li, Al-Rashed, Rostamzadeh, Kalbasi, Shahsavar & Afrand, 2019).

Use of PCM towards exterior side prevented heat from entering the room in summer and use of PCM in the internal side prevented heat from dissipating outside in the winter also, PCM Trombe wall in their research stored the low-temperature risidual heat in the room and released it when the room was cold improving thermal comfort (Li, Zhu, Hu, Lei & Deng, 2019).

ii. Phase Change Temperature and Set-Point Temperature

It can be understood that phase change temperature and set-point temperature are correlated to the energy savings, and optimal PCM product selection can be changed depending on the climate as the following works indicate.

It is shown that the PCM melting temperature should be close to the indoor air temperature which reduces heat transfer from PCM wall to the room (Xia, Meng, Chen, Liu, Chen, Lu & Chen, 2017).

In another work, Li found the optimum phase change temperature for PCM was 30°C when used towards exterior side and, 18°C when used on the interior side (Li, Zhu, Hu, Lei & Deng, 2019).

Childs and Stovall (2012) found that altering the cooling setpoint from its value while using PCM can reduce the effectiveness of the PCM significantly.

In the work of Peippo et al the authors have concluded that a melting temperature 1°C to 3°C above average room temperature is a good selection for optimal diurnal temperature in their research regarding the PCM wall concept for direct gains in a passive solar house (Peippo, Kauranen & Lund, 1991).

iii. Latent Heat

In some studies, excess latent heat gave rises to negative conclusions; according to Sharma & Rai (2020), in their simulation as the latent heat capacity of the PCM layer increases from 60 kJ/kg to 240 kJ/kg, it is found that it increases the envelope heat gain, which deteriorates the PCM performance. In the work of Xia et al (2017), the latent heat of PCM had no effect on the heat flux of the inner surface however, it effects significantly the phase change time.

iv. Thermal Conductivity

According to Li et al, the thermal conductivity of the PCM plays the most significant role in selecting the appropriate PCM; the amount of heat transferred to

the room decreases as the conductivity decreases (Li, Al-Rashed, Rostamzadeh, Kalbasi, Shahsavar & Afrand, 2019).

v. Thickness of the PCM Layer

For a solar wall, the optimal thickness is related to climate, latitude, and, heat loss (Hordeski ,2011) and the thickness of the solar wall mass is one parameter which contributes to the effectiveness of the solar wall (Saadatian et al, 2012). It should be mentioned that thickness is a parameter that can be changed for finding the optimum value for a particular design but the optimum value changes as the other parameters change. According to work of the building simulation analysis for Delhi, India by Sharma, the PCM-enhanced building envelope can reduce the summer heat gain by 12.6% to 36.2% depending on the PCM layer thickness and position (Sharma & Rai, 2020).

vi. Convection

Natural convection is the dominant mechanism for the heat transfer inside the buildings, when exterior surface recieves incident solar radiation and the heat is conducted to the interior surface, the adjacent thin air layer inside warms up and rising causing convective heat transfer (Dascalaki, Santamouris, Balaras & Asimakopoulos, 1994).

The result of the simulation done by Kylili & Fokaides (2015) indicated that in the PCM melting process, a zone of convection is quickly formed inside the liquid PCM that grows, and the top side of PCM melts faster compared to the lower side. It is stated that natural convection within the liquid PCM should be taken into consideration, which can directly affect the thermal performance and effectiveness of the PCM (Kylili & Fokaides, 2015).

vii. Insulation

The study by Guohui suggests that solar walls need proper insulation which is necessary to maximise the ventilation rate during summer (Guohui, 1998).

In the work of Zrikem & Bilgen, the authors studied a composite solar wall which consisted of a thermal mass wall, a glass panel, an insulation layer with vents between the thermal mass and insulation (Zrikem & Bilgen, 1987). The results showed that insulated composite wall displays better performance than the classic solar wall in the cold and cloudy weather and the researchers found that the insulation applied to composite wall can reduce the thickness of the solar wall (Zrikem & Bilgen, 1987).

In the study of Stazi et al, a super-insulated solar wall and, a normal solar wall were compared for heating and cooling seasonal energy demands (Stazi et al., 2011). The results show that for heating energy, super-insulated solar wall was using 16.21 kWh/m2, normal solar wall was using 58.33 kWh/m2 and, for cooling energy, super-insulated solar wall was 23.31 kWh/m2, normal solar wall was using 9.19 kWh/m2; which shows the setup of super-insulated solar wall saves up energy in winter, however, it uses more in summer compared to normal solar wall (Stazi et al., 2011). According to the work of Hagenau & Jradi (2020), it is found that more insulated envelopes enhances PCM performance.

2.1.5 PCM Application Techniques to Building Materials

There are different techniques for implementing the PCM to building materials according to Madessa (2014) as follows:

- In the immersion technique by immersing the building material into melted PCM, and with the help of the capillary action, the material absorbs the PCM.
- Direct incorporation is done by directly adding PCM into the construction material during the production process of the material, for an example PCM

powder and gypsum powder are mixed for manufacturing the PCM-gypsum board.

- The encapsulation methods have two forms, microencapsulation and macroencapsuation. In the technique of microencapsulaion, the particles or the droplets of PCM are coated with a continuous film of polymeric material for producing capsules.
- In the macroencapsulation technique, the PCM is put into large containers such as bags or tubes, and these containers are used in the building (Madessa, 2014).

It should be mentioned that, low thermal conductivity and macroencapsulation can end up with ineffective heat transfer; as shown in a previous experiment using macro-encapsulation, due to the poor conductivity feature of the PCM during the solidification process, the PCM first solidified around the edges, which prevented the heat transfer (Khudhair & Farid, 2004).

2.1.6 PCM Works from Various Studies

The following tables summarize studies conducted around the world on using different types of PCM applications, their testing locations, set point temperatures PCM parameters, testing equipment and/or software, and their outcomes (Table 2.3).

Table 2.3 Various PCM Studies from Literature

Source & Testing Location	PCM Application Type	Used PCM Parameters	Set Point(s) Temperature	Subject(s) of Research and Results	Simulation Software or Experiment
1 - Hagenau, M., & Jradi, M. (2020). Dynamic Modeling and performance evaluation of Building Envelope Enhanced with phase change material under Danish conditions. Odense, Denmark	PCM layer is applied to the building envelope.	17 different PCMs are investigated, Check the source for more information	Heating = 21°C Cooling = 24°C (different set points are also measured)	Different scenarios are analyzed and compared with the baseline case on savings, check the source for more information, - Selecting Best Performing PCM Product ; CrodaTherm 24 ; 11.98 GJ Total Saving - Optimum PCM Thickness ; 40 mm ; 13 GJ Total Saving - Best Location for PCM Layer ; Internal Wall Side ; 22.79 GJ Total Saving - PCM Performance and Insulation Relationship ; It is found that more insulated envelopes enhances PCM performance - Different Set-Point Temperatures with different PCM ; SP24E performs best with 10.45 GJ Total Savings in condition of cooling set point is 22 and the heating set point is 25. - Different Locations in Denmark and possible savings with application of PCM to envelope ; Base case(Odense 2018) ; 10.6 GJ Total Saving (34%) Odense 2004-2018 average ; 9.37 GJ Total Saving (36%) Copenhagen 2004-2018 average ; 8.75 GJ Total Saving (32%) Aalborg 2004-2018 average ; 8.51 GJ Total Saving (33%) Esbjerg 2004-2018 average ; 8.39 GJ Total Saving (32%)	Sketchup OpenStudio EnergyPlus
2 - Derradji, L., Errebai, F. B., & Amara, M. (2017). Effect of PCM in improving the thermal comfort in buildings. Algiers, Algeria	PCM is applied to the gypsum panels as interior Plaster. Total volume of Panels consists 30% PCM and 70% plaster.	Plaster Coating: Thickness = 15 mm Thermal Conductivity = 1.2 (W/m. °C) Density = 1800 (kg/m3) Specific Heat Capacity = 840 (J/kg. °C)	Not mentioned	PCM applied plaster is compared with the baseline case for indoor temperature fluctuations, - Office indoor temperature ; increased by 4 in the winter period and decreased by 7 in the summer - Energy savings on heating and cooling ; 25% savings	TRNSYS 17 with TYPE 204

Table 2.3 (continues)

Source & Testing Location	PCM Application Type	Used PCM Parameters	Set Point(s) Temperature	Subject(s) of Research and Results	Simulation Software or Experiment
3 - Vautherot, M., Maréchal, F., & Farid, M. M. (2015). Analysis of energy requirements versus comfort levels for the integration of phase change materials in buildings. Auckland City, New Zealand	PCM is applied to the Gypsum board.	5 different PCMs are investigated, which are PCM that have phase change temperatures of 18-23°C; 19-24°C; 20-25°C; 21-26°C; 22-27°C Thickness = 13 mm Latent Heat Storage = 33.5 (kJ/kg) Thermal Conductivity = 0.25 (W/m K) Density = 600 (kg/m3) Specific Heat Capacity = 1089 (J/kg K)	Heating = Goes from 20°C to 24°C with 1°C increments, for analyzing different cases Cooling = 25°C At night time however, the bedrooms are set to 18°C after 10 P.M.	The rooms are heated and cooled to meet the set-points with HVAC system monitoring energy use, - Best Scenario of PCM Phase Change Temperature and Heating Set Point for energy savings PCM 20-25°C 20°C is selected as a good scenario by researchers - Best Scenario for Increasing Comfort Hours ; PCM 20-25°C 24°C - Best Scenario for Comfort and Savings ; "Combining efficiency and comfort indicators, it turns out to be that the PCM with a phase change temperature range of 21–26 °C is the best regardless of the heating set point" - As the heating set point increased, more energy is used, it is less likely PCM integration will bring energy savings - "Regardless of the heating set point, the cooling load decreases sharply when the melting temperature range of the PCM increases" - "A general observation is that most of the savings occur from cooling and only little saving comes from Heating"	Design Builder EnergyPlus
4 - Poulad, E., Fung, A., & Naylor, D. (2011). Effects of convective heat transfer coefficient on the ability of PCM to reduce building energy demand. Toronto, Canada	PCM layer is applied to the building envelope.	Different thickness of same PCM are analyzed ; 1 mm PCM & 10 mm PCM Solidification Point = 22°C Melting Point = 23°C Density = 800 (kg/m3) Specific Heat Capacity = 1.6 (J/g K)	Heating (Winter) = 21°C Cooling (Summer) = 24°C Initial Temperature = 20°C Indoor Temperature (fixed) = 40°C	No PCM, 1 mm PCM and 10 mm PCM were analyzed while changing the h-value(convective heat transfer coeffecient) 0.5 to 10 (W/m2K) that which transfers heat between PCM and indoor air, - generally in the condition when the thickness of PCM increased, it is seen that it reduces energy demand except for h = 0.5 (W/m2K) - it is emphasized that due to more happening of more phase transitions in winter, PCM brings more energy saving in winter than summer - in summer it decreases the energy demand and keeps the zone temperature inside the set points (21°C- 24°C), in winter it results in more energy demand to keep the zone temperature higher than 21°C.	TRNSYS 16 with TYPE 204

Source & Testing Location	PCM Application Type	Used PCM Parameters	Set Point(s) Temperature	Subject(s) of Research and Results	Simulation Software or Experiment
5 - de Gracia, A., Navarro, L., Castell, A., Ruiz-Pardo, Á., Alvárez, S., & Cabeza, L. F. (2013). Experimental study of a ventilated facade with PCM during winter period.	Macro encapsulated PCM layer applied into Ventilated Air Chamber in a Double Skin Façade system.	Salthydrate SP-22 PCM used. Melting Point = 22°C	Set Points differ for the purposes of experiment, check the source for more İnformation	Two setup are compared, a baseline case which only has no double skin façade or PCM but the test equipment, second one has both double skin façade with test equipment. Three operational modes were assessed, Free Floating(no HVAC system, discharge happens at 12:00 to 18:00 in severe winter condition and between 18:00 to 23:00 in mild winter condition), Controlled Temperature(the indoor temperature of the cubicle is fixed with heat pumps while measuring energy consumption of the heat pumps, different set point temperatures analyzed), Demand Profile(where the HVAC systems were controlled by a timer in the mild season, which allows them to operate with the façade from 18:00 to 23:00, using mechanical and natural ventilation modes) check source for more information, - Use of ventilated façade with PCM, increased the temperature from 9 to 18 everyday in the severe winter conditions - Under severe winter conditions the system shows significant energy savings between 19% and 26% depending on the HVAC set point (21◦C and 19◦C respectively) and researchers state that "those values would have been even higher if a thermal control system would have been programmed depending on the energy demand, production and storage" - Use of mechanical ventilation is not necessary unless there is a requirement for a fast heating supply - Use of SP-22 did not provide any benefits as its solidification temperature is very low as 20◦C, regaring this researchers tell that the better utilization of PCM with its latent heat storage would be providing more higher thermal benefits - Controlled Temperature(CT) Mechanically Ventilated(MV) Severe Winter(SW) 21(Set Point) ; 19.1% savings - Controlled Temperature(CT) Mechanically Ventilated(MV) Severe Winter(SW) 19(Set Point) ; 26.1% savings - Controlled Temperature(CT) Naturally Ventilated(NV) Severe Winter(SW) 21(Set Point) ; 18.7% savings - Controlled Temperature(CT) Mechanically Ventilated(MV) Mild Winter(SW) 19(Set Point) ; 25.2% savings - Demand Profile(DP) Mechanically Ventilated(MV) Mild Winter(MW) 19(Set Point) ; 26.1% savings - Demand Profile(DP) Naturally Ventilated(NV) Mild Winter(MW) 19(Set Point) ; 86.2% savings - Demand Profile(DP) Trombe Wall(TW) Mild Winter(MW) 18(Set Point) ; 75,6% savings	Experiment

Table 2.3 (continues)

Source & Testing Location	PCM Application Type	Used PCM Parameters	Set Point(s) Temperature	Subject(s) of Research and Results	Simulation Software or Experiment
6 – Kishore, R. A., Bianchi, M. V. A., Booten, C., Vidal, J., & Jackson, R. (2020). Optimizing PCM-integrated walls for potential energy savings in U.S. buildings. United States, Phoenix United States, Las Vegas United States, Baltimore United States, Denver United States, Billings	PCM layer is placed between two layers of İnsulation.	Thickness(solid,liquid) = 6.4 mm Thermal Conductivity(solid) = 0.3 (W/m-K) Density(solid) = 887 (kg/m3) Specific Heat(solid) = 2.750 (kJ/kg-K) Latent heat(solid) = 100 (kJ/kg) U-value(solid) = 46.9 (W/m2-K) Thermal Conductivity(liquid) = 0.1 (W/m-K) Density(liquid) = 898 (kg/m3) Specific Heat(liquid) = 1.848 (kJ/kg-K) Latent heat(liquid) = 100 (kJ/kg) U-value(liquid) = 15.6 (W/m2-K) Phase transition temperature varies 12°C-32°C For the analysis and,its range is fixed to 4°C	Interior temperature varies in the range of 22°C-24°C	Studied combinatory effects of PCM-integrated wall in various climatic conditions, PCM transition temperature, PCM location in the wall on the energy savings in five U.S. cities, - "If the exterior temperature always remains higher than the interior temperature,no ambient cooling takes place, making the PCM ineffective in reducing the heat gains through the wall. Likewise, in heating season, if the exterior temperature is always lower than the interior temperature, there is no scope for ambient heating, making PCM ineffective in reducing the heat losses through the wall." - Some cases show adding PCM is not always beneficial for reducing heat gains, PCMs could be advantageos for a portion of the year while it could be disadvantageous during other times - Swings of diurnal temperature should be favorable to permit free ambient cooling/heating - PCM transition temperature should be optimized to enhance the utilization of the PCM - PCM location in the wall section should be optimized to make the PCM interact with the exterior and the interior - Use of PCM-integrated envelope is not beneficial in all climates but it is advantageous mostly in moderate climates	COMSOL Multiphysics version 5.4

Table 2.3 (continues)

Table 2.3 (continues)

Source & Testing Location	PCM Application Type	Used PCM Parameters	Set Point(s) Temperature	Subject(s) of Research and Results	Simulation Software or Experiment
7 – Onishi, J., Soeda, H., & Mizuno, M. (2001). Numerical study on a low energy architecture based upon distributed heat storage system.	PCM-concrete mix is used as a Trombe Wall in the cases with the following numbers 2-3-4-6-7.	Inorganic PCM was used; Concrete consists 25% PCM Different cases applied PCM with different phase transition temperature which are Case 1 = no PCM Case 2 = 30-31°C Case 3 = 35-36°C Case 4 = 20-21°C Case 5 = no PCM Case 6 = 30-31°C Case 7 = 35-36°C	Set Point Temperature = 18°C	Hybrid system including electrical heater and a passive system is measured with 7 different cases, - PCM systems have a lower cost and they consume less energy on fine days than the ones that with no PCM systems. - Optimum PCM phase change temperature for the system could be between 30-35 according to researchers. - The cost and energy consumption is nearly the same in both systems on a cloudy day which indicates PCM does not work on cloudy days efficiently.	CFD Simulation By Onishi, Takeya & Mizuno, 1995
8 – Jin, X., Shi, D., Medina, M. A., Shi, X., Zhou, X., & Zhang, X. (2017). Optimal location of PCM layer in building walls under Nanjing (China) weather conditions. Nanjing, China	PCM layer is applied to the building envelope.	Phase Change Temperature = 26-28°C Thickness = 5 mm Thermal Conductivity = 1.8 (solid) (W/mK) Thermal Conductivity = 2.4 (liquid) (W/mK) Density = 880 (solid) (kg/m3) Density = 760 (liquid) (kg/m3) Specific Heat Capacity = 2 (J/gK) Heat of Fusion = 179 (J/g)	Set Point Temperature = 26°C	The optimum location of PCM in the wall section is analysed using PCM with a range of phase temperature of 26-28°C, - The optimum location for PCM layer in the wall section = Spring (8/16 L), Summer (2/16 L), Autumn (5/16 L), Winter (8/16 L), Whole Year (4/16 L) - The most effective season = Summer - The optimum phase change temperatures and the related optimum location = Spring (24-26°C – 0/16 L), Summer (26-28°C – 2/16 L), Autumn (24-26°C – 1/16 L), Winter (20-22°C – 3/16 L), Whole Year (24-26°C – 0/16 L) - Optimal PCM phase change temperature and the optimal PCM location in a whole year were more suitable for spring and autumn, not summer or winter. - According to researchers if the conditions,the outdoor environment,the indoor environment, thermal properties of the wall materails were different, the results may be different. For example, in the case of optimal PCM location for summer condition was 2/16 L and the thickness of the PCM was 5 mm, when the PCM amount is increased, the layer should be moving to the outdoor environment.	-

Table 2.3 (continues)

Source & Testing Location	PCM Application Type	Used PCM Parameters	Set Point(s) Temperature	Subject(s) of Research and Results	Simulation Software or Experiment
9 – Kishore, R. A., Bianchi, M. V. A., Booten, C., Vidal, J., & Jackson, R. (2021). Parametric and sensitivity analysis of a PCM-integrated wall for optimal thermal load modulation in lightweight buildings. Phoenix, United States Las Vegas, United States Nevada, United States Arizona, United States	PCM layer is applied to the building envelope.	The Phase Change Temperature Range = 23-26°C Thickness Range = 5-20 mm Distance Range from interior side = 0-0.3 L (L means total width of the wall cavity) Latent Heat Range = 10 – 100 (kJ/kg) Specific Heat Range= 200-2000 (solid) (J/kg-K) Specific Heat Range= 200-2000 (liquid) (J/kg-K) Thermal Conductivity Range = 0.1- 0.7(solid) (W/m-K) Mass Density Range = 250-1000 (kg/m3) Transition Range = 4-16 °C	Initial Temperature = 23°C Interior Temperature = a sinusoidal variation from 22°C at 8:00 to 24°C at 20:00	For a south-facing wall cooling loads analyzed only while changing the parameters, location of the PCM in the wall section, transition temperature of the PCM, thickness, latent heat capacity, transition temperature range of the PCM, specific heat capacity of the PCM, mass density, thermal conductivity, - Thermal load modulation was the highest when PCM was located nearest to the interior of the building.This setup reduces the heat gain during the peak period, but it does increase the total daily heat gain - The load modulation and total heat gain reduce as the PCM layer moves away from the interior to exterior. - Placement of the PCM at a 10% cavity width from the interior side results with a peak period heat gain reduction of 67% in Phoenix and 75% in Las Vegas with no increase in the total heat gain - With PCM transition temperature of 24-25°C, the maximum thermal load modulation occured in both Phoenix and Las Vegas - 67% reduction in the peak period heat gain was calculated in Phoenix with a mean transition temperature of 25°C with no increase in the total heat gain - 75% reduction in the peak period heat gain was calculated in Las Vegas with a mean transition temperature of 24°C with no increase in the total heat gain - It is found that with an increase in PCM thickness, the heat gain during the peak period decreases, but the total heat gain increases - The mass density and the PCM latent heat were found to have a strong relationship with thermal load modulation. The peak period heat gain reduces with the increase in the latent heat or mass density, but there was a dimishing return - There is a negative relation with thermal load modulation and PCM transition temperature range. With an increase in transition range, the peak period heat gain was increased gradually - The latent heat capacity of a PCM is usually much higher than the specific heat capacity; therefore, on the thermal performace of the PCM in buildings, the specific heat has no major influence - It is found that the strongest parameter affecting the thermal load modulation was the PCM transition temperature which is followed by, PCM location and PCM thickness. After that PCM latent heat and density were found to be having the next order of priority followed by the transition temperature range. PCM thermal conductivity and PCM specific heat showed no impact.	COMSOL Multiphysics version 5.5

Table 2.3 (continues)

Source & Testing Location	PCM Application Type	Used PCM Parameters	Set Point(s) Temperature	Subject(s) of Research and Results	Simulation Software or Experiment
10 – Peippo, K., Kauranen, P., & Lund, P. D. (1991). A multicomponent PCM wall optimized for passive solar heating. Helsinki, Finland Madison, United States	PCM impregnated plasterboard was used.	Thickness = Applied to 13 mm thick plasterboard Eutectic Point = 21.4 °C Specific Density = 950 (kg/m3) Latent Heat(PCM-Gypsum Board)=46 (kJ/kg) Latent Heat(PCM) = 152 (kJ/kg) Thermal Conductivity = 0.2 (W/m °C) Specific Heat Capacity = 1200 (kJ/kg)	Two scenarios are assessed, Minimum Energy Approach, Set Point allows a temperature swing between 18°C-26°C Maximum Comfort Approach, Set Point allows a narrower temperature swing between 19°C-21°C	PCM-Gypsum panels were analyzed with 2 scenarios using capric-myristic acid compound as PCM, - PCM wall reduces the heating demand by 6% in Helsinki and 15% in Madison - Energy savings are slightly larger in the maximum energy approach - The performance of the storage is significantly effected by the climatic conditions as is evident in Madison simulation - Less insulation results with less energy savings - The insolation level is important for heat storage techniques in buildings	FHOUSE Code Based on NBSLD Program

2.2 Trombe Walls

A classic Trombe Wall is a passive heating system for buildings which is made of a high mass wall (generally concrete) and its exterior side is painted black and then applied with a glazing layer while leaving an air gap in between (Figure 2.5). The reason why the wall is painted black is to increase the absorption of the incoming solar energy (Agrawal & Tiwari, 2011). The inventor of the classical Trombe Wall was Edward Morse who is an American engineer that patented his design in 1881 (Agrawal & Tiwari, 2011).

The main function of both techniques is to absorb direct and diffused solar rays, convert them to heat energy during the day, then transfer the energy to the interior by conduction or convection at night. For this purpose, high heat storage capacity materials such as bricks, concrete stone, and adobe are used generally, and the air gap between the glass and the wall ranges from 3 cm to 6 cm (Saadatian, Sopian, Lim, Asim & Sulaiman, 2012). Depending on the location in the world, the sun-facing side changes as in the northern hemisphere it is the south-facing façade that provides high solar exposure and for the southern hemisphere, the north-facing façade is selected for the solar Trombe wall setup.

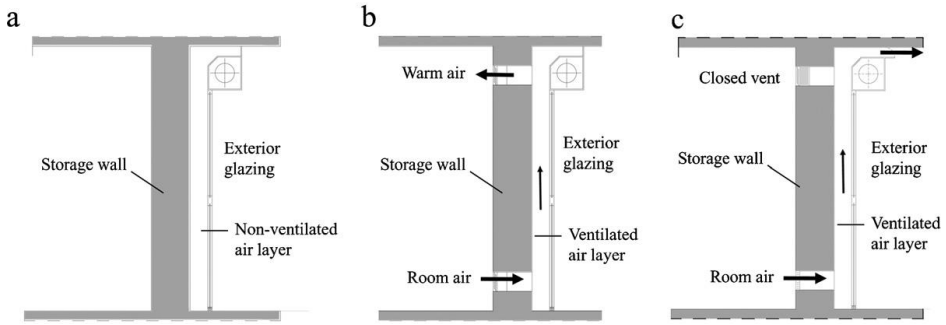

Figure 2.5 Operating schemes: non-ventilated solar wall (a); Trombe wall in winter mode with air thermo-circulation (b); Trombe wall in summer mode with cross ventilation(c) (Stazi, Mastrucci & Perna, 2012)

2.2.1 Zigzag Trombe Wall

Zigzag Trombe Wall consists of three sections, while one section faces south, the other two sections are formed as an inward V-shaped wall (Figure 2.6, Figure 2.7), mainly in one of the sections of the V-shaped wall, a window that is facing southeast provides light and heat in the morning cold, and the other part collects and stores heat for the cold night hours (Saadatian et al, 2012). This technique aims to reduce the excessive heat gain and glare on sunny days to avoid overheating during summer days, this design also consists of an exterior overhang (Saadatian et al, 2012).

Figure 2.6 Zigzag Trombe Wall , Residential structure built near Asheville, North Carolina (Sokol, 2008)

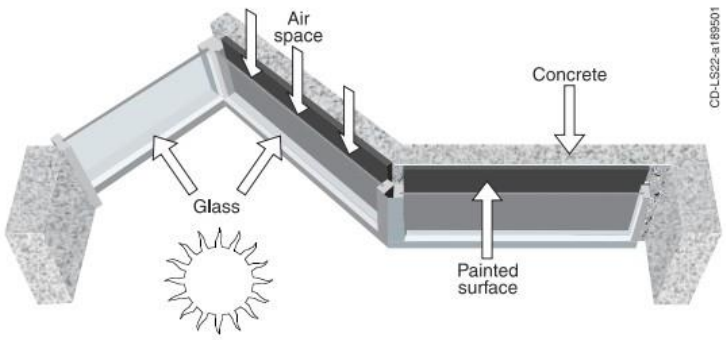

Figure 2.7 Section of Zigzag Trombe wall proposed by NREL, NREL Visitors Center, Denver, Colorado (NREL, n.d.)

2.2.2 Water Trombe Wall

Water Trombe Wall (Figure 2.8) utilizes water instead of a masonry heat storage unit, which is more beneficial as the surface temperature of the water does not rise as high as that of masonry and in this way, less heat is reflected back to the glazing (Hordeski, 2002) (Saadatian et al., 2012). In this type of setup, to increase the absorption of solar radiation, the exterior facing side of the wall is darkened and additionally, the glass layer is insulated in the case of harsh cold climates (Saadatian et al, 2012).

The water wall can be used for both heating and cooling purposes and it is mentioned that the specific heat of the water (0.999 cal/gram°C (Engineering ToolBox, (n.d.)) is higher than any other building material which makes this even more effective, however it is hard to contain comparing with masonry that's why it is not appreciated as much as a classic Trombe wall (Saadatian et al., 2012).

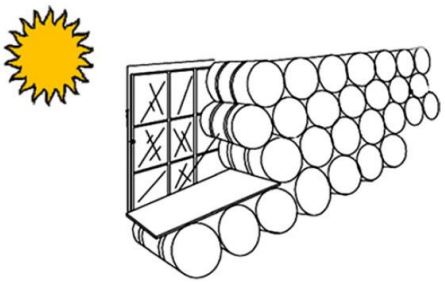

Figure 2.8 A sketch of Solar Water Wall, the containers of water are in front of the glazing (Saadatian et al, 2012)

2.2.3 Solar Transwall

A Transwall is a transparent modular water wall (Figure 2.9) (Garg & Prakash, 2000). It is built on a metal frame that holds a water container made from glass and a semi-transparent absorbing plate that is placed between walls. Such a semitransparent plate absorbs 80% of the solar energy and transmits the rest inside; on the other hand, this unit requires adding gelling and bio-inhibiting agents for

increasing the viscosity and preventing the microorganisms to grow in the water (Saadatian et al., 2012).

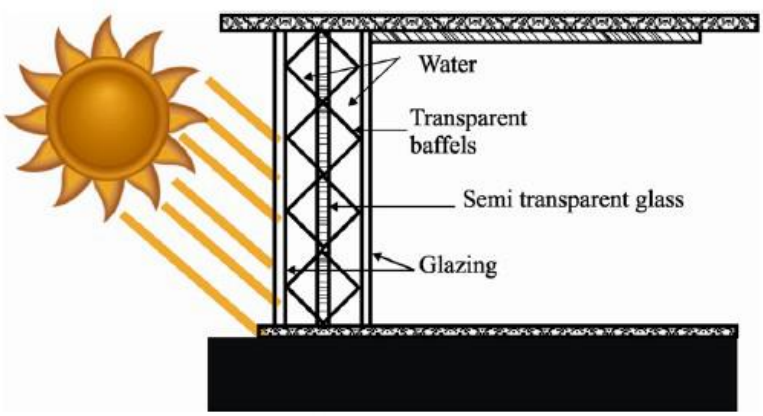

Figure 2.9 Section of a Solar Transwall (Saadatian et al, 2012)

2.2.4 Solar Hybrid Wall

Unlike the Trombe wall which is generally aimed to be used in cold climate conditions, Solar Hybrid Wall (Figure 2.10) is an evaporative cooling wall that acts like a solar wall in the winter and provides cooling in the summer (Melero, Morgado, Neila, et al, 2011). With an external thermal insulation blind which avoids any direct solar gain and the special ceramic material used in the wall can absorb significant amounts of water thus, in hot weather conditions, ceramic is wetted with a water nozzle which allows the Trombe wall to act as an evaporative cooling unit (Melero et al, 2011).

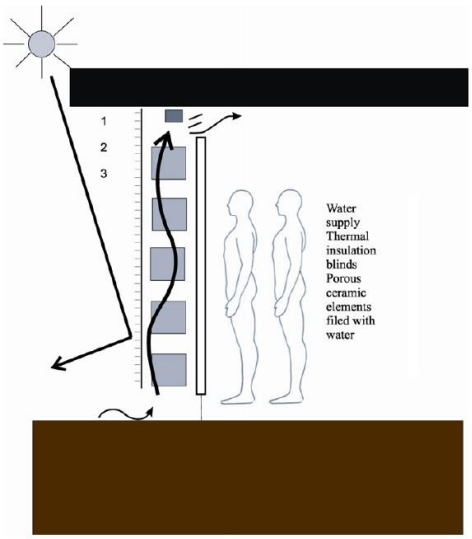

Figure 2.10 Solar Hybrid Wall. (Melero et al ,2011)

2.2.5 Trombe Wall with PCM

This kind of Trombe Wall is considered to be a new type, which accompanies a phase change material (PCM) such as “eutectic salts or salt hydrates” to enhance efficiency (Saadatian et al., 2012). The introduction of PCM to Trombe Walls allows it to be lighter and smaller in volume than a thick massive wall which increases the building’s dead loads (Cabeza, Castello, Nogue, et al, 2007) (Zalewski, Joulin, Lassue, Dutil & Rousse, 2012). Bourdeau indicates that a 3.5 cm PCM wall can perform similarly to a 15 cm concrete wall (Bourdeau, 1980).

It has been proven that the utilization of PCM has benefits for energy consumption reduction in buildings (Onishi et al.,2001). Results of experiments show that latent heat storage applied solar wall is more efficient than a concrete wall (Bourdeau, 1980).

2.2.6 Composite Trombe Wall

The composite Trombe wall consists of different layers, such as “a semi-transparent cover, a thermal mass heating wall, a closed cavity, a ventilated air cavity, and an insulating panel” (Figure 2.11) (Saadatian et al., 2012). This type of wall helps with two deficiencies of Trombe walls which are loss of heat during cloudy winter days and undesired heat inputs during hot weather (Zhai et al., 2011). As the light passes through the glazing the storage wall gets heated, and the collected heat is transferred to the interior by convection occurring in the ventilation channel and conduction from the wall (Saadatian et al., 2012).

In this method, users can adjust the heating by controlling the flow of air into the ventilation channel and the thermal resistance of the solar wall is extremely high due to insulation in the wall and ventilation channel (Saadatian et al., 2012). One downside of this combination is that it needs a mechanism for reversing the thermo-circulation that happens when the storage wall becomes colder than the interior ambient temperature (Zalewski et al., 2012) which can be solved by placing a plastic film in the vent that functions as a thermal diode (Zalewski et al., 1997).

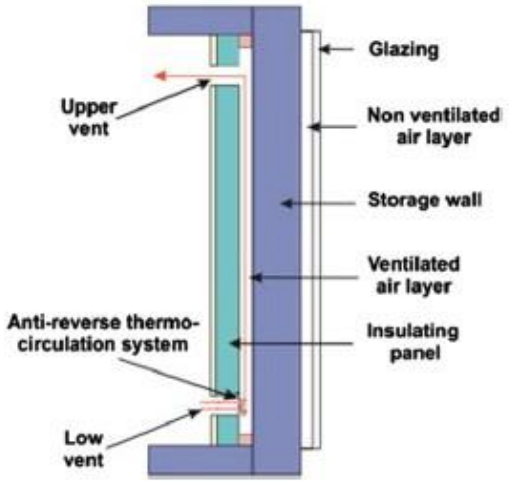

Figure 2.11 Composite Trombe Wall (Zalewski et al., 2012)

2.2.7 Fluidised Trombe Wall

Fluidised Trombe Wall is like a classic Trombe Wall but the exterior gap between the wall and the glazing unit is filled with low density highly absorbent fluid (Figure 2.12) (Sadineni, Madala & Boehm, 2011) (Sayigh, 1991) (Tunç & Uysal, 1991). A fan blows air into the exterior gap where the solar energy is gained by the absorptive fluid which heats the air and leads it into the room (Saadatian et al., 2012). Two filters are placed which are located at the top and bottom of the air channel, which helps to prevent the entering of the fluidised particles into the room (Sadineni et al., 2011).

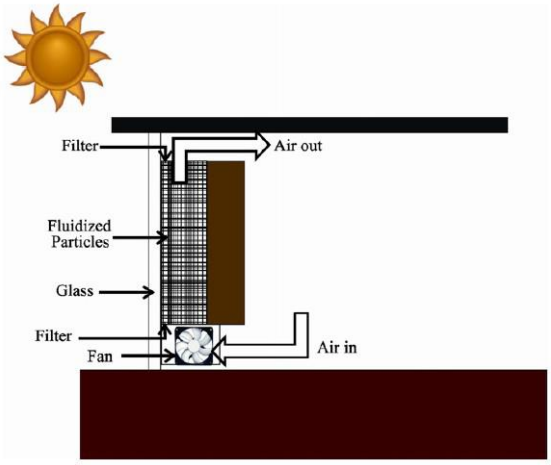

Figure 2.12 Fluidised Trombe Wall (Sadineni et al., 2011)

2.2.8 Photovoltaic Trombe Wall

In the PV-Trombe Wall technology, photovoltaic panels(PV) are placed in the glazing units' exterior face and they convert solar radiation into heat (Figure 2.13) (Sun, Ji, Luo & He, 2011). Interior cool air is drawn in from the lower vent to the exterior gap and gets heated, therefore, moving upwards through the upper vent, carrying heat into the interior (Saadatian et al., 2012). As a downside, a study

reveals that the installation of photo voltaic panels over the glazing decreases the thermal performance by up to 17% due to its obstruction of penetrating the sun's rays into the thermal mass wall (Sun et al., 2011).

Figure 2.13 PV Trombe Wall, a hot box constructed on the roof-top of an office building located at 37.86 N latitude (Sun et al., 2011)

2.3 ASHRAE Thermal Comfort Standards

Indoor thermal comfort is an important aspect of building design which can cause the buildings to increase their energy demand to stabilize the temperature in a suitable range for occupant comfort. For maintaining human comfort, the related temperature ranges are stated in the documents of ASHRAE (American Society of Heating, Refrigerating and Air-Conditioning Engineers). According to ASHRAE Standard 55-2017, Thermal Environmental Conditions for Human Occupancy states that for maintaining thermal comfort at homes, indoor temperature could range approximately between 67 °F - 82 °F (19.44 °C – 27.7 °C) (ASHRAE, 2017).

It is also essential that HVAC systems must be able to maintain a humidity ratio of at or below 0.012 and it is been recommended that "relative humidity in occupied spaces be controlled to less than 65% to reduce the likelihood of conditions that can lead to microbial growth"(ASHRAE, 2016). Another aspect is airflow which contributes to indoor comfort. ASHRAE recommends in its Standard

62.2-2016 that homes should receive 0.35 air changes per hour but not less than 15 cubic feet of air per minute (cfm) per person, this data is given for presenting the required air circulation which may contribute effects on the convective heat transfer due to airflow.

CHAPTER 3

MATERIAL AND METHODOLOGY

3.1 Material of Research

This research was carried out to validate the innovative PCM integrated Trombe wall designed by the author called the “ISICEBİ” or the “Heat Pocket”, which is described in section 3.1.1. The other material were the software used to model, render and simulate the energy produced by the Heat Pocket system; as well as the types of material selected for the design and simulations.

3.1.1 Design of the Heat Pocket

The proposed technology named “ISICEBİ” or the “Heat Pocket”, advances the static characteristics of the Trombe Wall in a way that allows flexible dynamic use. Its function is to convert the solar energy to heat and store it in the PCM which aims to improve the buildings’ energy absorption efficiency and energy storage capacity.

PCM provides greater heat capacity as Bourdeau indicates that a 3.5 cm PCM wall can perform similarly to a 15 cm concrete wall (Bourdeau, 1980). This means using PCM as heat capacity material, the unit weight will be much less than using a concrete wall instead to store the energy which allows to use this technique in already existing buildings due its lightweight potential.

The Heat Pocket achieves this by using individual aluminum box panels which contain PCM and their exterior-looking face is applied with a solar energy selective black coating finish that converts the solar energy to heat efficiently (Figure 3.1). These boxes with a size of 4 cm x 38 cm x 280 cm are installed into a sliding

profile which is located behind the building's glass façade envelope. Sliding profiles allow panels to be stored in the hot summer season when the panels are not needed or to be planted to collect solar energy in the cold winter times (Figure 3.2, Figure 3.3).

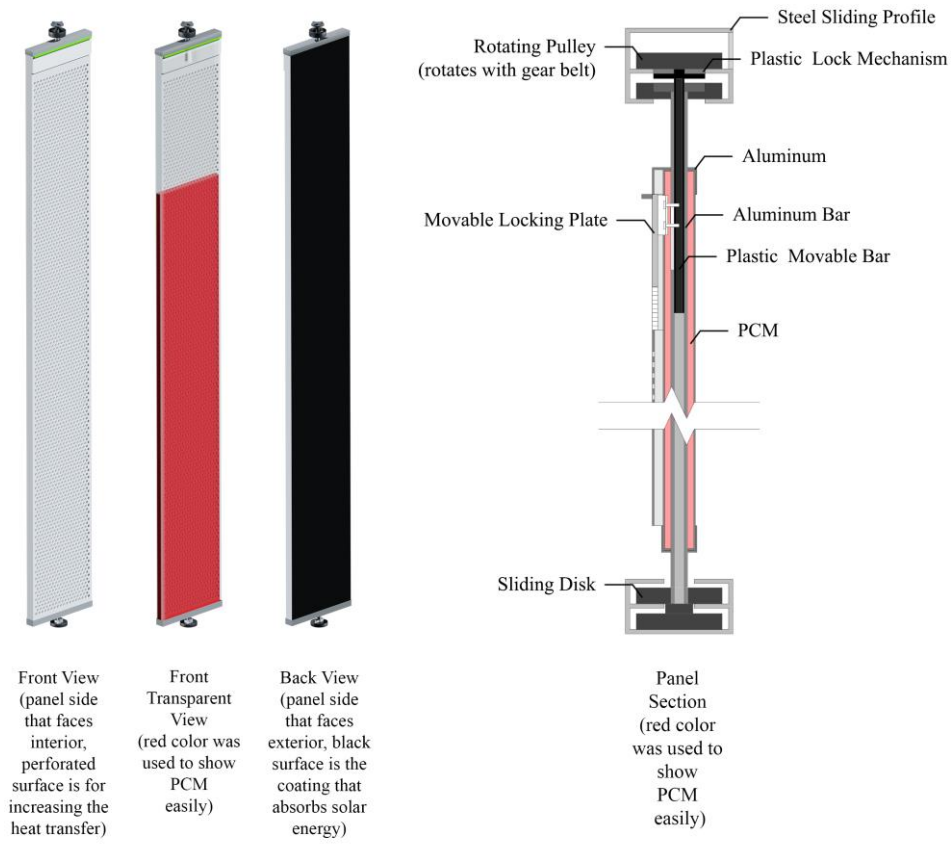

Figure 3.1 Panel Views (Front, Front Transparent, Back), Panel Section (PCM is shown with red to emphasize clearly in both images)

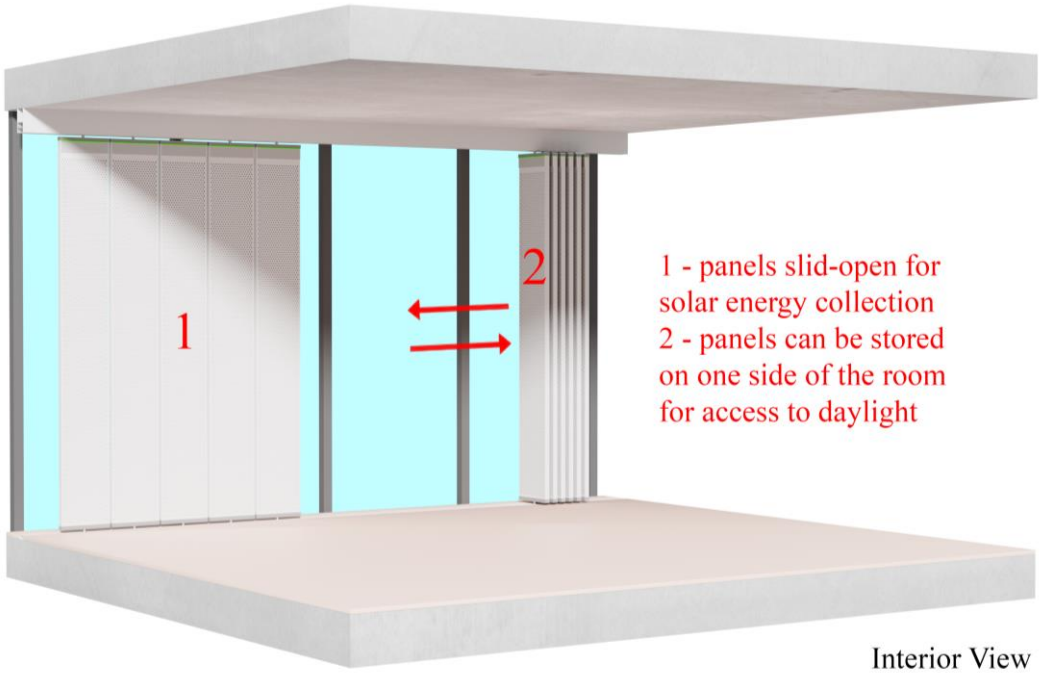

Figure 3.2 Heat Pocket System Interior View

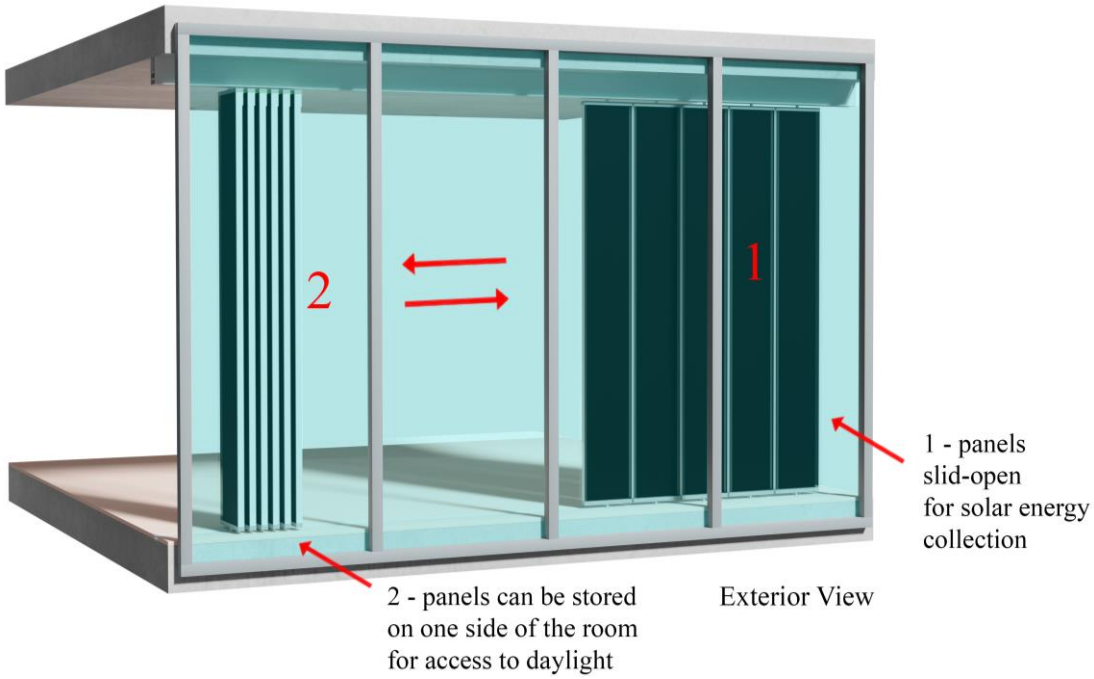

Figure 3.3 Heat Pocket Exterior View

With this design, the time lag of heating in the classic Trombe Wall is decreased by increasing conduction with aluminum material so it can raise the temperature of the room faster, which is desired in cold winter mornings. A layer of perforated aluminum is added to the interior-looking face of the panel that increases the heat interaction surface area and thus, increasing convective heat transfer between the surface of aluminum and air (Figure 3.4)

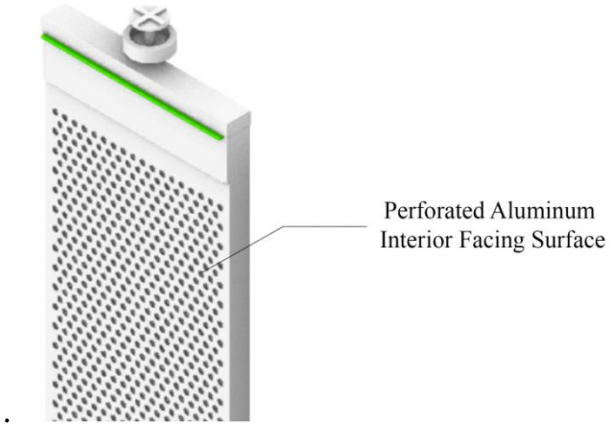

Figure 3.4 Panel Perforated Aluminum Surface

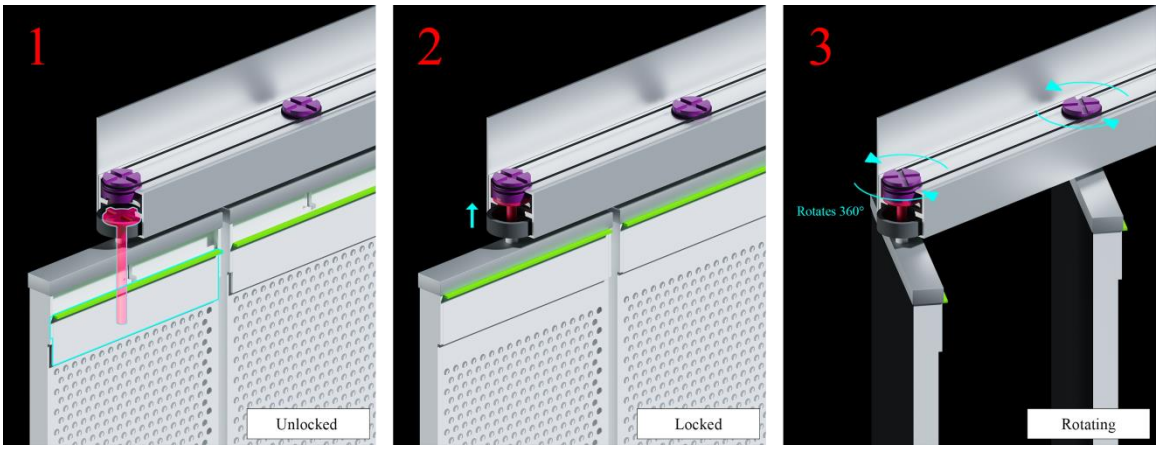

Figure 3.5 Suntracking Mechanism

The system is designed in a fashion that includes a rotational mechanism, which allows the boxes to rotate and track the sun's location for perpendicular exposure with the help of a motor and pivot rotating pulleys (Figure 3.5). In this study, due to the fact that it should be performed in a real-life situation, sun-tracking and stationary versions could not be compared to evaluate their effect on the efficiency of performance. This approach should be seen as a future development phase.

3.1.2 Modeling, Drafting Rendering and Energy Simulation Softwares

There are various software used for different purposes in the preparation of the article which are described in the following paragraphs.

For modeling the test room, Rhino software was used. Briefly, Rhino is a 3D modelling software that provides complex 3D modeling tools and is used by industries such as architecture and product design. In Rhino users "can create, edit, analyze, document, render, animate, and translate NURBS curves, surfaces and solids, subdivision geometry(SubD), point clouds and polygon meshes". It is accurate and compatible with other design and analysis software. It was chosen because of its export capabilities to ABAQUS. The objects that are modeled in the Rhino Software were exported as Standard for the Exchange of Product Data(STEP) file format with a file extension of *.stp and then imported to ABAQUS component by component.

(https://www.rhino3d.com/features/)

In order to perform the energy analysis and calculate the system's effect on indoor temperature changes, ABAQUS software was used. ABAQUS software is an analysis program that utilizes finite element analysis and has wide use in various engineering fields such as automotive, aerospace, and industrial product industries. It is both a modeling and analysis software for mechanical components and assemblies, which visualizes analysis in the 3D space over time. It can calculate multi-physics, such as "coupled acoustic-structural, piezoelectric, and structural-

pore capabilities". ABAQUS was chosen because it can perform the required calculations for conduction, forced convection, and latent heat (it can perform the crystallization and melting aspect) in the 3D space. To perform the analysis more easily, the real-life model was simplified which is going to be discussed in the following section.

(https://www.pdc.kth.se/software/software/Abaqus/index_general.html)

For rendering purposes in the real-life images of the system, Blender was used. Blender is an open source, free 3D creation software. It is used for rendering representative images.

For drafting the plan and section drawings, AutoCAD was used which is a commercial computer-aided design (CAD) software. AutoCAD is used in the field of architecture, engineering, graphic design, and other professions.

3.1.3 Selection of the Used PCM

The important properties for selecting the right PCM for the panel are:

- the selected PCM melting temperature should be close to the room setpoint temperature for PCM to act as a temperature resistance point

- the selected PCM's melting temperature should be a little bit higher because the system will load with solar energy. This criterion can be regarded as analogous to a battery, if the PCM melting temperature range is lower than the operational temperature (20°C), at the operational temperature (20°C) the PCM is already melted which is similar to the battery is already full and you can't load it with energy. But if the melting temperature range is higher than the operational temperature (20°C), the PCM is not loaded with energy and its solid meaning the battery is at 0% in terms of latent heat, then you can load it with solar energy.

In terms of satisfying the properties described above, Crodatherm 24W Paraffin PCM is selected is due to its melting temperature range (22°C - 24°C) for

the article's scenario of a room with a temperature of 20°C. Also, Crodatherm 24W was not corrosive with the use of the aluminum box and sustainable as it can withstand many melting crystallization phases.

3.1.4 Climate Data for the Analysis

The location of the test unit was selected as Van because it has very cold winter months and it snows in winter. The energy model aims to perform in the worst case scenario and the data for the harshest conditions for both temperature and the lowest solar radiation was used; and according to the work of Uçkan (2018) this is December month for Van. Weather data for Van is showns in Figure 3.6, Figure 3.7, and Figure 3.8 as temperature values, amount of snow and global solar radiation.

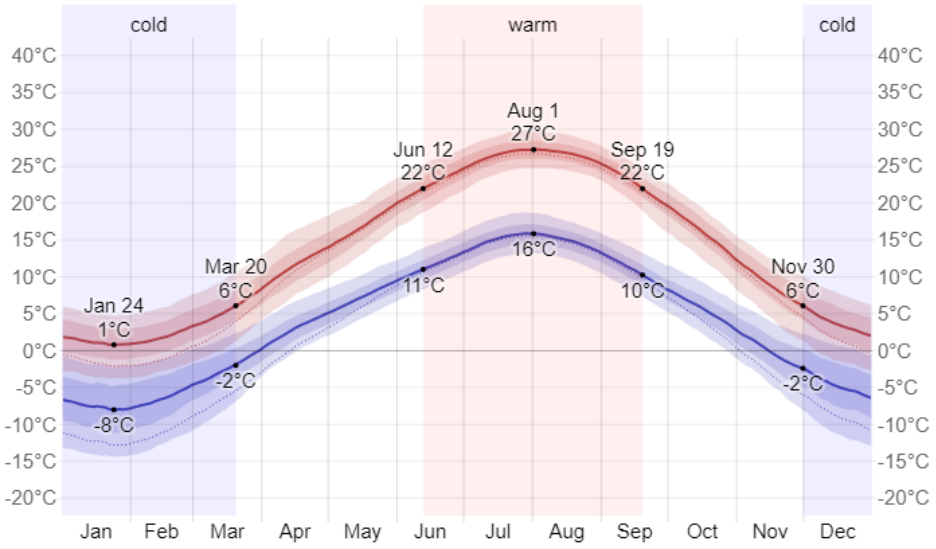

Figure 3.6 Average High and Low Temperature in Van (Weather Spark)

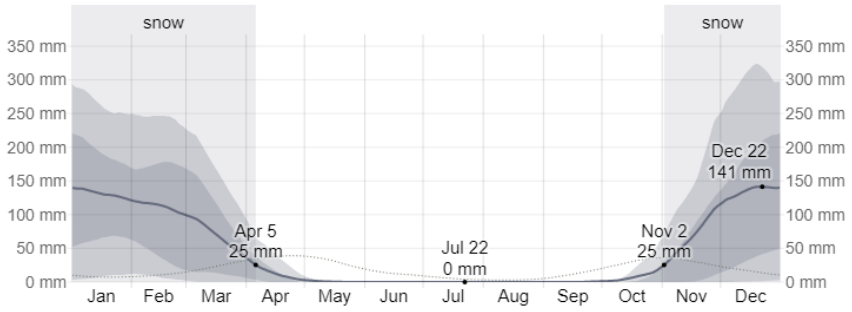

Figure 3.7 Average Monthly Snowfall in Van (Weather Spark)

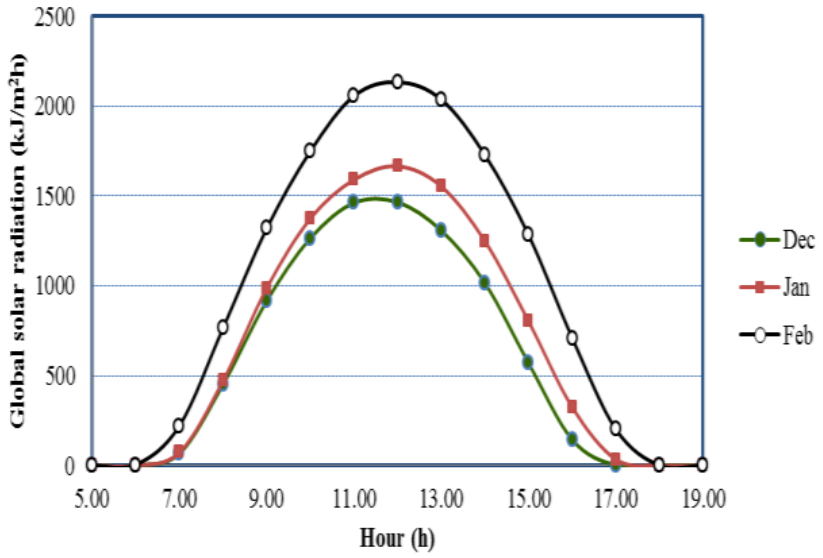

Figure 3.8 Variation of annual average clearness index at situation Van between the years of 1993 and 2007 (Uçkan, 2018)

3.2 Research Methodology

In this research, the proposed ISICEBİ system was tested to select the best PCM fill rate scenario for the panel in relation to the proposed 3D energy model and tested to observe if the selected panel scenario satisfies the ASHRAE indoor thermal comfort levels in this energy model during the analysis time.

At first, the Heat Pocket system for the novel PCM-integrated Trombe wall was designed; as described in section 3.1.1. The drawings were produced in Autocad and the 3D components of the system were designed and tested with Rhino for the actual product. After this, the panel model was modeled in a simplified way and multiple simplified panels were merged into a big one panel for the energy analysis which was described in Section 3.2.1.

Then the indoor space of the case study room of a highly glazed building was modeled in Rhino including the big simplified merged panel placed into the room; this model was exported as *.stp file format component by component and imported to ABAQUS.

Then the input data of material properties for conductivity, specific heat, density, latent heat, emissivity, thickness, solar energy transmittance, PCM melting temperature, and PCM flashpoint was collected from various sources on the web and related product sheets. After this, climate data of Van, Turkey was collected from the literature and Weather Spark. The hourly solar radiation power that was measured for Van, Turkey (Uçkan, 2018) was converted from kJ/m2h unit to W/m2, and the resulting power was multiplied by 63% which is the LandVac glass solar transmission rate and then this value was multiplied with coating absorption rate. The resulting power was used as a tabular graph in ABAQUS and then applied to the exterior facing surface of the panel during the transient-analysis step.

There are two phases of study which were in order. In both phases, the same 3D room model was used, except in phase 1 the PCM fill rate of the panel was changed.

In phase 1, three analyses were performed to select the best scenario PCM fill rate for the panel between the following fill rates 50%,75%, and 100%. In the 50% filled panel scenario, it was expected that the temperature on the panel would rise due to lack of PCM, which may result in hazardous situations for the system which made this phase necessary to investigate.

In phase 2, the best PCM fill rate scenario for the panel was used to observe if the system satisfies ASHRAE thermal comfort standards during the day cycle. To achieve this, in the 3D model total indoor air volume was divided into 7 individual 1 m deep air volume sections (Figure 3.13). In this way, the temperature data collection of different points was possible which was used to measure and evaluate whether or not the data collection point temperature values were in the range of ASHRAE thermal comfort levels. In addition to that, the equilibrium temperature for the energy analysis was calculated to observe if the system gains or loses energy when one day of simulation time was over.

3.2.1 Energy Analysis Model

First, the system is modeled in a simplified way using Rhino software. For the scenario, it is expected that all of the panels are not going to be utilized by the users for solar collection in daily life so the users can benefit from sunlight also, therefore as an assumption, only the $1/3^{rd}$ area of the total panel collection area was used for solar collection and the other $2/3^{rd}$ left for daylight use. Normally, the unit is consisting of individual slideable aluminum panels. However, in order to simulate how the total façade unit behaves easily, all of the individual panels ($1/3^{rd}$) are merged into a simplified single big panel that is filled with PCM (Figure 3.9, Figure 3.10). This gives a panel size of 152 cm x 280 cm x 4 cm for solar heat collection (Figure 3.9).

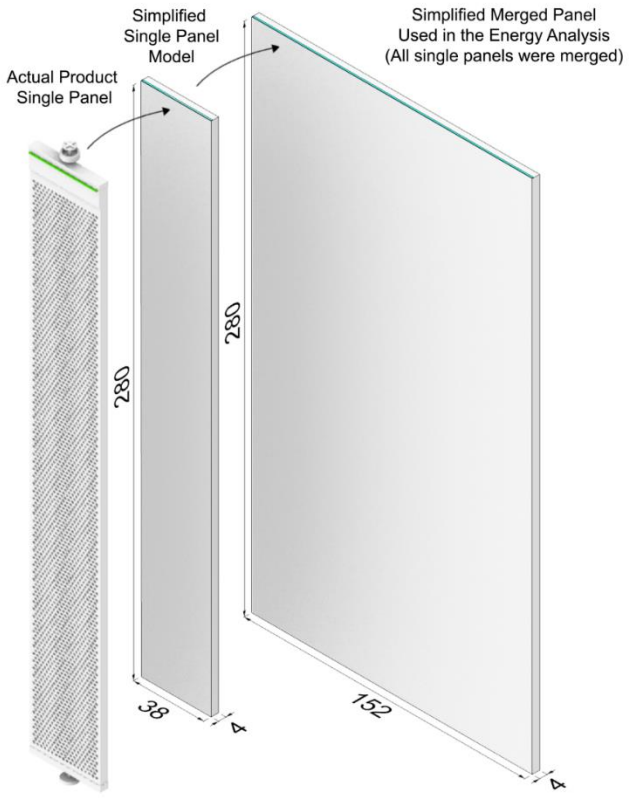

Figure 3.9 Simplification of the Product for Energy Analysis

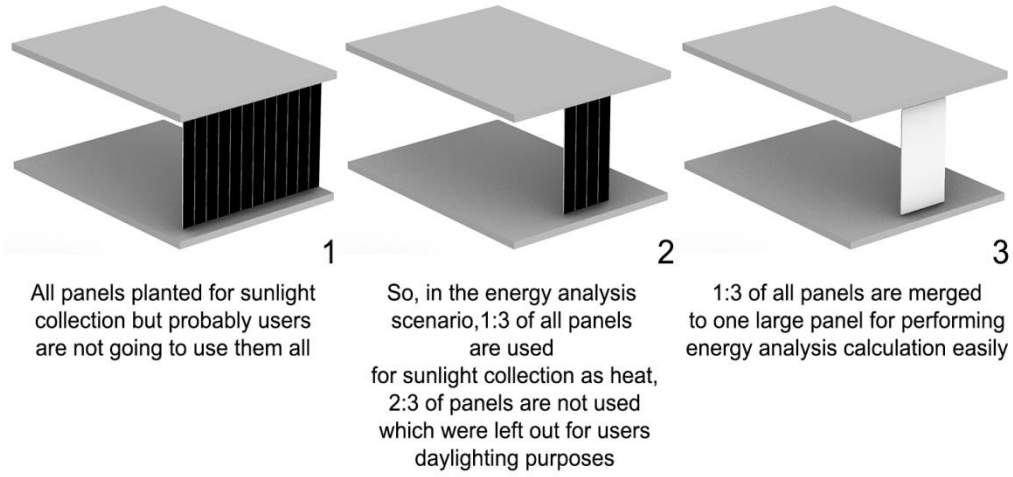

Figure 3.10 Merging of Simplified Panels in the Scenario for the Energy Analysis

The perforated surface in the representation model increases the contact surface between the panel and air which was also added in the analysis model however, it is not perforated and it is modeled as a flat surface in the analysis (Figure 3.11). Also, details such as the bars, steel railing structures, flooring, and ceiling finishes are removed in the analysis in order to simplify the model for faster simulations. Therefore, the energy analysis model only consists of concrete flooring, concrete ceiling, indoor air, heat pocket panel, and glass façade (Figure 3.13).

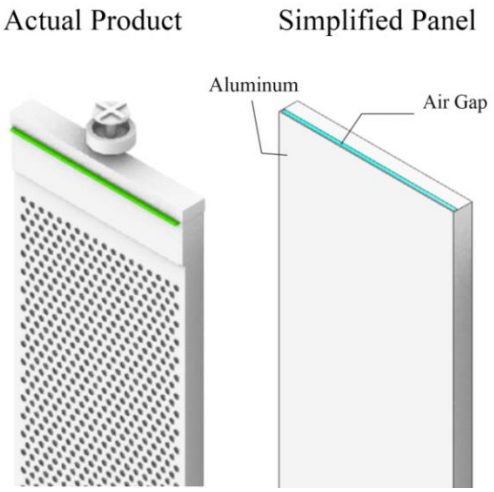

Figure 3.11 Actual Product and Simplified Panel are shown to represent the perforated surface and its simplified version as a flat aluminum surface enclosure that has an air gap inside

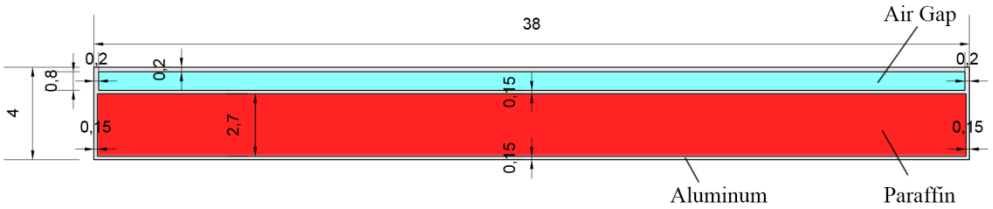

Figure 3.12 Plan of the Simplified Panel Section Used in the Energy Analysis

The test unit was integrated into the virtual room space in ABAQUS which represents a scenario of an office or a residential living room, in a glass façade building with a room size of 5.4 m x 7.3 m x 3.5 m (Figure 3.13).

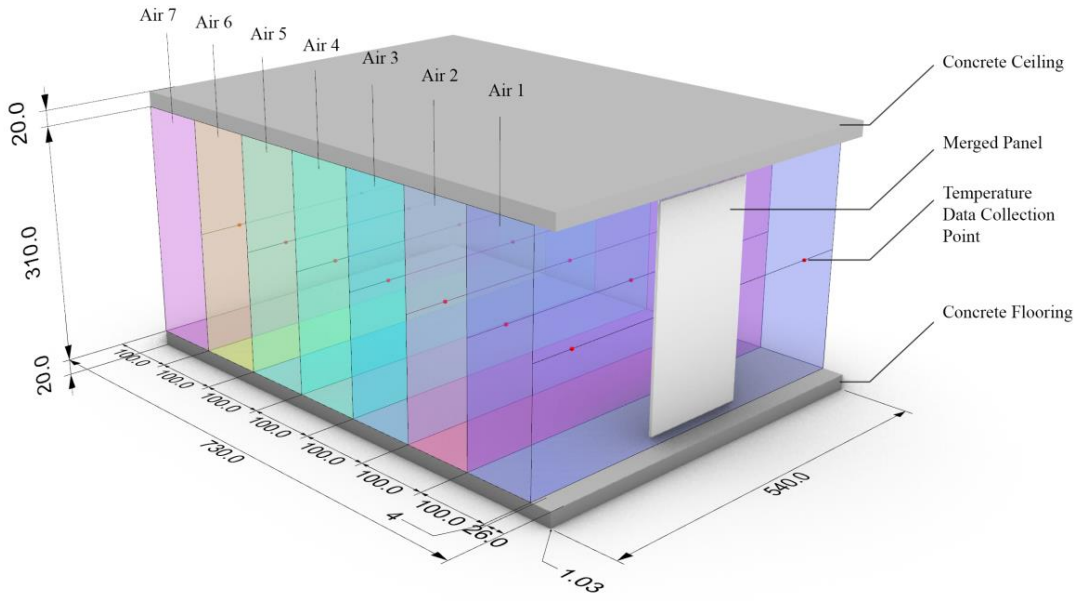

Figure 3.13 The Energy Analysis Model, Panel is shown with white, Indoor air volume is divided to 7 parts of 1 meter air volumes (dimensions are in cm)

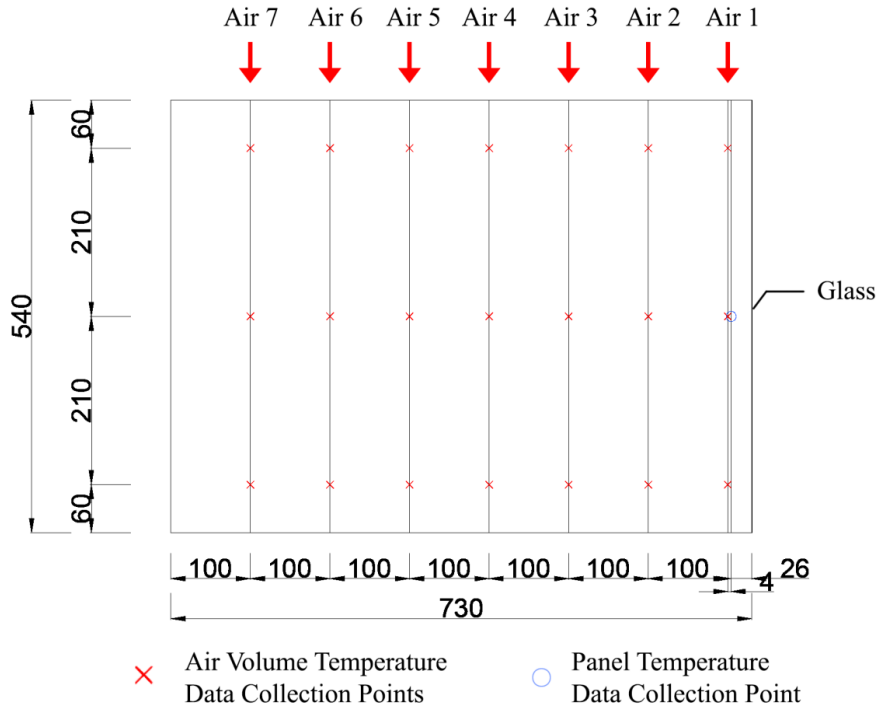

Figure 3.14 The Energy Analysis Model Plan, temperature collection points are shown (dimensions are in cm)

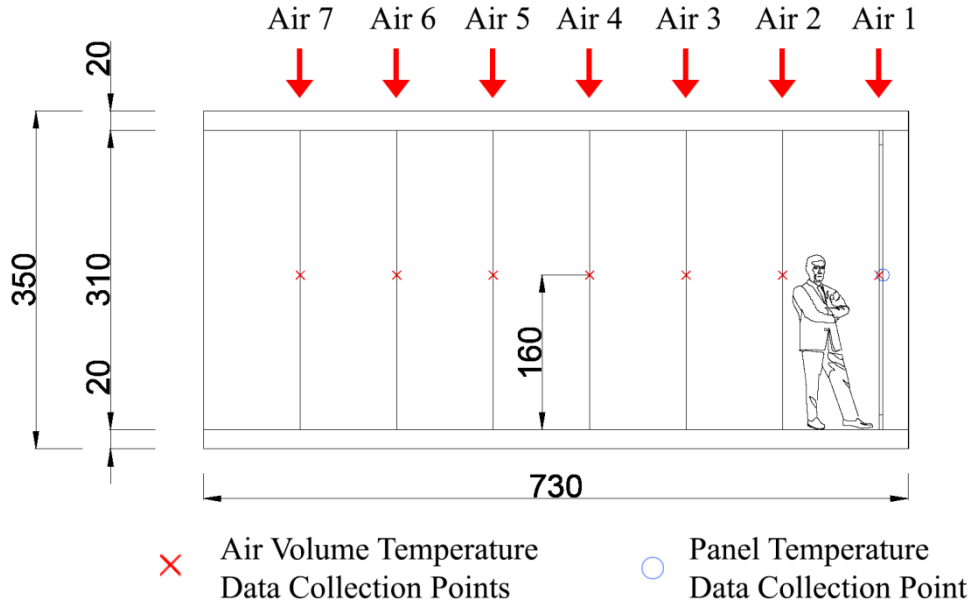

Figure 3.15 The Energy Analysis Model Section View, temperature collection points are shown (dimensions are in cm)

3.2.2 Material Properties Used in the Analysis

In order to analyze the thermal conditions within the space, “Forced convection” and “diffusion” elements were applied to the air volumes, however the latent heat property was assigned to the PCM, which made impossible to assign PCM with “Forced convection” and “Diffusion” due to the ABAQUS program limitations. All of the used material parameters in the analyses are shown in the Table 3.1.

Table 3.1 Material Parameters Used in the Analysis

	Conductivity (W/m.K)	Specific Heat (kJ/kg.C)	Density (kg/m3)	Latent Heat (J/kg)	Emissivity (W/m2.K)	Thickness (m)	Solar Energy Transmittance (%)	Melting Temperature (°C)	Flash Point (°C)	Sources
Aluminum	237	0.897	2712	-	-	-	-	-	-	Wikimedia Foundation. List of thermal conductivities. Specific heat of common substances. Engineering ToolBox. Metals and alloys - densities. Engineering ToolBox.
Concrete	1	0.88	2500	-	-	-	-	-	-	Wikimedia Foundation. List of thermal conductivities. Specific heat of common substances. Engineering ToolBox. Density of K5 materials in KG/M3 and LB/FT3. The Constructor.
Air	0.024	1.006	1.204	-	-	-	-	-	-	Thermal conductivity. (n.d.) Air. Density, heat capacity, thermal conductivity. Material Properties. Wikimedia Foundation. Density of air.
CrodaTherm 24W	0.22 (solid) 0.16 (liquid)	3.7 (solid) 2.2 (liquid)	906 (at 20 °C) 843 (at 40 °C)	184000(melting) 182000(crystallisation) 183000(taken as average)	-	-	-	22 °C - 24 °C	226 °C	Phase change material 24W. Energy Technologies. (n.d.).
Glass	0.00679	0.84	2500	-	-	-	-	-	-	Specific heats and molar heat capacities for various substances at 20 C. Table of Specific Heats. (n.d.). Solids - densities. Engineering ToolBox. (n.d.).
LandVac Glass (5TL +0.3V+5T) High Transmittance	0.009579	0.84	2500	-	0.93	0.0103	63%	-	-	Specific heats and molar heat capacities for various substances at 20 C. Table of Specific Heats. (n.d.). Solids - densities. Engineering ToolBox. (n.d.). LandGlass. (n.d.). LandVac 100% Tempered Vacuum Insulated Glass.

3.2.3 Calculation of the Absorbed Energy

The city of Van in Turkey was selected for the energy model to take place as the building heating demands are very high in this location; and in order to explore what the proposed Heat-Pocket system can achieve in worst conditions, December is taken as the month when the energy input from the sun is at its minimum. The solar energy (kJ/m2h) data (Figure 3.8) are obtained from the work belonging to Uçkan (2018). It should be mentioned that the values are not exact but approximate because the data was derived from the graph; to do so the charted data was projected on a surface in Rhino and the curves were traced as lines to extract the hourly values of approximate energy input in the graph. After that, kJ/m2h units are converted to W/m2 units.

In the analysis scenario as a highly efficient glass LandVac (5TL +0.3V+5T) (Vacuum Insulated Glass/High Transmittance Series) is selected as the glazing unit. In order to calculate the reflection loss, the incoming energy is multiplied with the value of solar transmittance according to documents of LandVac (LandGlass, n.d.). Then the transmitted energy is multiplied with the absorption rate of the black coating which was 90%. The resulting energy input is applied to the exterior facing surface of the aluminum box which was facing the south orientation in the analysis (Table 3.2).

Table 3.2 Solar Radiation Input Power Calculation for Analysis (Power Absorbed By Coating data was applied to the panel's exterior looking face)

Hours	Global Solar Radiation (kJ/m2h)	Global Solar Radiation (W/m2)	Power Reaching Indoors (W x 63%)	Power Absorbed By Coating ((W x 63%)x90%)	Time (seconds)
07:00:00	68.03	18.897	11.90511	10.714599	0
07:30:00	222.62	61.838	38.95794	35.062146	1800
08:00:00	445.08	123.633	77.88879	70.099911	3600
08:30:00	679.37	188.71	118.8873	106.99857	5400
09:00:00	914.25	253.958	159.99354	143.994186	7200
09:30:00	1100.64	305.73	192.6099	173.34891	9000
10:00:00	1263.87	351.075	221.17725	199.059525	10800
10:30:00	1380.81	383.558	241.64154	217.477386	12600
11:00:00	1466.27	407.297	256.59711	230.937399	14400
11:30:00	1482.6	411.833	259.45479	233.509311	16200
12:00:00	1466.66	407.405	256.66515	230.998635	18000
12:30:00	1401.47	389.29	245.2527	220.72743	19800
13:00:00	1308.54	363.48	228.9924	206.09316	21600
13:30:00	1177.73	327.147	206.10261	185.492349	23400
14:00:00	1015.08	281.966	177.63858	159.874722	25200
14:30:00	792.85	220.236	138.74868	124.873812	27000
15:00:00	570.62	158.505	99.85815	89.872335	28800
15:30:00	356.96	99.155	62.46765	56.220885	30600
16:00:00	143.3	39.805	25.07715	22.569435	32400
16:30:00	40.32	11.2	7.056	6.3504	34200
17:00:00	0	0	0	0	36000
17:30:00	0	0	0	0	37800
18:00:00	0	0	0	0	39600
18:30:00	0	0	0	0	41400
19:00:00	0	0	0	0	43200
20:00:00	0	0	0	0	46800
21:00:00	0	0	0	0	50400
22:00:00	0	0	0	0	54000
23:00:00	0	0	0	0	57600
00:00:00	0	0	0	0	61200
01:00:00	0	0	0	0	64800
02:00:00	0	0	0	0	68400
03:00:00	0	0	0	0	72000
04:00:00	0	0	0	0	75600
05:00:00	0	0	0	0	79200
06:00:00	0	0	0	0	82800
07:00:00	0	0	0	0	86400

3.2.4 Calculation of the Glass Material Properties

The following properties of the glazing were necessary to perform the heat transfer analysis in ABAQUS. The following input data used for the simulation are given in the following paragraphs; sources of the calculation methods are also indicated alongside:

i. Thermal Conductivity

The thermal conductivity of a material is a measure of its ability to conduct heat. The selected glazing was modeled with the LandVac documentation and its conductivity was calculated with the following formula :

Thermal conductivity = U-value * thickness (W/mK)

According to the Landvac manufacturer's factsheet, this material has a U-value of 0.93 W/m2k which is %50 lower than the U-value of normal glazing, which is 1.8 W/m2k. This value is considerably lower than conventional glazing. Using the equation above, the thermal conductivity of this type of glass with a thickness of 0.0103 m is calculated to be 0.009579 W/mK.Thermal conductivity = 0.93 * 0.0103 = 0.009579 (W/mK)

ii. Density

The density for the glass material is taken from internet sources and according to the manufacturers, the LandVac glass has a 0.3 mm vacuum insulation between the two glass panes, which was significantly low and disregarded in the density calculation. Therefore, the glass density was taken as the widely used value of 2500 kg/m3.

iii. Film Coefficient

The film coefficient was calculated with the calculator from Overall heat transfer coefficients, in the Engineering ToolBox online calculator. Used parameters for the film coefficient calculation are given in Figure 3.16, the value for the convective heat transfer coefficient inside wall and outside wall was gathered from the section of the book "Exploring Engineering", Chapter 12 – Mechanical Engineering (Kosky, Balmer, Keat & Wise, 2013).

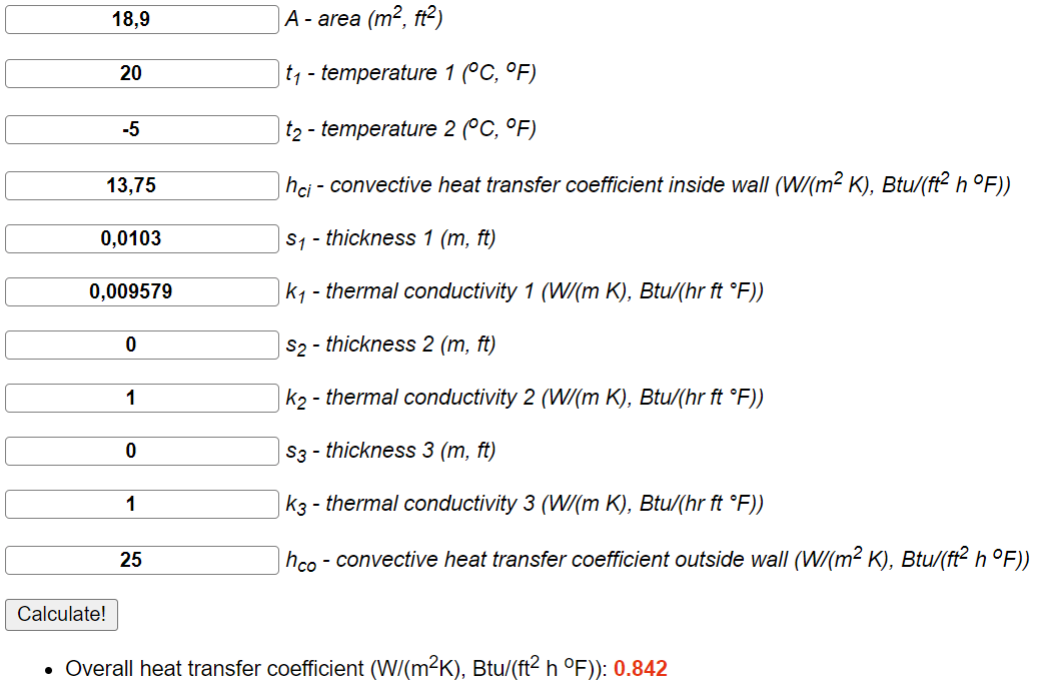

Figure 3.16 Overall heat transfer coefficient calculation, Engineering Toolbox

3.2.5 Simulation Steps

The energy model interactions are given below in Figure 3.17 and all of the simulations in this article took place in three steps in the following manner:

i. Initial Step

In the initial step, the whole model was set to 20 °C except for the exterior facing glass surface, which is set to -5 °C (Weather Spark, n.d.) as predefined temperature set-points.

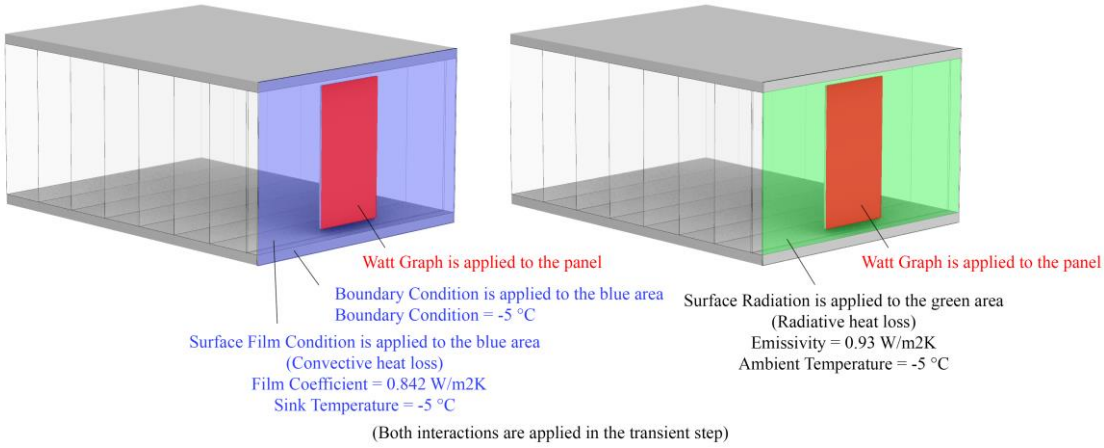

Figure 3.17 The Energy Analysis Interactions (Load (applied to red plane), Boundary Condition (applied to blue plane), Surface Film Condition (applied to blue plane), Surface Radiation (applied to green plane))

ii. Transient Heat Transfer Step

In this step, the solar energy values are taken from the Van Solar Radiation data (Table 3.2) were used and applied to the aluminum panel's exterior facing surface (shown as red in Figure 3.17). Except for the exterior facing glass surface, all side surfaces of the room are adiabatic walls. A uniform boundary condition with -5°C is set to the exterior facing glass surface, this means the exterior temperature is -5°C throughout the analysis time during the transient heat transfer step (shown as blue in Figure 3.17). Radiative heat loss (Surface Radiation interaction) is applied to the Front Air Volume 1 exterior facing surface (shown as green in Figure 3.17) with an emissivity value of 0.93 (W/m2K) and the ambient temperature value of -5°C. The convective heat loss interaction is applied to the

exterior surface of the glass with a film coefficient of 0.842 (W/m2K) (Surface Film Condition). Temperature values of selected points were calculated for every 1 hour period for the whole model. The duration of this step was 86400 seconds (1 day).

iii. Steady-state Equilibrium Step

To calculate what would be the average temperature after the analysis, a steady-state heat transfer step is introduced lasting 24 hours until the temperature settles into its equilibrium state. The loaded energy from the sun during the day and the lost energy from the façade interactions during the day were completed when the transient step is ended which means one day is past, considering this, to calculate the equilibrium temperature, Boundary Condition, Surface Radiation interaction and Surface Film Condition are deactivated in this step. Duration of this step is also 86400 seconds (1 day).

3.3 Phases of the Analysis

This study consists of two phases which are described below.

In Phase 1, multiple PCM fill rate panel scenarios were tested for selecting the best fill rate for the system. For this, three analyses were performed using 50%, 75%, and 100% PCM-filled panels in the 3D energy model (Figure 3.13). This phase was performed because when some part of the panel is not filled with PCM, for example in the 50% PCM filled panel case, the empty part that does not touch with PCM can not dissipate the absorbed energy instantly, resulting in increased temperature for that location of the panel which may bring problems of safety due to the fact that used paraffin material may flash after 226 °C.

In Phase 2, after selecting the best panel PCM fill rate for the system, the selected panel configuration was used in the 3D energy model (Figure 3.13) for

calculating its effects on the indoor temperature changes to determine if the system satisfies ASHRAE thermal comfort standards during the day cycle.

3.4 Limitations of the Study

This study does not calculate the energy savings due to the limitations of the simulation program ABAQUS. The purpose of this research is to find the temperature values in the conditions of the proposed scenario and test if these values are in the range of ASHRAE recommended thermal comfort levels.

- This analysis is based on heat transfer through conduction.
- The energy analysis model is thermally isolated except for the glass layer's exterior facing surface for boundary condition, surface film condition and surface radiation loss.
- This analysis can only capture the surface radiation loss, so if the total volume of the indoor air is considered in the calculation for radiation loss, it is expected to be higher, as the volume of gas increases, this can end up with more energy loss values than the reality.
- This analysis does not include CFD analysis for natural convection in the indoor air volumes, due to the fact that ABAQUS does not provide such option of performing natural convection; however, all Air Volumes are applied with forced convection and radiation nodes. This increases the heat flow between units but as it can be seen in the results section, in the real life scenario where natural convection exists, the heat is expected to be dissipated faster.
- The contact surface of aluminum and paraffin is minimized due to the fact that energy analysis model is simplified by joining individual box panels into one big one. Hence, the total volume of PCM remains the same but the area of the sides of boxes is ignored. It can be expected the contact surface area in reality would be higher and so more aluminum material will be present in the system; therefore, the temperature on the front face of the

panels would drop faster as the thermal energy from the heated aluminum box would go into the PCM at a faster rate.

- The analysis only uses 1/3rd of the total glazed façade area for solar heat collection and utilizes 2/3rd of the façade area for daylighting purposes. Otherwise the temperature values achieved inside the space could be higher if all the façade area was used for solar heat collection.
- The analysis excludes the radiation loss from the angular reflection which happens in real life when the sunlight energy is transmitted into interiors with an amplitude in regards to its impact angle to façade glass. To calculate such complex phenomenon was not possible to be analysed in ABAQUS software, therefore, the energy analysis uses the solar transmittance percentage from the glass product documentations.
- The analysis excludes the ambient light energy input. Ambient light amplitude is expected to be higher as the snowfall increases in the winter and snow disperses the light which increases overall ambient daylight.

CHAPTER 4

RESULTS AND DISCUSSION

4.1 Results

The results of the simulations are presented here in two main sections related to the two phases of the research, as described in Chapter 3.

4.1.1 Phase 1 Results

In phase 1, as it was described in the previous chapter three scenarios of PCM fill rates in the panel were compared which were 50%, 75%, and 100% using the same 3D model (Figure 3.13). The results for the panel and the PCM surface temperatures are given below.

I. Panel Temperatures

The following results of temperature data for the panel were taken from the top and the below front surface of the panel (Figure 4.1).

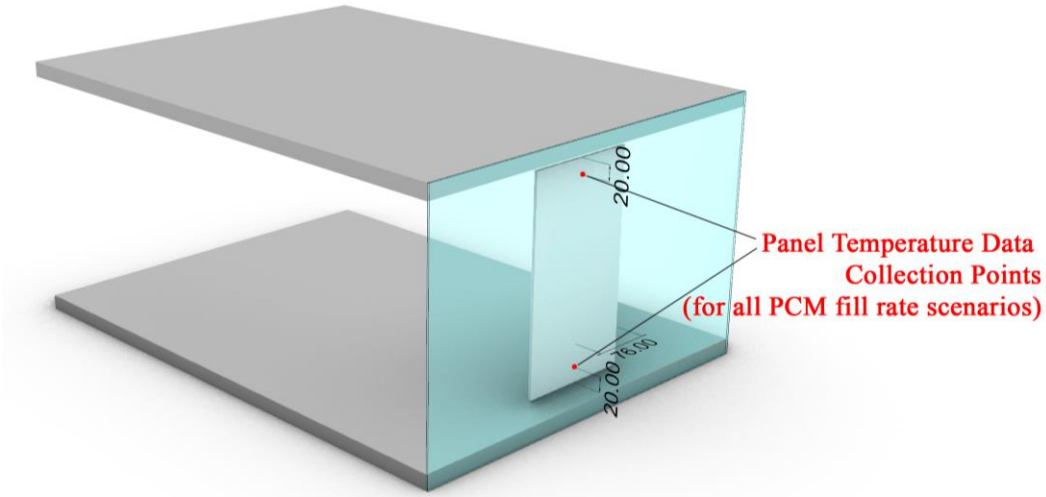

Figure 4.1 Panel Temperature Data Collection Points for all of the scenarios of Phase 1

i. Panel Front Top Surface Temperatures

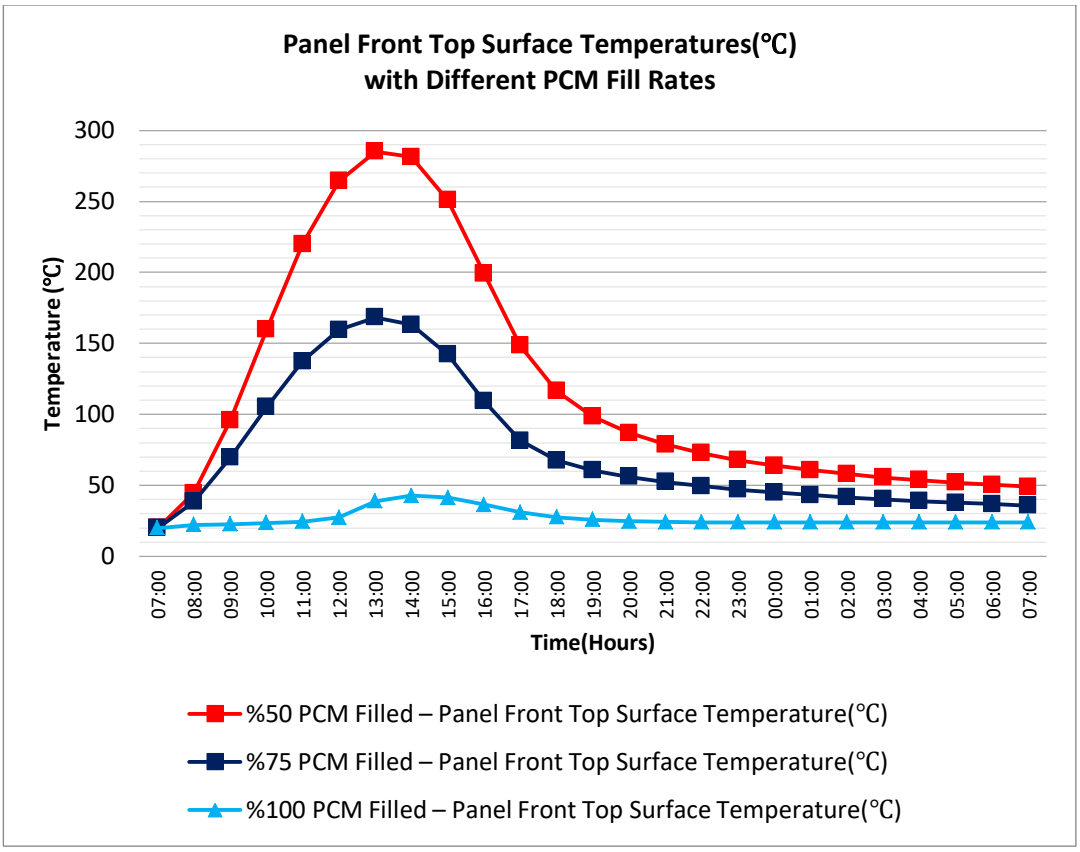

Figure 4.2 Panel Front Top Surface Temperatures(℃) with Different PCM Fill Rates

It can be seen in the 50% fill rate scenario, the temperature of the panel's front facing top surface is reaching up to 285.13 ℃ at 13:00 PM as maximum value which is dangerous due to the fact that the PCM has a flashing point of 226 ℃ (Figure 4.1, Figure 4.2). If this case happens in real life, the PCM would explode through out the façade and cause fire. This part of the study was specifically given to inform the readers about this issue to ensure user safety.

It must be stated that the hot air will lift up and heat the top part more therefore, local energy accumulations are expected at the top of the panel in a real life case however, due to the lack of natural convection in this analysis this phenomenon could not be observed (Figure 4.1).

In the 75% fill rate scenario, the temperature of the panel's front facing top surface is reaching up 168.31 ℃ at 13:00 PM as maximum value (Figure 4.1, Figure 4.2). It is too hot to touch panel while it's operating which may cause safety problems for the user.

It can be seen in the 100% fill rate scenario, the temperature is reaching up to 42.78 ℃ at 14:00 PM as maximum value which is ideal and safe to use (Figure 4.1, Figure 4.2).

ii. Panel Front Below Surface Temperatures

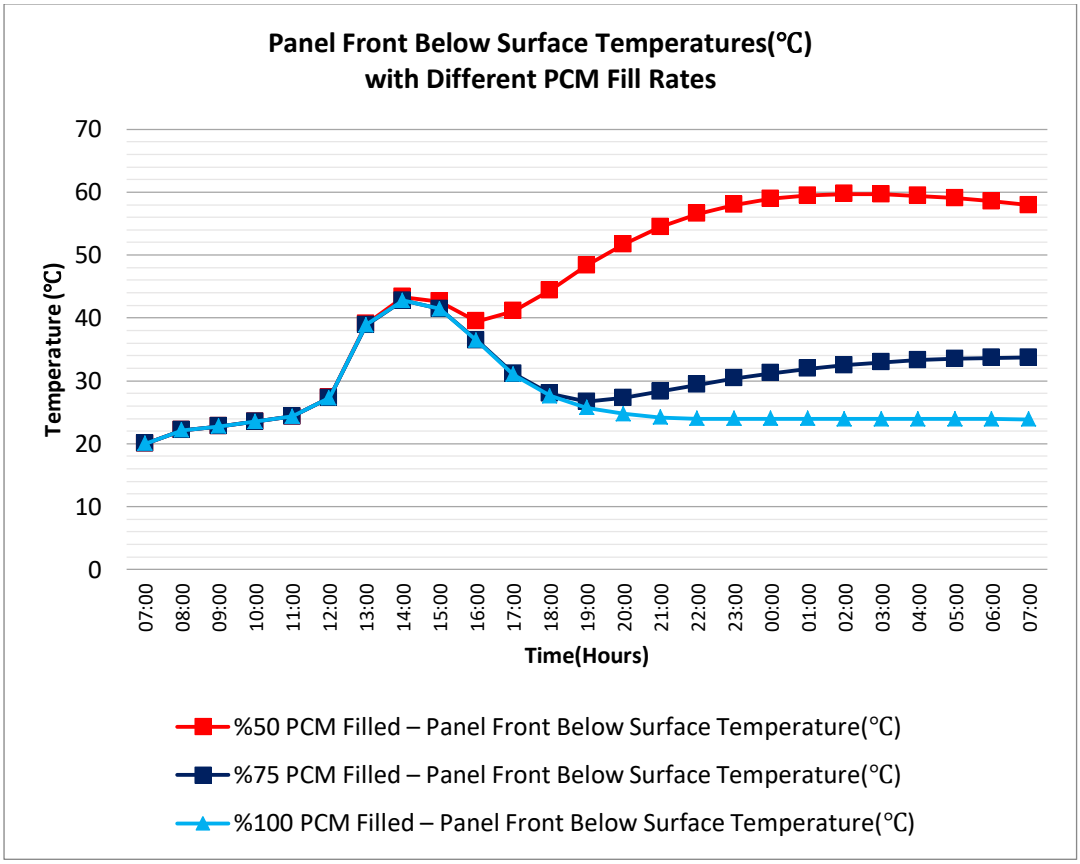

Figure 4.3 Panel Front Below Surface Temperatures(℃) with Different PCM Fill Rates

In the 50% fill rate scenario, the temperature of the panel's front facing below surface is reaching up to 59.69 ℃ at 02:00 AM next day as maximum value (Figure 4.1, Figure 4.3).

In the 75% fill rate scenario, the temperature of the panel's front facing below surface is reaching up to 42.77 ℃ at 14:00 PM next day as maximum value (Figure 4.1, Figure 4.3).

In the 100% fill rate scenario, the temperature of the panel's front facing below surface is reaching up to 42.78 ℃ at 14:00 PM next day as maximum value (Figure 4.1, Figure 4.3).

For all of the results for the bottom temperature collection point, the temperature increase is slowed down between 7:00 AM to 11:00 AM first day which was caused by PCM being melted in that time (Figure 4.1, Figure 4.3).

In the scenarios of 50% and 75% filled panels, the excess energy accumulation at the top part of the panel where there is no PCM is dissipating to the below part of the panel, that's why the temperature at the below part increases after 16:00 PM for the 50% filled panel and after 19:00 PM (Figure 4.1, Figure 4.3).

II. PCM Temperatures

The following results of temperature data for the PCM were taken from the top and below front surface of the PCM layer, the points for each simulation are shown in the following figures (Figure 4.4, Figure 4.5, Figure 4.6).

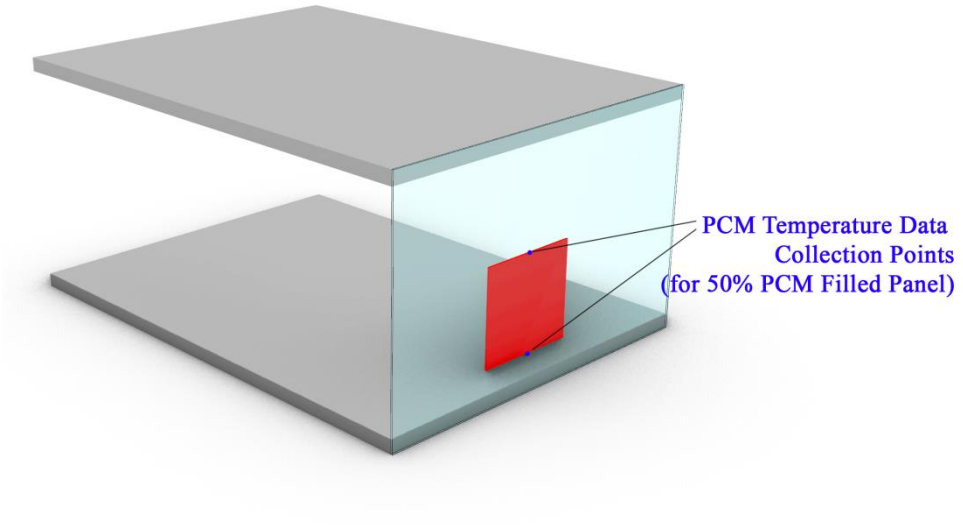

Figure 4.4 PCM Temperature Data Collection Points for 50% PCM Filled Panel, Phase 1

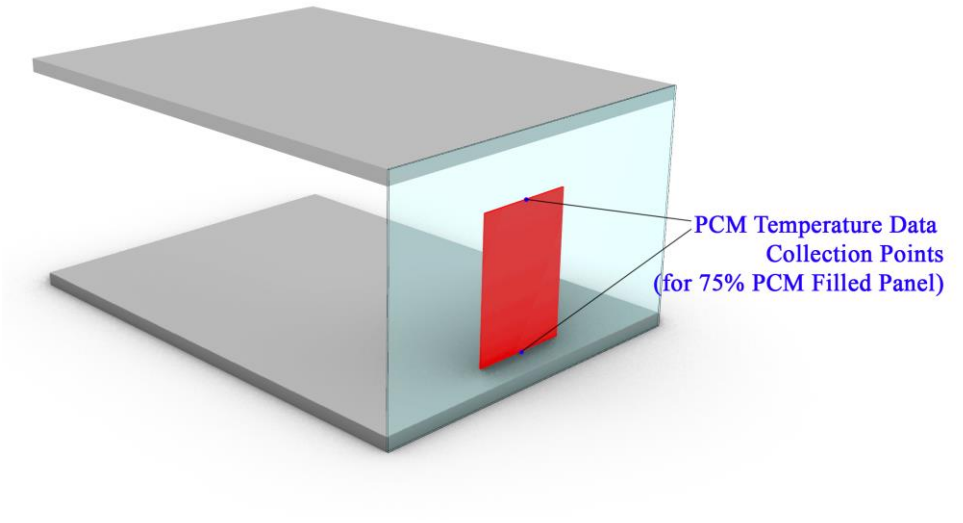

Figure 4.5 PCM Temperature Data Collection Points for 75% PCM Filled Panel, Phase 1

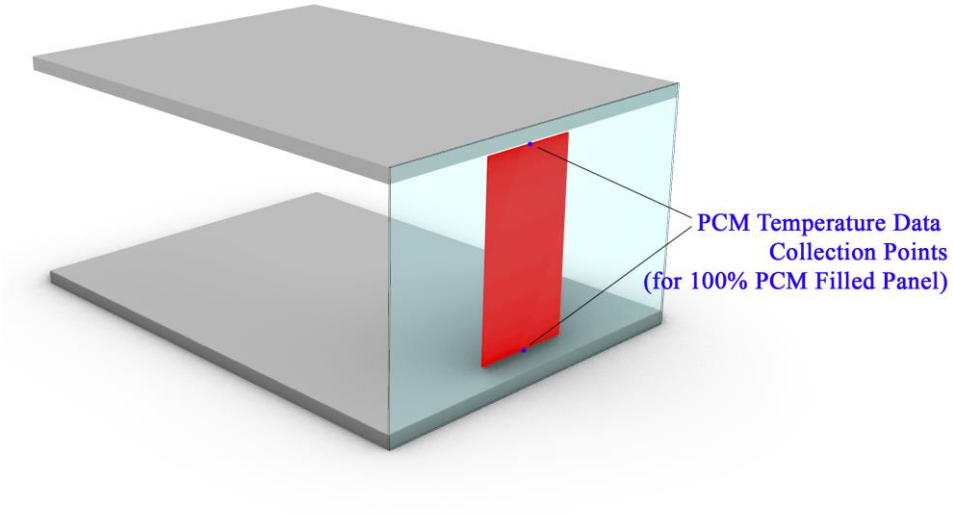

Figure 4.6 PCM Temperature Data Collection Points for 100% PCM Filled Panel, Phase 1

i. PCM Front Top Surface Temperatures

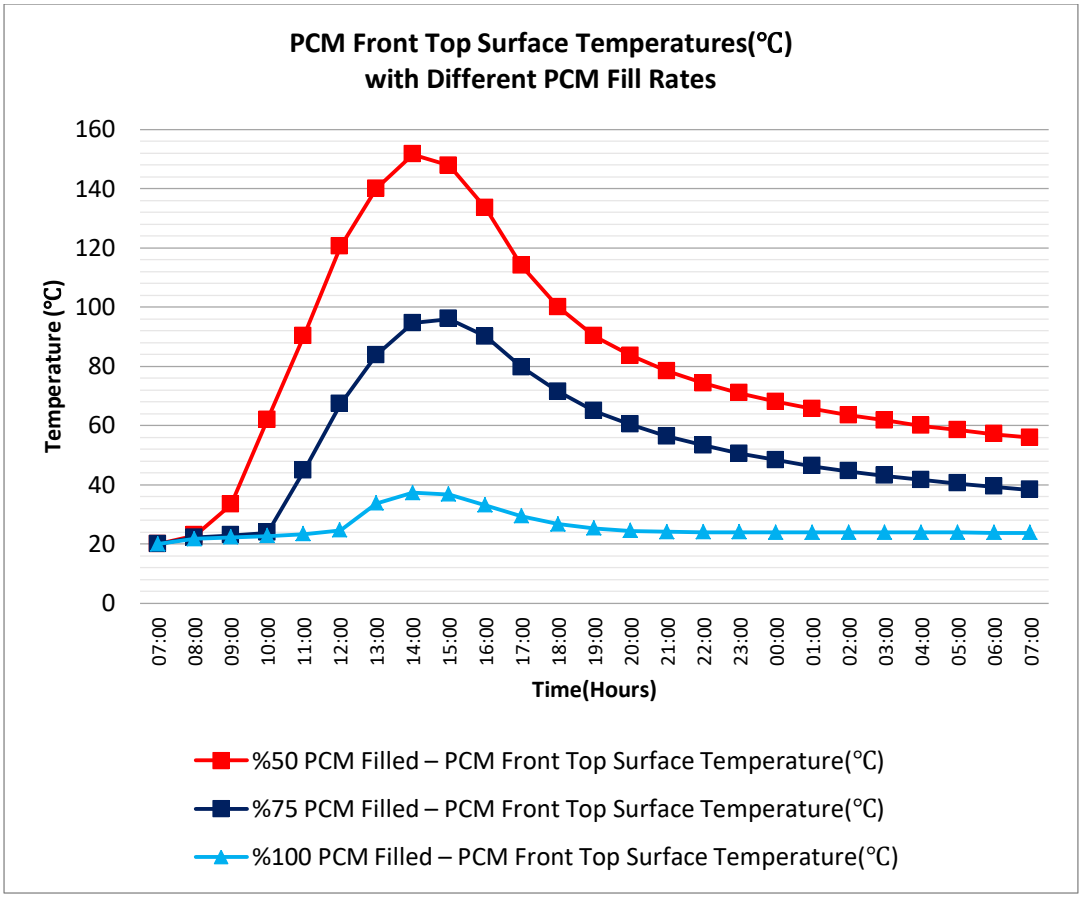

Figure 4.7 PCM Front Top Surface Temperatures(°C) with Different PCM Fill Rates

For the PCM layer, in the 50% fill rate scenario the temperature of the PCM's front facing top surface is reaching up to 151.55 °C at 14:00 first day. The reason for the gradual decrease after 14:00 PM is due to excess energy at the top of the panel and top of the PCM layer flows to the surroundings and the PCM layer below during the day (Figure 4.4, Figure 4.7).

In the 75% fill rate scenario the temperature of the PCM's front facing top surface is reaching up to 95.97 °C at 15:00 PM first day. The reason for the gradual decrease after 15:00 PM is due to excess energy at the top of the panel and top of

the PCM layer flows to the surroundings and the PCM layer below during the day (Figure 4.5, Figure 4.7).

In the 100% fill rate scenario the temperature of the PCM's front facing top surface is reaching up to 37.29 ℃ at 14:00 PM first day. The reason for the gradual decrease after 14:00 PM is due to excess energy at the top of the panel and top of the PCM layer flows to the surroundings during the day (Figure 4.6, Figure 4.7).

ii. PCM Front Below Surface Temperatures

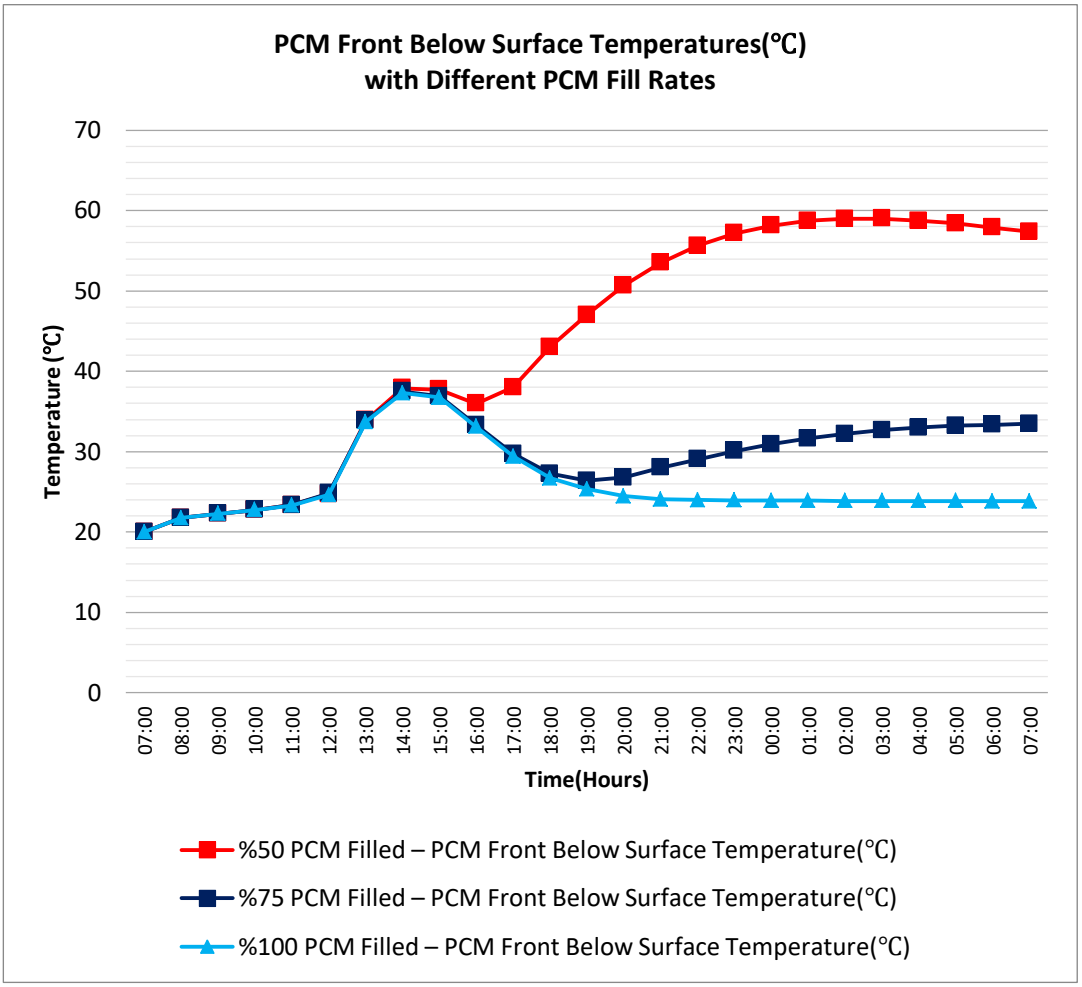

Figure 4.8 PCM Front Below Surface Temperatures(℃) with Different PCM Fill Rates

In the 50% fill rate scenario the temperature of the PCM's front facing below surface is reaching up to 58.98 °C at 03:00 AM next day as maximum value (Figure 4.4, Figure 4.8). The reason for the gradual increase of temperature after 16:00 PM is due to excess energy at the top section flows to the PCM layer below.

In the 75% fill rate scenario the temperature of the PCM's front facing below surface is reaching up to 37.48 °C at 14:00 PM first day as maximum value (Figure 4.5, Figure 4.8). The reason for the gradual increase of temperature after 19:00 PM is due to the excess energy at the top of the panel flowing into the PCM below.

In the 100% fill rate scenario the temperature of the PCM's front facing below surface is reaching up to 37.29 °C at 14:00 PM first day (Figure 4.6, Figure 4.8).

For all of the scenarios the reason for the gradual decrease of temperature after 14:00 PM first day is due to the energy flows to the surroundings during the day (Figure 4.8).

4.1.2 Selected PCM Fill Rate

The equilibrium temperatures for the configurations are given in the following: 56.68 °C for 50% PCM filled panel, 35.94 °C for 75% filled version and 23.64 °C for 100% filled version. The reason that the equilibrium temperatures are different is due to lack of PCM, when there is more PCM present in the system it absorbs the excess solar energy such in the case of 100% filled panel which decreases the overall temperature and when there is less PCM present in the system, the excess energy flows into the room increasing the overall temperature for the system.

The best scenario that was suitable for users in terms of safety was the 100% PCM filled panel as its temperatures for the setup does not exceed 42.78 °C therefore it won't flash and it is safe to touch while it's operating.

4.1.3 Phase 2 Results

The selected 100% PCM filled panel was tested how it effects the indoor air temperature. Results for the simulation of the test room obtained from ABAQUS software are presented and evaluated in the following sections. The thermal data obtained for each air layer is discussed one by one ; the location of the seven air layers is indicated on the plans shown in Figures 4.9, 4.11, 4.13, 4.15, 4.17, 4.19 and 4.21 and the graphs for the 3 data points are given in Figures 4.10, 4.12, 4.14, 4.16, 4.18, 4.20 and 4.22, respectively.

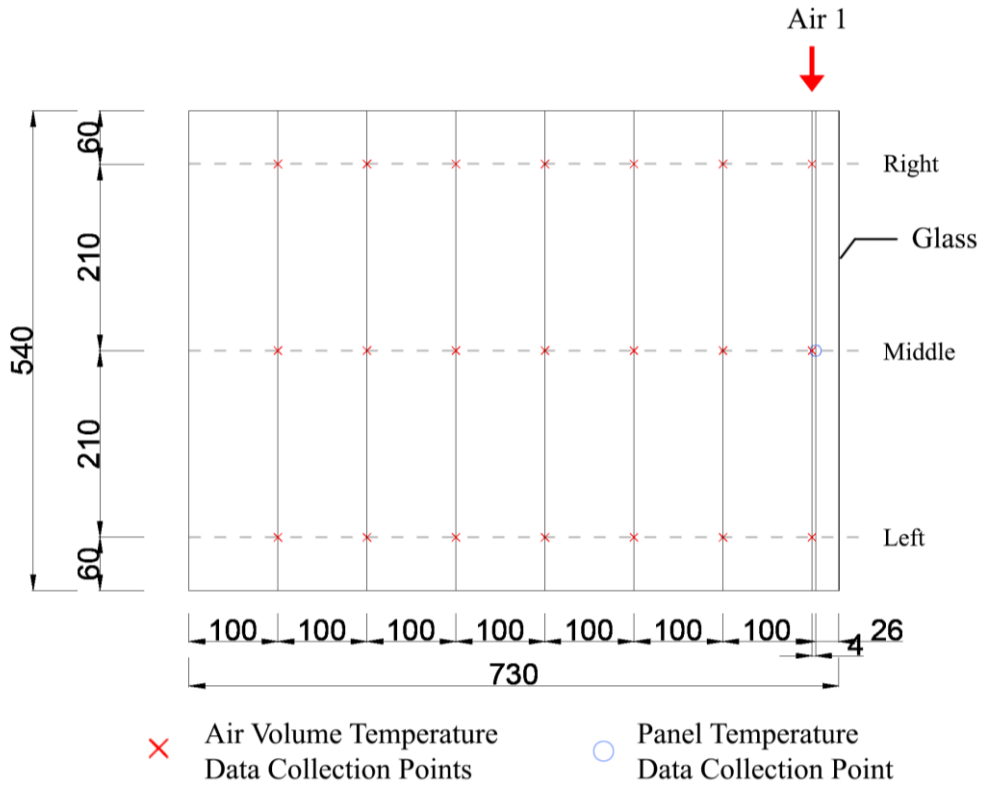

Figure 4.9 Air 1 Layer's Location Plan

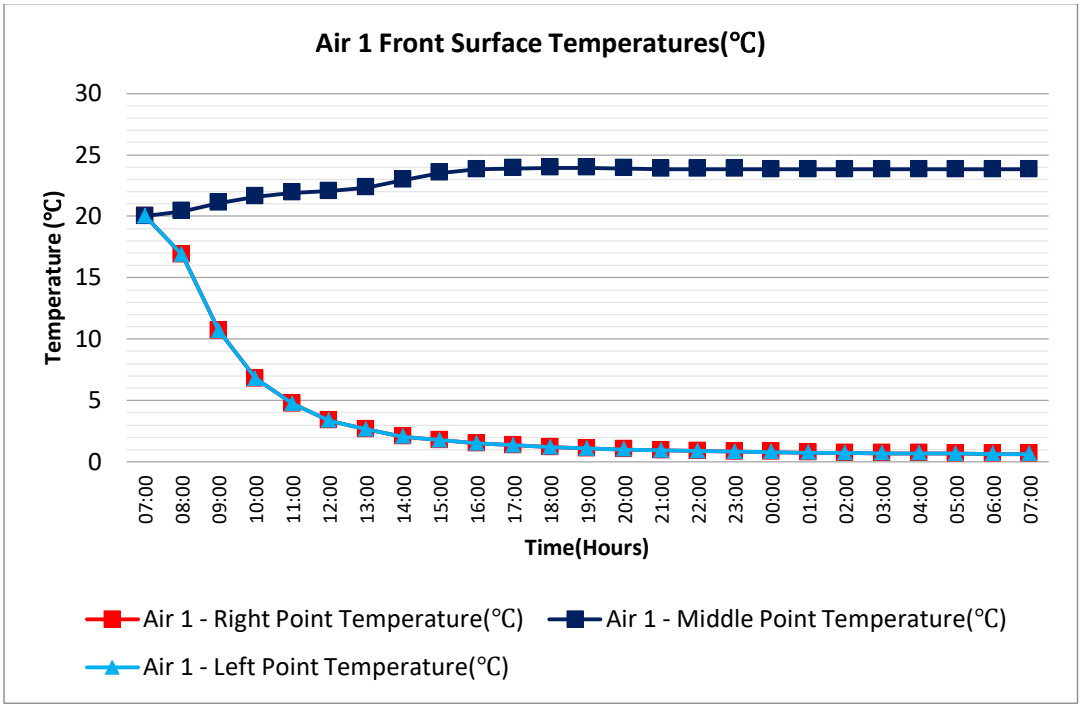

Figure 4.10 Air 1 Front Surface Temperatures(°C)

Results for Air 1 show that just behind the panel, the middle point complies with ASHRAE thermal levels throughout the day, however the temperature values at the left and the right points do not stay in the range of comfort levels after 7:00 AM first day when the analysis starts and at the end of the analysis drop significantly, to 1 °C due to losses through the glass to the exterior (Figure 4.9, Figure 4.10). Since a CFD analysis for natural convection could not be performed in this simulation, in a real life scenario with the help of natural convection, the temperature values at Air 1 level are not expected to drop that significantly as in the analysis and expected to be getting closer to equilibrium temperature for the system.

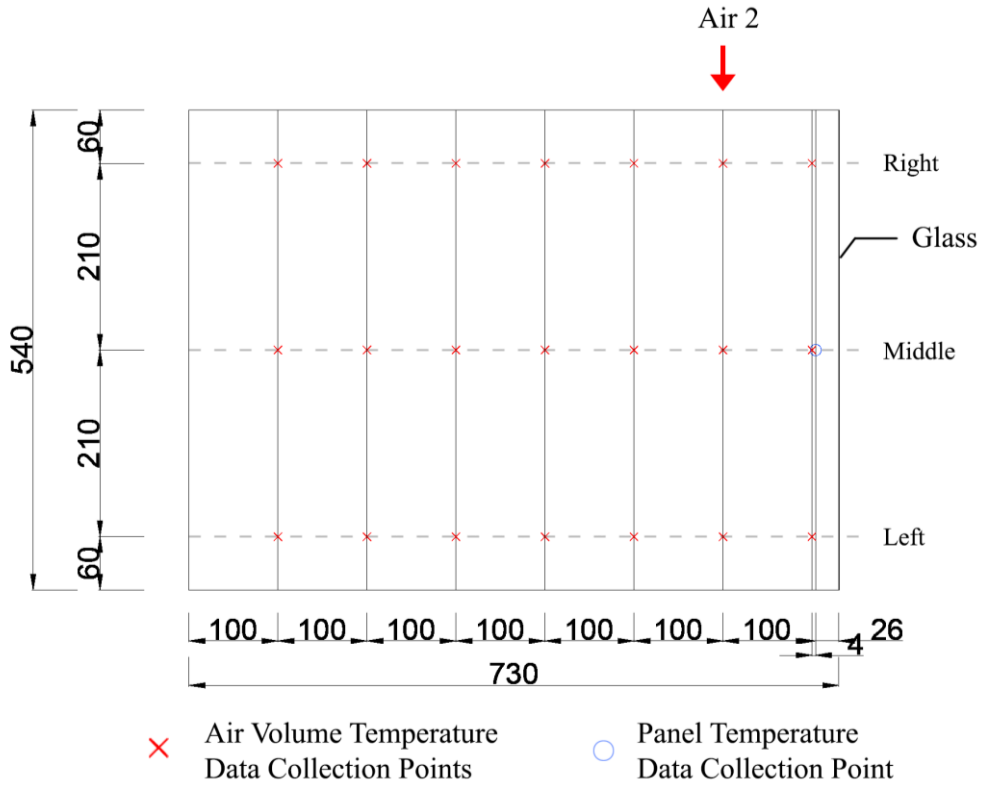

Figure 4.11 Air 2 Layer's Location Plan

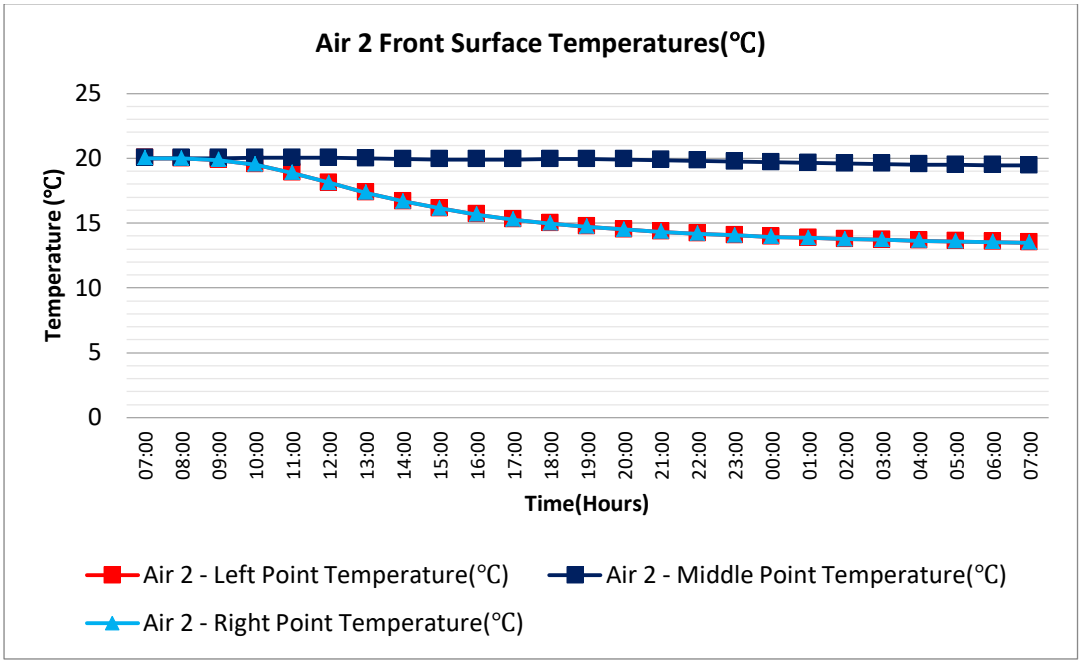

Figure 4.12 Air 2 Front Surface Temperatures(°C)

It can be seen from the results in the Air 2 layer, the front surface temperature that temperature value behind the panel does not alter and stays same through out the day (Figure 4.11, Figure 4.12); this layer is only 1 m away from the exterior conditions of -5°C; hence a 19 degrees improvement is achieved in the thermal conditions due to the PCM trombe wall.

When the middle point temperature of Air 2 is compared with the middle point temperature of Air 1, due to the distance which is 1 m to the panel, the heat could not be transferred from the panel in the case of Air 2 middle point. This case again is not expected in a real life scenario where the natural convection phenomenon exists and it is expected that the Air 2 middle point temperature would increase by absorbing energy from Air 1 middle volume (Figure 4.10, Figure 4.12).

Air 2 left and right temperature values conclude a falling curve as they are exposed to the coldness that is coming from the glass in contrast to Air 2 middle point. It can be said that the panel act as a heat barrier for the middle points in both Air 1 and Air 2 (Figure 4.10, Figure 4.12).

The Air 2 middle point satisfies the ASHRAE thermal comfort levels until 6:00 AM next day however, Air 2 left and right points satisfy the thermal comfort levels until 10:00 AM first day (Figure 4.12).

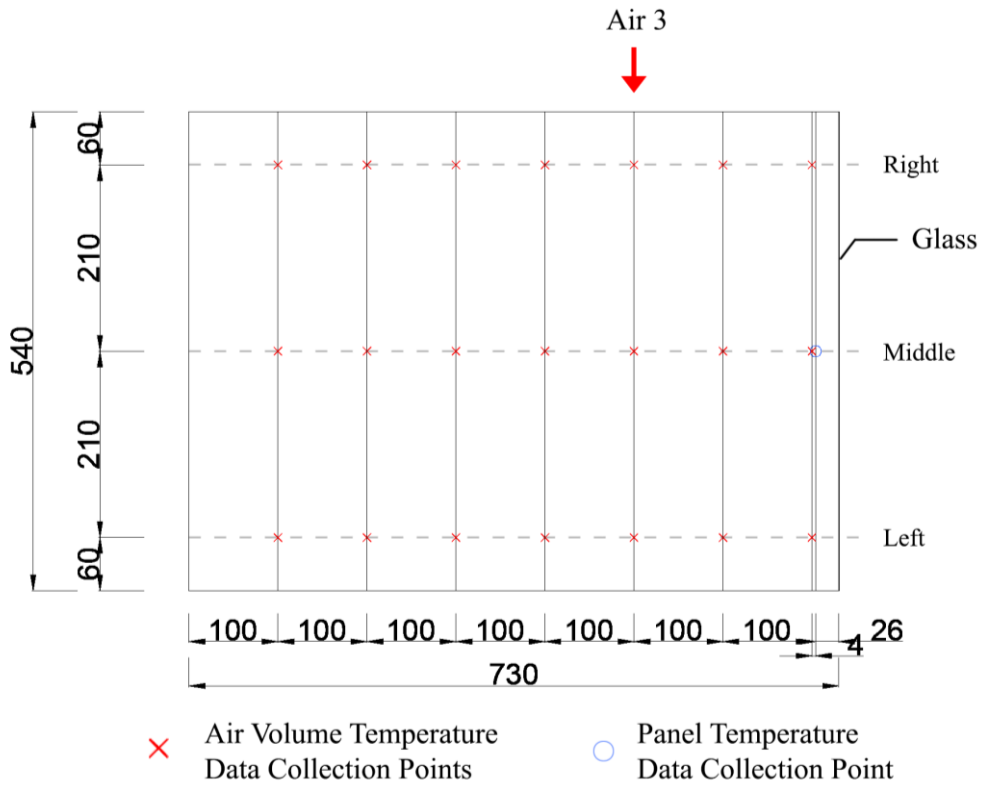

Figure 4.13 Air 3 Layer's Location Plan

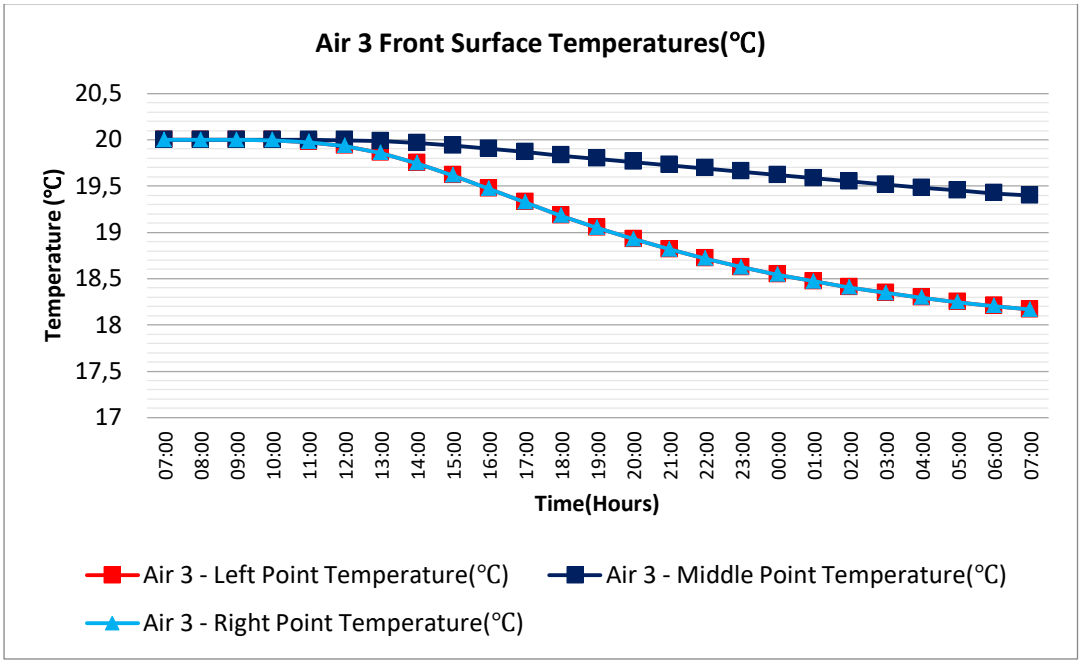

Figure 4.14 Air 3 Front Surface Temperatures(°C)

It can be seen for left, middle and right points, the temperature value drops in a smoother fashion in comparison to Air 2 (Figure 4.13, Figure 4.14).

The Air 3 middle point satisfies the ASHRAE thermal comfort levels until 5:00 AM next day however, Air 3 left and right points satisfy the thermal comfort levels until 16:00 PM first day (Figure 4.14). Nevertheless, the minimum temperature at this surface is 24°C (19°C +5°C) higher than the exterior.

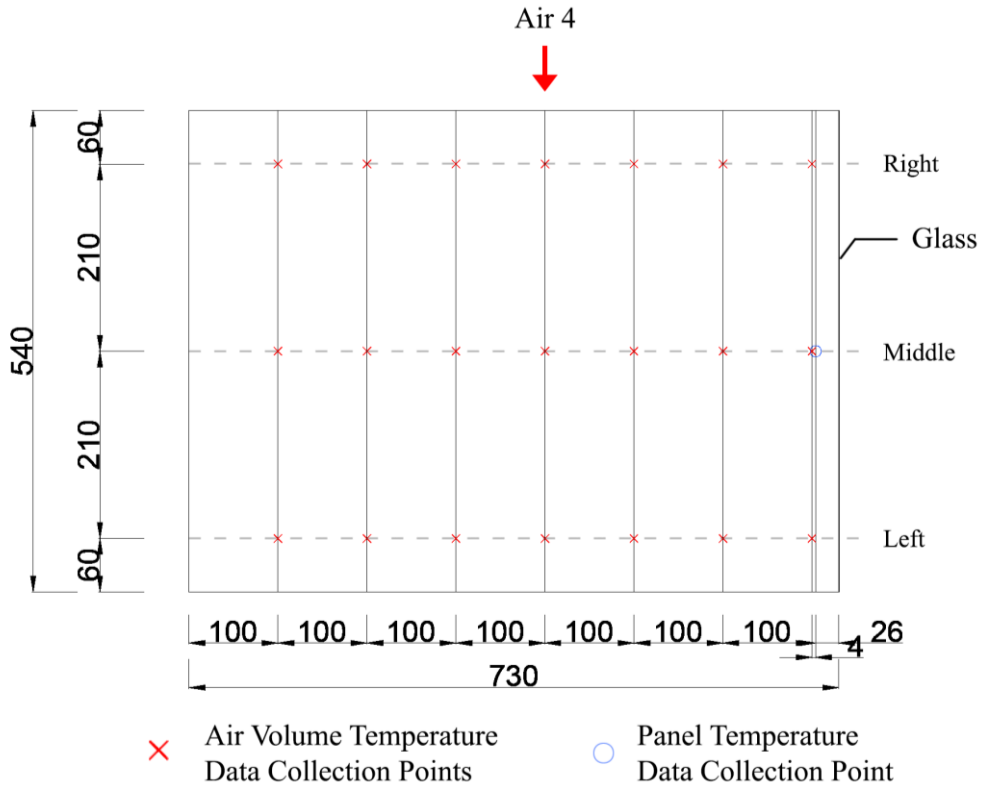

Figure 4.15 Air 4 Layer's Location Plan

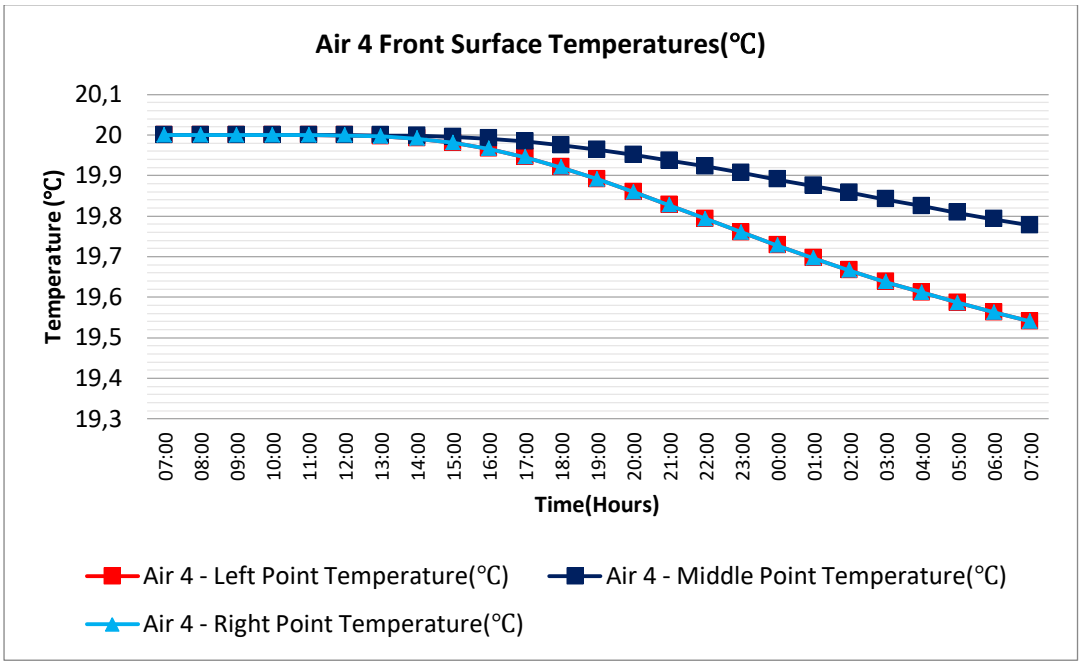

Figure 4.16 Air 4 Front Surface Temperatures(°C)

It can be seen from the energy analysis results that all the points of Air 4 front surface satisfy ASHRAE thermal comfort levels through out the day (Figure 4.15, Figure 4.16).

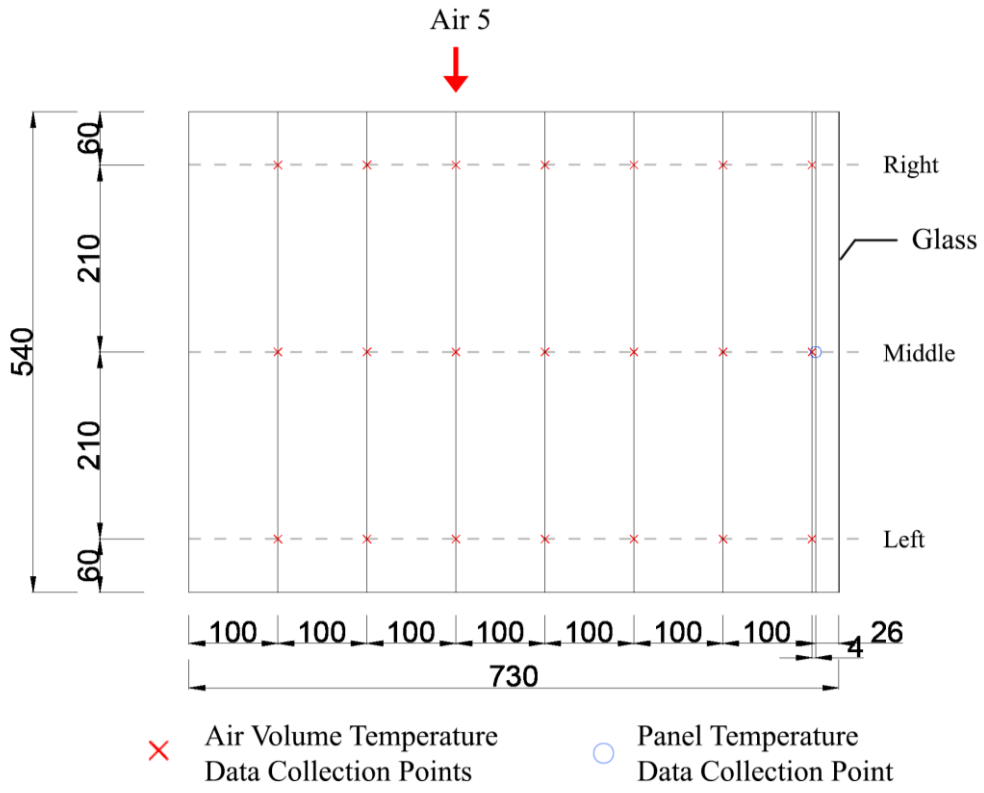

Figure 4.17 Air 5 Layer's Location Plan

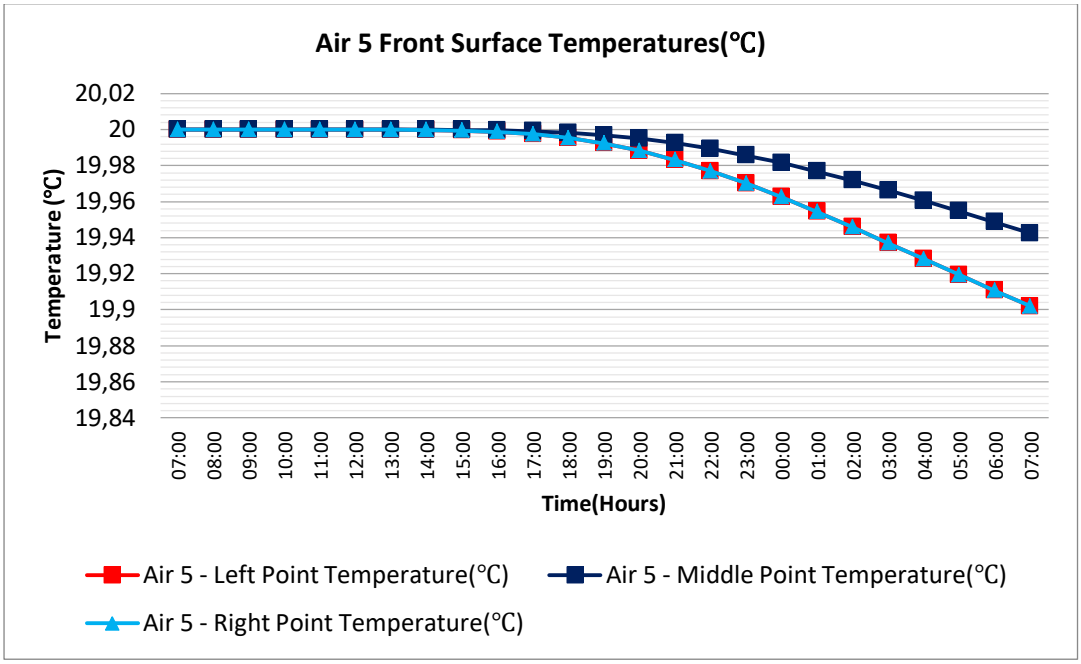

Figure 4.18 Air 5 Front Surface Temperatures(°C)

It can be seen from the energy analysis results that, all the points of Air 5 front surface satisfy ASHRAE thermal comfort levels through out the day (Figure 4.17, Figure 4.18). The temperature values of Air 5 front surface do not change too much, this could be the result of non existence of natural convection in the analysis.

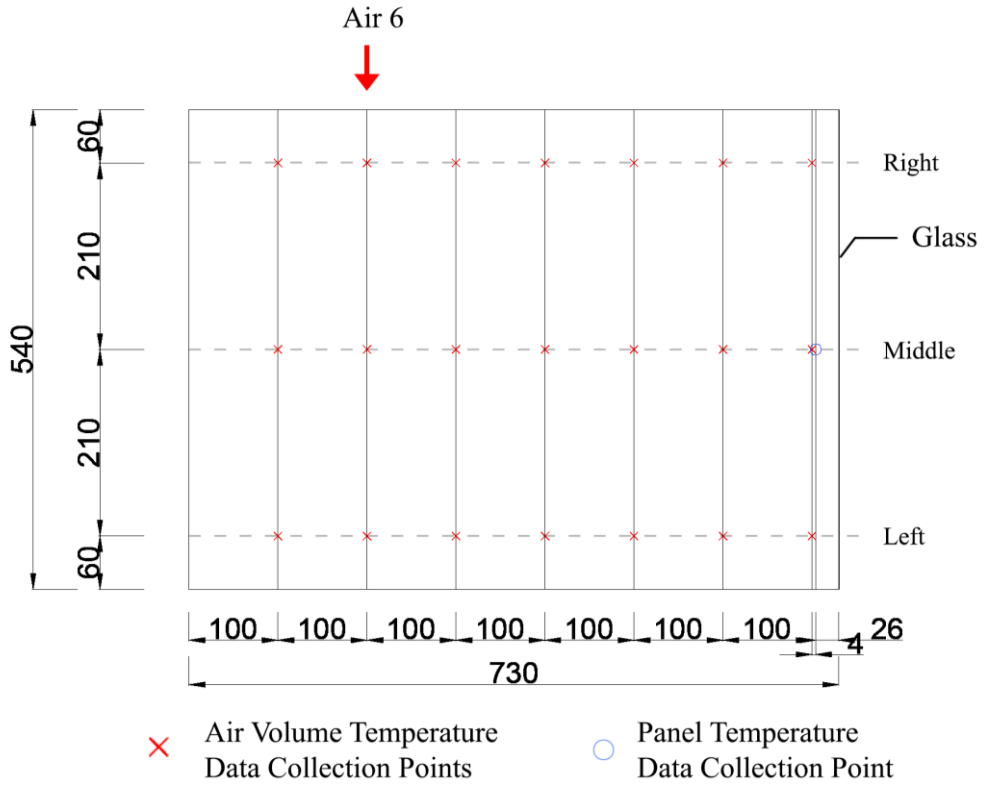

Figure 4.19 Air 6 Layer's Location Plan

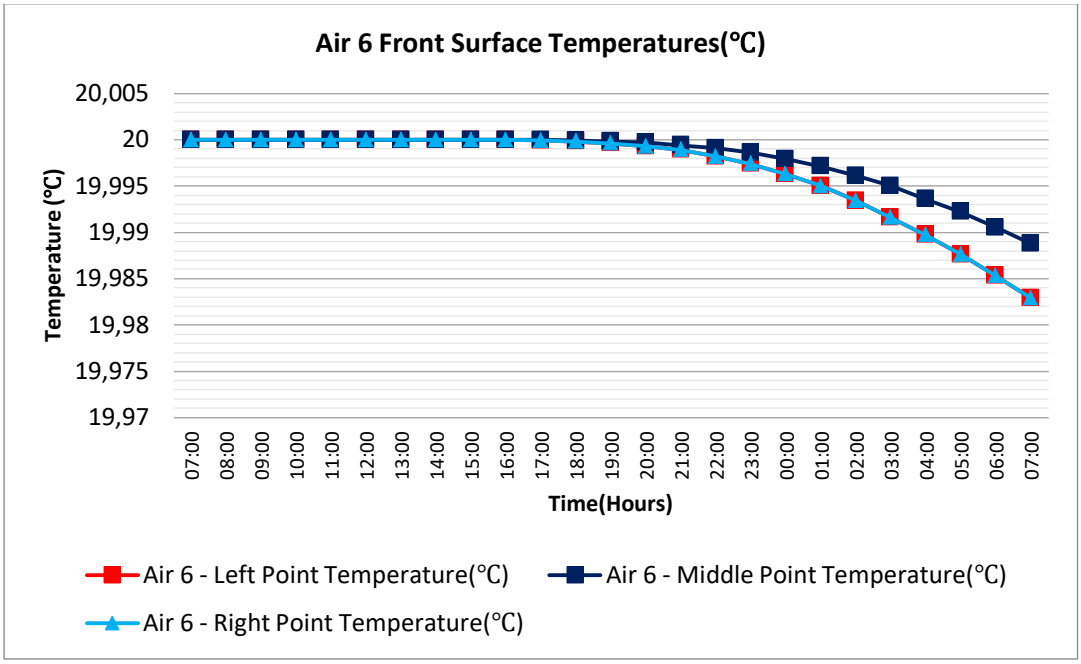

Figure 4.20 Air 6 Front Surface Temperatures(°C)

It can be seen from the energy analysis results that, all the points of Air 6 front surface satisfy ASHRAE thermal comfort levels through out the day (Figure 4.19, Figure 4.20). The temperature values of Air 6 front surface do not change too much, this could be the result of non existence of natural convection in the analysis.

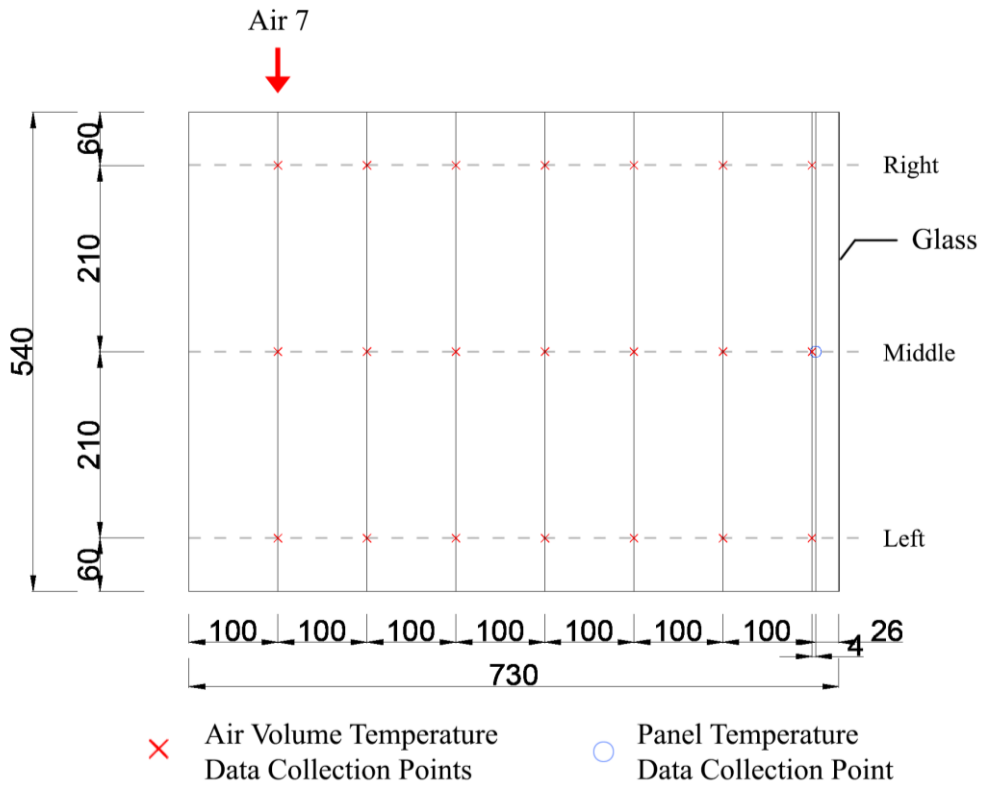

Figure 4.21 Air 7 Layer's Location Plan

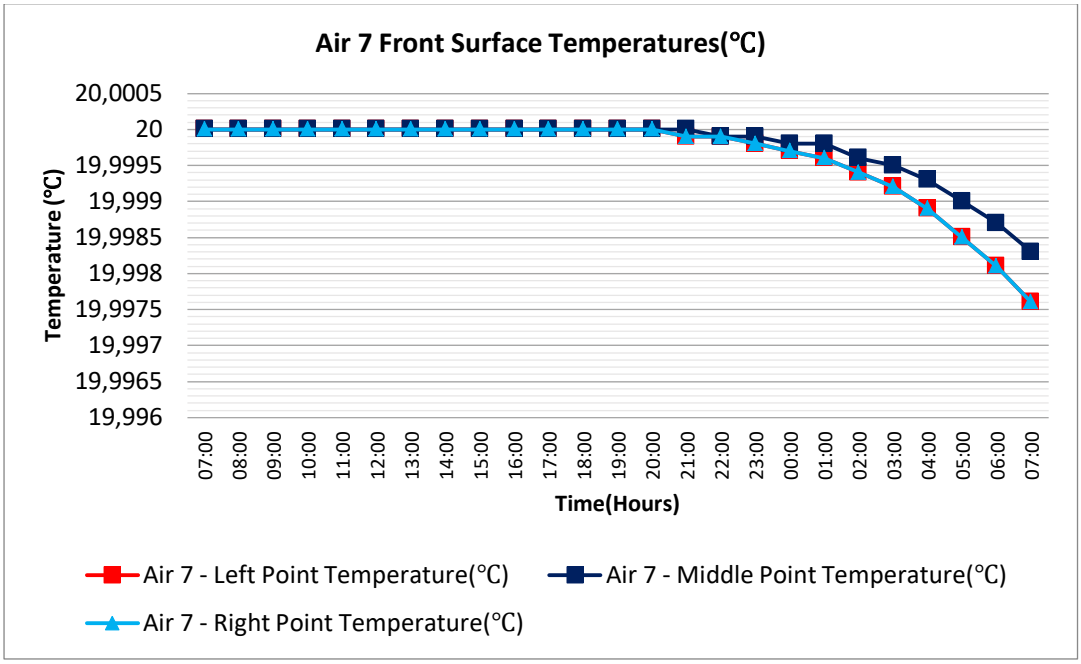

Figure 4.22 Air 7 Front Surface Temperatures(°C)

It can be seen from the energy analysis results that, all the points of Air 7 front surface satisfy ASHRAE thermal comfort levels through out the day (Figure 4.21, Figure 4.22). The temperature values of Air 7 front surface do not change too much, this could be the result of non existence of natural convection in the analysis.

It can be seen from the results that with 100% PCM filled panel scenario, Dynamic Trombe Wall, Heat Pocket can satisfy the ASHRAE thermal comfort levels after Air 3 volume under given conditions through out the day (Figure 4.16) and also, the temperature values taken from the middle region behind the panel approximately stay in the ASHRAE thermal comfort levels through the day.

It should be considered that the model only loses energy from the façade area, not from the sides, top or below because the spaces beyond were taken as adiabatic in the model. It should be also noted that only 1/3rd of the total panel area is utilized for the room to collect solar energy. In phase 2, the temperature data collection point locations for the panel and the PCM are different from the phase 1. New temperature data collection points on the panel and the PCM surfaces are

indicated in Figures 4.23 , Figure 4.24 and Figure 4.26, respectively. The temperature graphs for these data collection points on the panel and in the PCM are shown in Figures 4.25 and 4.27, respectively.

These graphs show us that a considerable amount of heat energy is stored in the PCM panels; hence, for home applications that are not used in the daytime, when most occupants go out for work in daytime and do not need to heat their homes during the day, this technology is expected to provide positive results in terms of energy savings.

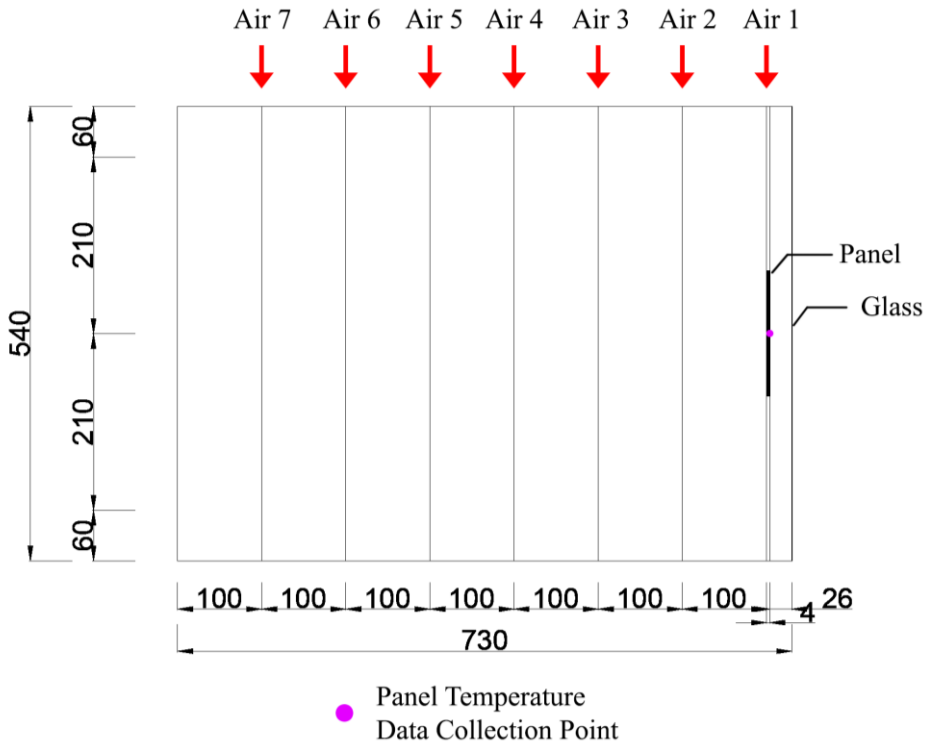

Figure 4.23 Panel Temperature Data Collection Point Plan

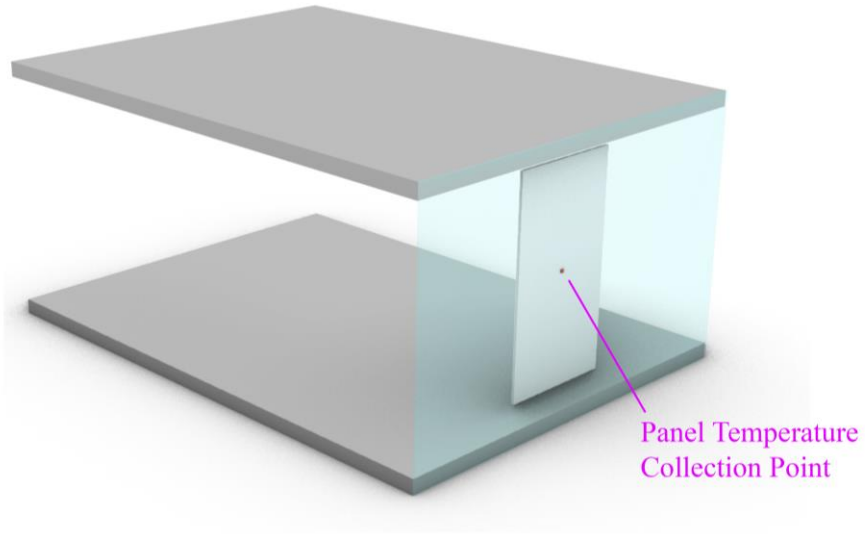

Figure 4.24 Panel Temperature Collection Point Location Perspective

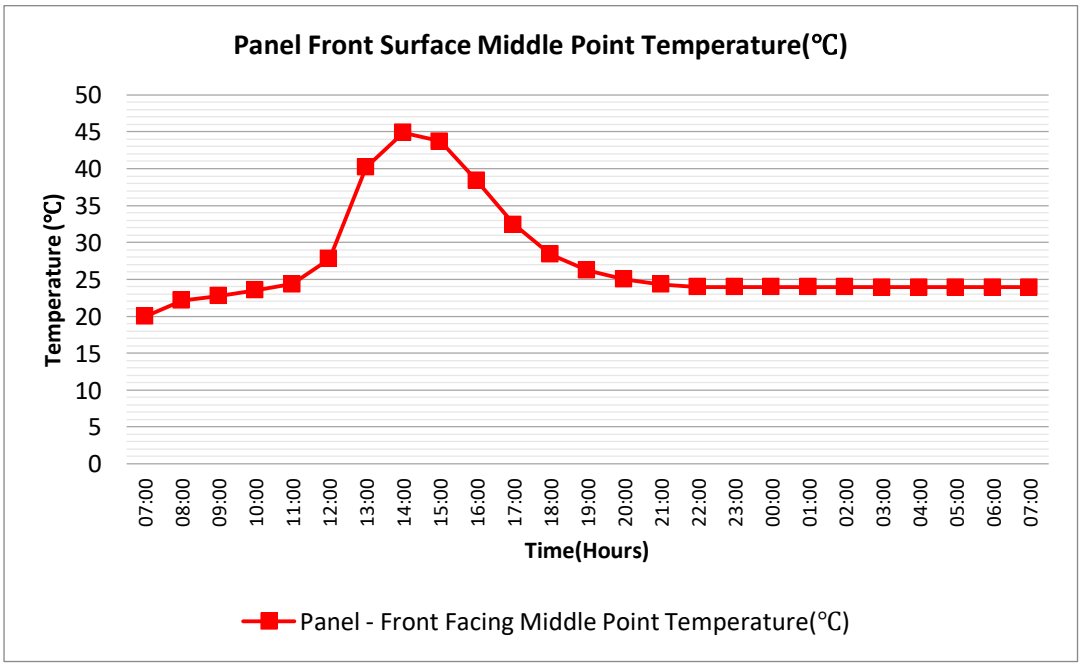

Figure 4.25 Panel Front Surface Middle Point Temperature(°C)

The panel's front middle surface is reaching up to a maximum of 44.86 °C at 14:00 first day (Figure 4.25). It can be seen from the panel results that the PCM is

absorbing energy between 22 °C - 24 °C, that's why the temperature increase slows down between 08:00 – 11:00 first day.

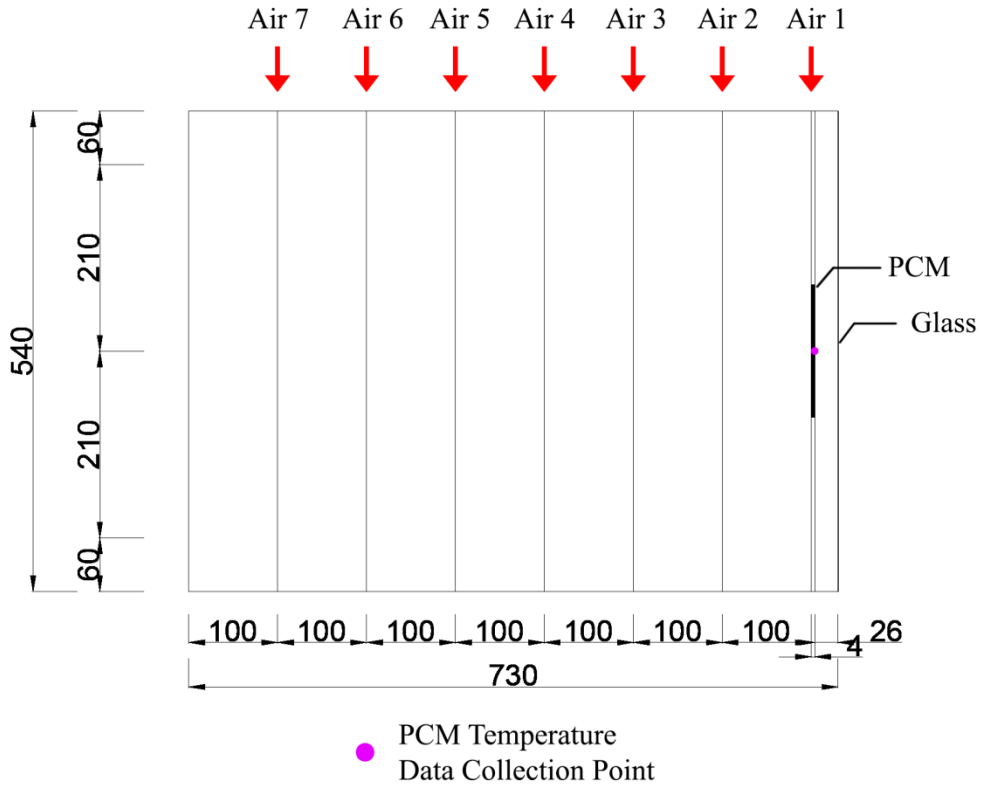

Figure 4.26 PCM Temperature Data Collection Point Plan

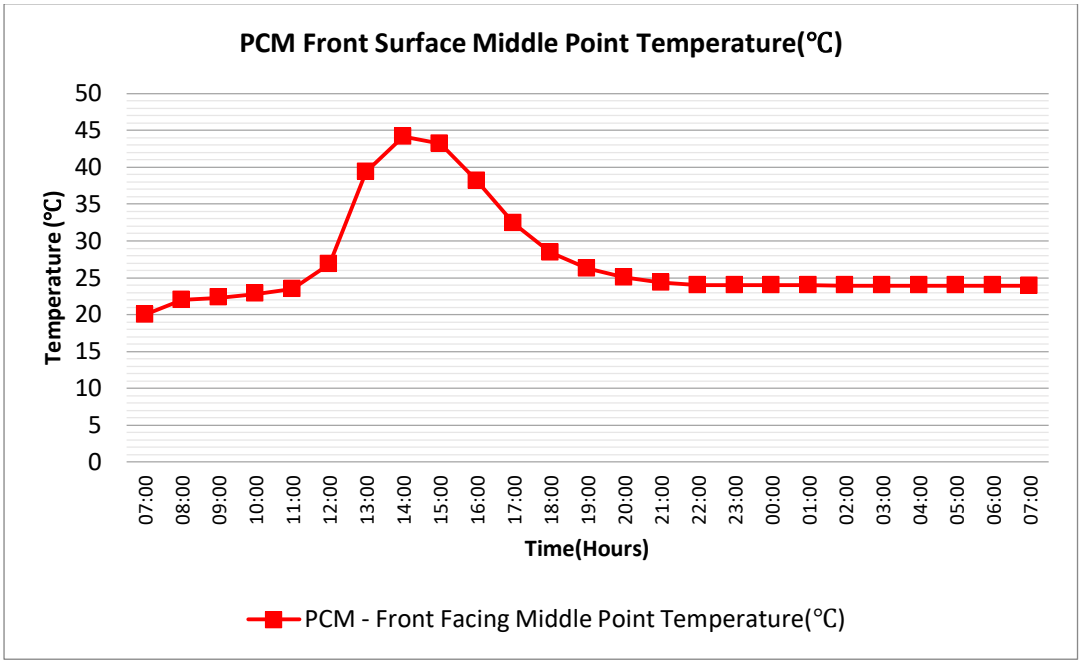

Figure 4.27 PCM Front Surface Middle Point Temperature(°C)

PCM Front surface middle point reaches up to 44.14 °C at 14:00 PM first day (Figure 4.27). It can be seen that the PCM front surface absorbs heat from the panel as the temperature collection point on the PCM is placed just behind the temperature collection point of the panel. The temperature increase slows down between 08:00 – 11:00 AM first day when the PCM goes through melting. The PCM curves down to 23.91 °C at 7:00 next day at the end of the analysis time which means it holds more energy than the initial temperature when the simulation was started for this scenario.

This system can be analogous of a heavy iron wheel which is ready to be loaded with energy by rotating it, which would give it momentum. PCM stores energy within the range of its melting just like this analogy. This means that this technology can be used in the buildings that are close or a little bit below to the temperatures of PCM's melting temperature, which are ready to be loaded with energy thereby, the solar energy will load the PCM with thermal energy which give the behaviour that PCM temperature point acts as the room temperature resistance against temperature decrease within PCM's melting temperature, similar to a

rotating heavy wheel. If the setpoint would be higher than the melting point of PCM, the system will use energy to sustain the setpoint, a stabilization point would never be achieved therefore, unnecessary energy consumption is expected.

4.2 Discussion

If the proposed Heat Pocket product is tested in a real-life experiment it is expected that the top sides of the boxes would get hotter as the hot air rises and there would be a formation of a convection zone because of the PCM melting which in turn is expected to increase the convective heat transfer rate inside the paraffin medium.

The simulation results of this study show that the surface contact area between the air and panel should be increased for increased heat dissipation.

As can be seen from the findings, in the scenarios of 50% and 75% fill rate, the panel gets too hot to be used, and touching them can harm users. This is why it must be stated that the panel should be designed carefully and PCM should be carefully selected due to safety reasons. For using Crodatherm 24W as PCM, the temperature must stay well below 226 °C degrees so it won't ignite and can cause hazardous consequences for such PCM products to use. It may end up with chain explosions throughout the building façade considering there are temperature gradients forming due to convection as heat rises up and leads to localized energy accumulations on the panel.

Additional findings that are not included in this work show, in phase 1 there is a tradeoff between the heat stored in the paraffin versus the heat sent indoors, when the boxes get hotter significantly such was the case in 50% filled panel, the room gets heated faster and when the boxes get hotter slowly which was the case in 100% filled panel, there is a smooth transition of energy transfer to the indoors. According to the analysis, it can be seen that the more the paraffin fill rate, the lesser the temperature of the panels will increase because the heat is transferred

into the paraffin medium faster as the heat storage increases and the contact surface area increases between the aluminum surface and the paraffin surface.

4.3 Recommendations

If it is possible, another definitive similar analysis should be simulated to see how much this system can benefit the user by comparing it with the same room, under the same interactions but without the heat pocket. This analysis must include the following: setpoint temperature, use of HVAC and related savings, convective heat transfer in the fluids of air and PCM, angular interaction of reflectivity between the glass and the incoming solar energy and, to assess the efficiency of the panels on the different façade orientations (north, south, east, west), the façade directions and related energy input should be studied as both direct solar energy input and indirect ambient solar energy input changes as the earth rotates.

As a further study, the sun-tracking module and stationary module could be compared in a real-life experiment to observe how much box rotation in regards perpendicular exposure influences the heat absorption from direct solar energy. In this study, this comparison could not be included because there were no calculation modules in ABAQUS program for this specific job and it can be said that it is difficult to calculate such a complex phenomenon of radiation-matter interactions. To study this, a panel that is parallel to glass and, a rotating sun-tracking one could be compared to see how it affects the efficiency either vertically or horizontally.

CHAPTER 5

CONCLUSION

In the literature, PCM and their application in buildings have been studied by many researchers showing their potential in terms of cooling and heating energy demand reduction by stabilizing the indoor temperature fluctuations, peak-load reduction in grids which decreases the inefficient energy production, maintaining the user thermal comfort in the built environment and thereby, decreasing the related CO2 emissions. Hence, the subject of PCM application is promoting a thinking style that questions how could the world be built smarter which gives architects a broader way to figure out the functional possibilities and provides a method of exploration for decreasing the energy consumption in the built environment.

Moreover, with the help of computation tools such as various energy simulation software, architects now can analyze the approximate energy consumption behavior before the construction processes. This procedure gives architects insight into how to use these products, helping them calculate complex physical behavior easily and allowing them to choose the correct materials for specific building applications in regard to PCM usage.

This approach is functional because, in the cases of using PCM, different PCM products can represent different behaviors due to their latent heat storage in comparison with normal materials which generally store the thermal energy as sensible heat. Therefore, utilizing simulation software can help designers calculate such complex energy interactions while calculating the related savings and prevent

such cases of the wrong PCM uses that can result in more energy consumption which can be regarded as a direct loss of money and effort for no gain in real life. This is why the energy simulation method is used for assessing the proposed product.

In this study, the aim was to observe the impact of the Heat Pocket product and assess if the energy model can satisfy the ASHRAE thermal comfort levels in a scenario of an office or residential space. For the design of the product, the main ideas of simple design, high efficiency, low cost, fast production, retrofit ability user comfort, and dynamic use were taken into consideration which was essential to generate a promising product. This was an attempt to form an alternative technology to the old one of the conventional/ traditional Trombe Wall. The use of PCM as the heat storage material meets with these aspects, which allowed to implement of a lightweight system in contrast to a classic massive Trombe Wall, and also, the use of solar selective coating allowed to gather energy faster and more efficiently and use of aluminum allowed for faster heat transfer to the environment. To achieve the objective of this study, the proposed design of Heat Pocket was formed that utilizes multiple aluminum panels that were filled with PCM in order to allow the intended latent heat storage capacity for any possible case which aims to increase the thermal energy storage and solar absorption in the winter months for glazed buildings. This approach can bring an opportunity for the office buildings which are mostly occupied during the day time. Therefore, they need the instant transfer of the heat. In this case, the use of PCM with aluminum containers offers an extra advantage for office buildings. To make this system user-friendly, a railing system that panels can slide on was introduced which allows users to select between the use of sunlight for lighting purposes and energy collection, also when it is not used users can slide and store the panels at the end of the room.

It was important to choose the suitable PCM product for the specific case. It was found that when the set point temperature is close to the PCM melting

temperature, it has positive effects on the energy savings which was discussed in Chapter 2. In this respect, Crodatherm 24W PCM was used in the analysis which was close to the expected indoor set point temperature with its melting temperature, which was 22°C - 24°C. Also, Crodatherm 24W was not corrosive with the use of the aluminum box and sustainable as it can withstand many melting crystallization phases.

To analyze this system, the study model was selected for a scenario where $1/3^{rd}$ of the total panels were used ($2/3^{rd}$ of them were not used in the scenario due to utilizing sunlight for interiors) and the location for the analysis was selected as Van, Turkey with a room size of 5.4 m x 7.3 m x 3.5 m. The model was simplified by merging all of the simplified panels into one big panel element which has a size of 152 cm x 280 cm x 4 cm. The room's indoor air volume is divided into seven 1 meter deep layers to calculate the temperature change behavior of certain points that are located on these layers' front facing surfaces. This simulation was performed for one day cycle in December when the solar radiation was the lowest throughout the year in Van, Turkey and the exterior temperature was taken as -5 °C constantly. After that, the energy analysis was left to rest in thermal isolation where all of the sun energy inputs and exterior temperatures were removed to affect the system for calculating the thermal equilibrium. This step is done to compensate for the natural convection analysis which could not be performed in this work due to ABAQUS program limitations.

The study consists of two phases and both phases used the same 3D model except the panel PCM fill rates were changed in phase 1.

In phase 1, panels with PCM fill rates 50%, 75%, and 100% were calculated to select the best scenario of PCM fill rate. This phase is actually to observe how hot the panel gets when the panel lacks PCM to a certain amount in some locations which may cause high temperatures due to energy accumulation. This was

expected to cause safety issues for the users such as the panel getting too hot to touch or worse used PCM Crodatherm 24W may ignite after the flashing point. Results for phase 1 showed that in the 50% fill rate scenario, the temperature of the panel's front facing top surface is reaching up to 285.13 ℃ at 13:00 PM as the maximum value which is dangerous considering that the PCM has a flashing point of 226 ℃ (Figure 4.1, Figure 4.2). If this case happens in real life, the PCM would explode throughout the façade and cause a fire. In the 75% fill rate scenario, the temperature of the panel's front facing top surface is reaching up 168.31 ℃ at 13:00 PM as the maximum value (Figure 4.1, Figure 4.2) which is too hot to touch the panel while it's operating which may cause safety problems for the user. Finally, in the 100% fill rate scenario, the temperature is reaching up to 42.78 ℃ at 14:00 PM as the maximum value which is found ideal and safe to use (Figure 4.1, Figure 4.2) therefore, this panel design was selected to be used in phase 2.

In phase 2, another simulation was performed calculating indoor temperatures using the selected 100% PCM-filled panel in the 3D setup which aims to observe if the Heat Pocket product satisfies the ASHRAE indoor thermal standards during the analysis time of 1 day.

Results showed that with 100% PCM filled panel scenario, Dynamic Trombe Wall, Heat Pocket can satisfy the ASHRAE thermal comfort levels after Air 3 volume under given conditions throughout the day (Figure 4.16) and also, the temperature values taken from the middle region behind the panel approximately stay in the ASHRAE thermal comfort levels through the day.

It can be seen in the results, the proposed technology can achieve an increase in the overall temperature for the scenario in the winter conditions for Van, Turkey at the end of 24 hours of analysis time; as could be observed according to the thermal analysis equilibrium temperature that is given by the steady-state step which was 23.64 °C. It should be mentioned that even though the system is set to work by $1/3^{rd}$ of the power of solar input due to the used surface area for collection, the

system can outperform itself by increasing the panels, allowing for more energy collection. Considering the results, Heat Pocket did achieve the required thermal comfort levels for occupants in such a room with the given conditions throughout the analysis time. It should be emphasized strongly that the room was thermally isolated except for the glass exterior surface, if the room's other surfaces were also exposed to the exterior cold temperature conditions, this result would change. This study model should be considered as a section / slice / part of a highly glazed building that the rooms next to it would be close to the room temperature, theoretically.

To compensate for this low fidelity simulation experiment which lacks convective and radiative heat transfer analyses study, a computational fluid dynamics (CFD) simulation in air and PCM should be conducted, while calculating savings as discussed in Chapter 4. This can be followed by a cost analysis study that should be conducted for the proposed design to assess its realization.

REFERENCES

Agrawal, B., & Tiwari, G. N. (2011). Building Integrated Photovoltaic Thermal Systems for Sustainable Developments. RSC Pub.

Air: Density, heat capacity, thermal conductivity. Material Properties. (2021, June 30). Retrieved August 4, 2022, from https://material-properties.org/air-density-heat-capacity-thermal-conductivity/#:~:text=Specific%20heat%20of%20Air%20is,degree%20or%20energy%20per%20kelvin.

Alana. (n.d.). Thermal conductivity. Retrieved June 1, 2022, from https://ewistore.co.uk/thermal-conductivity-u-values/#:~:text=U%2Dvalue%20%3D%20Thermal%20conductivity%20%2F,it%20is%20a%20better%20insulator.

ASHRAE. (2016). Standard 62.1-2016, Ventilation for Acceptable Indoor Air Quality. American Society of Heating, Refrigerating and Air-Conditioning Engineers.

ASHRAE. (2016). Standard 62.2-2016, Ventilation and Acceptable Indoor Air Quality in Residential Buildings. American Society of heating, refrigerating and air-conditioning engineers.

ASHRAE. (2017). Standard 55-2017 Thermal environmental conditions for human occupancy. American Society of Heating, Refrigerating and Air-Conditioning Engineers.

Barbi, S., Barbieri, F., Marinelli, S., Rimini, B., Merchiori, S., Bottarelli, M., & Montorsi, M. (2022). Phase change material evolution in thermal energy storage systems for the building sector, with a focus on ground-coupled heat pumps. Polymers, 14(3), 620. https://doi.org/10.3390/polym14030620

Bourdeau LE (1980) Study of two passive solar systems containing phase change materials for thermal storage. In: Proceedings of the 5th national passive solar conference, Amherst, MA, 19–26 October. Newark, DE: American Section of the International Solar Energy Society.Building a better Trombe wall - NREL. (n.d.). Retrieved July 13, 2022, from https://www.nrel.gov/docs/legosti/fy98/22834.pdf

Cabeza LF, Castello´ n C, Nogue´s M, et al. (2007) Use of microencapsulated PCM in concrete walls for energy savings. Energy and Buildings 39: 113–119.

Childs, K. W., & Stovall , T. (2012). Potential energy savings due to phase change material in a building wall assembly: An examination of two climates. Retrieved May 9, 2022, from https://info.ornl.gov/sites/publications/files/Pub34268.pdf.

Collier, R. K., & Grimmer, D. P. (1979). Experimental evaluation of phase change material building walls using small passive test boxes (LA-UR-79-175; CONF-790106-4). Los Alamos Scientific Lab., NM (USA). https://www.osti.gov/biblio/6416100

Core Writing Team, & Pachauri, R. K. (2014). IPCC, 2014: Climate Change 2014: Synthesis Report. Contribution of Working Groups I, II and III to the Fifth Assessment Report of the Intergovernmental Panel on Climate Change (L. A. Meyer, Ed.). IPCC. https://www.ipcc.ch/report/ar5/syr/

de Abreu, D. D., Neto, R. C., Aelenei, L., & Silva, C. A. (2019). Modelling and experimenting thermal energy storage through the use of PCM in low thermal inertia office. 2019 International Conference on Power Generation Systems and Renewable Energy Technologies (PGSRET). https://doi.org/10.1109/pgsret.2019.8882725

de Gracia, A., Navarro, L., Castell, A., Ruiz-Pardo, Á., Alvárez, S., & Cabeza, L. F. (2013). Experimental study of a ventilated facade with PCM during winter period. Energy and Buildings, 58, 324–332. https://doi.org/10.1016/j.enbuild.2012.10.026

Density of construction materials in KG/m3 and LB/FT3. The Constructor. (2021, June 9). Retrieved August 2, 2022, from https://theconstructor.org/building/density-construction-materials/13531/

Derradji, L., Errebai, F. B., & Amara, M. (2017). Effect of PCM in improving the thermal comfort in buildings. Energy Procedia, 107, 157–161. https://doi.org/10.1016/j.egypro.2016.12.159

Farid, M. M., & Chen, X. D. (1999). Domestic electrical space heating with heat storage. Proceedings of the Institution of Mechanical Engineers, Part A: Journal of Power and Energy, 213(2), 83–92. https://doi.org/10.1243/0957650991537455

Farid, M. M., & Sheriff, A. (2016). 16 Phase change materials for energy storage and thermal comfort in buildings. In Materials for Energy Efficiency and Thermal Comfort in Buildings (pp. 384–398). essay, WOODHEAD.

Garg, H. P., & Prakash, J. (2000). Solar energy : fundamentals and applications (1st ed.). New Delhi.

Gawande, A. M., & Wasokar, A. P. (2016). Thermal Energy Storage by Phase Change Material. International Research Journal of Engineering and Technology, 03(10).

Gencel, O., Hekimoglu, G., Sarı, A., Ustaoglu, A., Subasi, S., Marasli, M., Erdogmus, E., & Memon, S. A. (2022). Glass fiber reinforced gypsum composites with microencapsulated PCM as novel building thermal energy storage material. Construction and Building Materials, 340, 127788. https://doi.org/10.1016/j.conbuildmat.2022.127788

Ghoneim, A. A., Klein, S. A., & Duffie, J. A. (1991). Analysis of collector-storage building walls using phase-change materials. Solar Energy, 47(3), 237–242. https://doi.org/10.1016/0038-092x(91)90084-a

Global Climate Change: Evidence. (2008, June 15). Retrieved January 9, 2021, from http://climate.nasa.gov/evidence/

Guohui, G. (1998). A parametric study of Trombe walls for passive cooling of buildings. Energy and Buildings 27: 37–43.

Hagenau, M., & Jradi, M. (2020). Dynamic Modeling and performance evaluation of Building Envelope Enhanced with phase change material under Danish conditions. Journal of Energy Storage, 30, 101536. https://doi.org/10.1016/j.est.2020.101536

Hordeski, M. F. (2002). New Technologies for Energy Efficiency. Fairmont Press.

Hordeski, M.F. (2011). New Technologies for Energy Efficiency. New York: Fairmont Press.

Ismail, K. A. R., Salinas, C. T., & Henriquez, J. R. (2008). Comparison between PCM filled glass windows and absorbing gas filled windows. Energy and Buildings, 40(5), 710–719. https://doi.org/10.1016/j.enbuild.2007.05.005

Jin, X., Medina, M. A., & Zhang, X. (2016). Numerical Analysis for the optimal location of a thin PCM layer in frame walls. Applied Thermal Engineering, 103, 1057–1063. https://doi.org/10.1016/j.applthermaleng.2016.04.056

Jin, X., Shi, D., Medina, M. A., Shi, X., Zhou, X., & Zhang, X. (2017). Optimal location of PCM layer in building walls under Nanjing (China) weather conditions. Journal of Thermal Analysis and Calorimetry, 129(3), 1767–1778. https://doi.org/10.1007/s10973-017-6307-3

Kedl, R J, & Stovall, T K. (1989). Activities in support of the wax-impregnated wallboard concept. United States.

Khudhair, A. M., & Farid, M. M. (2004). A review on energy conservation in building applications with thermal storage by latent heat using phase change materials. Energy Conversion and Management, 45(2), 263–275. https://doi.org/10.1016/s0196-8904(03)00131-6

Kishore, R. A., Bianchi, M. V. A., Booten, C., Vidal, J., & Jackson, R. (2020). Optimizing PCM-integrated walls for potential energy savings in U.S. buildings. Energy and Buildings, 226, 110355. https://doi.org/10.1016/j.enbuild.2020.110355

Kishore, R. A., Bianchi, M. V. A., Booten, C., Vidal, J., & Jackson, R. (2021). Parametric and sensitivity analysis of a PCM-integrated wall for optimal thermal load modulation in lightweight buildings. Applied Thermal Engineering, 187, 116568. https://doi.org/10.1016/j.applthermaleng.2021.116568

Kosky, P., Balmer, R., Keat, W., & Wise, G. (2013). Mechanical engineering. Exploring Engineering, 259-281. https://doi.org/10.1016/b978-0-12-415891-7.00012-1

Kylili, A., & Fokaides, P. A. (2015). Numerical simulation of phase change materials for building applications: A Review. Advances in Building Energy Research, 11(1), 1–25. https://doi.org/10.1080/17512549.2015.1116465

LandGlass. (n.d.). LandVac 100% Tempered Vacuum Insulated Glass. Retrieved June 1, 2022, from https://www.importproducts.nl/data/upload/files/e-catalogue.pdf

Li, D., Wu, Y., Wang, B., Liu, C., & Arıcı, M. (2020). Optical and thermal performance of glazing units containing PCM in buildings: A Review. Construction and Building Materials, 233, 117327. https://doi.org/10.1016/j.conbuildmat.2019.117327

Li, D., Zheng, Y., Liu, C., & Wu, G. (2015). Numerical analysis on thermal performance of roof contained PCM of a single residential building. Energy Conversion and Management, 100, 147–156. https://doi.org/10.1016/j.enconman.2015.05.014

Li, S., Sun, G., Zou, K., & Zhang, X. (2016). Experimental research on the Dynamic Thermal Performance of a novel triple-pane building window filled with PCM. Sustainable Cities and Society, 27, 15–22. https://doi.org/10.1016/j.scs.2016.08.014

Li, S., Zhu, N., Hu, P., Lei, F., & Deng, R. (2019). Numerical study on thermal performance of PCM Trombe Wall. Energy Procedia, 158, 2441–2447. https://doi.org/10.1016/j.egypro.2019.01.317

Li, Z. X., Al-Rashed, A. A. A. A., Rostamzadeh, M., Kalbasi, R., Shahsavar, A., & Afrand, M. (2019). Heat transfer reduction in buildings by embedding phase change material in multi-layer walls: Effects of repositioning, thermophysical properties and thickness of PCM. Energy Conversion and Management, 195, 43–56. https://doi.org/10.1016/j.enconman.2019.04.075

Madessa, H. B. (2014). A review of the performance of buildings integrated with phase change material: Opportunities for application in Cold Climate. Energy Procedia, 62, 318–328. https://doi.org/10.1016/j.egypro.2014.12.393

Melero S, Morgado I, Neila J, et al. (2011) Passive evaporative cooling by porous ceramic elements integrated in a Trombe wall. In: Bodart M and Evrard A (eds) PLEA 2011: Architecture & Sustainable Development. Paris, France: Presses univ. de Louvain.

Metals and alloys - densities. Engineering ToolBox. (n.d.). Retrieved August 2, 2022, from https://www.engineeringtoolbox.com/metal-alloys-densities-d_50.html

Metals, metallic elements and alloys - thermal conductivities. Engineering ToolBox. (n.d.). Retrieved August 2, 2022, from https://www.engineeringtoolbox.com/thermal-conductivity-metals-d_858.html

Noh-Pat, F., Gijón-Rivera, M., Xamán, J., Zavala-Guillén, I., Aguilar, J. O., & Rodríguez-Pérez, M. (2019). Modelling of an energy-efficient open double-glazing unit for the main climatic conditions of Mexico. Indoor and Built Environment, 29(5), 746–764. https://doi.org/10.1177/1420326x19862601

Onishi, J., Soeda, H., & Mizuno, M. (2001). Numerical Study on a low energy architecture based upon distributed heat storage system. Renewable Energy, 22(1-3), 61–66. https://doi.org/10.1016/s0960-1481(00)00049-5

Onishi, J., Soeda, H., & Mizuno, M. (2001). Numerical Study on a low energy architecture based upon distributed heat storage system. Renewable Energy, 22(1-3), 61–66. https://doi.org/10.1016/s0960-1481(00)00049-5

Overall heat transfer coefficients. Engineering ToolBox. (n.d.). Retrieved November 10, 2022, from https://www.engineeringtoolbox.com/overall-heat-transfer-coefficient-d_434.html

Peippo, K., Kauranen, P., & Lund, P. D. (1991). A multicomponent PCM wall optimized for passive solar heating. Energy and Buildings, 17(4), 259–270. https://doi.org/10.1016/0378-7788(91)90009-r

Phase change material 24W. Energy Technologies. (n.d.). Retrieved August 4, 2022, from https://www.crodaenergytechnologies.com/en-gb/product-finder/product/1365-crodatherm_1_24w

Poulad, E., Fung, A., & Naylor, D. (2011). Effects of convective heat transfer coefficient on the ability of PCM to reduce building energy demand. Proceedings of Building Simulation 2011: 12th Conference of International Building Performance Simulation Association.

Saadatian, O., Sopian, K., Lim, C. H., Asim, N., & Sulaiman, M. Y. (2012). Trombe walls: A review of opportunities and challenges in research and development. Renewable and Sustainable Energy Reviews, 16(8), 6340–6351. https://doi.org/10.1016/j.rser.2012.06.032

Sadineni, S. B., Madala, S., & Boehm, R. F. (2011). Passive Building Energy Savings: A review of Building Envelope Components. Renewable and Sustainable Energy Reviews, 15(8), 3617–3631. https://doi.org/10.1016/j.rser.2011.07.014

Sayigh AAM, World Renewable Energy Congress Company and Institute of Energy (1991) Energy conservation in buildings: the achievement of 50% energy saving – an environmental challenge? In: Proceedings of NORTHSUN 90, An International Conference, University of Reading, UK, 18–21 September 1990. Berkshire, UK: Pergamon Press.

Sharifi, N. P., Shaikh, A. A., & Sakulich, A. R. (2017). Application of phase change materials in gypsum boards to meet building energy conservation goals. Energy and Buildings, 138, 455–467. https://doi.org/10.1016/j.enbuild.2016.12.046

Sharma, V., & Rai, A. C. (2020). Performance assessment of residential building envelopes enhanced with phase change materials. Energy and Buildings, 208, 109664. https://doi.org/10.1016/j.enbuild.2019.109664

Silva, T., Vicente, R., Rodrigues, F., Samagaio, A., & Cardoso, C. (2015). Development of a window shutter with phase change materials: Full Scale Outdoor Experimental Approach. Energy and Buildings, 88, 110–121. https://doi.org/10.1016/j.enbuild.2014.11.053

Sokol, D. (2008). Off the wall: Trombe walls at a visitor's center bask in the sunshine green source. The Magazine of Sustainable Design.

Solids - densities. Engineering ToolBox. (n.d.). Retrieved August 4, 2022, from https://www.engineeringtoolbox.com/density-solids-d_1265.html

Song, M., Niu, F., Mao, N., Hu, Y., & Deng, S. (2018). Review on Building Energy Performance Improvement Using Phase Change Materials. Energy and Buildings, 158, 776–793. https://doi.org/10.1016/j.enbuild.2017.10.066

Souayfane, F., Fardoun, F., & Biwole, P.-H. (2016). Phase change materials (PCM) for cooling applications in buildings: A Review. Energy and Buildings, 129, 396–431. https://doi.org/10.1016/j.enbuild.2016.04.006

Specific heat of common substances. Engineering ToolBox. (n.d.). Retrieved August 2, 2022, from https://www.engineeringtoolbox.com/specific-heat-capacity-d_391.html

Specific heats and molar heat capacities for various substances at 20 C. Table of Specific Heats. (n.d.). Retrieved August 4, 2022, from http://hyperphysics.phy-astr.gsu.edu/hbase/Tables/sphtt.html

Stazi, F., Mastrucci, A., & di Perna, C. (2012). The behaviour of solar walls in residential buildings with different insulation levels: An experimental and Numerical Study. Energy and Buildings, 47, 217–229. https://doi.org/10.1016/j.enbuild.2011.11.039

Stritih, U., Tyagi, V. V., Stropnik, R., Paksoy, H., Haghighat, F., & Joybari, M. M. (2018). Integration of passive PCM Technologies for net-zero energy buildings. Sustainable Cities and Society, 41, 286–295. https://doi.org/10.1016/j.scs.2018.04.036

Sun, W., Ji, J., Luo, C., & He, W. (2011). Performance of PV-trombe wall in winter correlated with south façade design. Applied Energy, 88(1), 224–231. https://doi.org/10.1016/j.apenergy.2010.06.002

The Causes of Climate Change. (n.d.). Climate Change: Vital Signs of the Planet. Retrieved January 16, 2021, from https://climate.nasa.gov/causes/#:%7E:text=On%20Earth%2C%20human%20activities%20are,air%20to%20make%20CO2.

Thermal conductivity. (n.d.). Retrieved August 4, 2022, from http://hyperphysics.phy-astr.gsu.edu/hbase/Tables/thrcn.html

Tunç, M. & Uysal, M. (1991) Passive solar heating of buildings using a fluidized bed plus Trombe wall system. Applied Energy 38: 199–213.

Tyagi, V. V., & Buddhi, D. (2007). PCM thermal storage in buildings: A state of art. Renewable and Sustainable Energy Reviews, 11(6), 1146–1166. https://doi.org/10.1016/j.rser.2005.10.002

Uçkan, İ. (2018). Analysis of solar radiation data in Van, Turkey. Celal Bayar Üniversitesi Fen Bilimleri Dergisi, 421–427. https://doi.org/10.18466/cbayarfbe.434552

Vautherot, M., Maréchal, F., & Farid, M. M. (2015). Analysis of energy requirements versus comfort levels for the integration of phase change materials in buildings. Journal of Building Engineering, 1, 53–62. https://doi.org/10.1016/j.jobe.2015.03.003

Weather Spark. (n.d.). Van Bölgesinde Aralık Hava Durumu. Retrieved June 1, 2022, from https://tr.weatherspark.com/m/102775/12/Aral%C4%B1k-ay%C4%B1nda-Van-T%C3%BCrkiye-Ortalama-Hava-Durumu#Figures-Temperature

Wi, S., Yang, S., Lee, J., Yun, B. Y., Park, J. H., & Kim, S. (2019). Dynamic heat transfer analysis on hwangtoh with PCM/eco-material for improving thermal inertia. IOP Conference Series: Materials Science and Engineering, 609(6), 062019. https://doi.org/10.1088/1757-899x/609/6/062019

Wikimedia Foundation. (2022, July 30). Density of air. Wikipedia. Retrieved August 5, 2022, from https://en.wikipedia.org/wiki/Density_of_air#:~:text=At%20IUPAC%20standard%20temperature%20and,approximately%201.2754%20kg%2Fm3.

Wikimedia Foundation. (2022, July 8). List of thermal conductivities. Wikipedia. Retrieved August 2, 2022, from https://en.wikipedia.org/wiki/List_of_thermal_conductivities

Xia, X., Meng, E., Chen, Y., Liu, Y., Chen, Q., Lu, Y., & Chen, J. (2017). Numerical Study of the thermal performance of the PCM wall under periodical outside Temperature waves. Procedia Engineering, 205, 3478–3484. https://doi.org/10.1016/j.proeng.2017.09.892

Zalewski, L., Chantant, M., Lassue, S., & Duthoit, B. (1997). Experimental thermal study of a solar wall of composite type. Energy and Buildings, 25(1), 7–18. https://doi.org/10.1016/s0378-7788(96)00974-7

Zalewski, L., Joulin, A., Lassue, S., Dutil, Y., & Rousse, D. (2012). Experimental study of small-scale solar wall integrating phase change material. Solar Energy, 86(1), 208–219. https://doi.org/10.1016/j.solener.2011.09.026

Zhai, X. Q., Song, Z. P., & Wang, R. Z. (2011). A review for the applications of solar chimneys in buildings. Renewable and Sustainable Energy Reviews, 15(8), 3757–3767. https://doi.org/10.1016/j.rser.2011.07.013

Zrikem, Z. & Bilgen, E. (1987). Theoretical study of a composite Trombe-Michel wall solar collector system. Solar Energy 39: 409–419.